

University of Dayton

eCommons

Graduate Theses and Dissertations

Theses and Dissertations

2008

Photochemical characterization of intensity dependence in multiphoton-reactive systems: application to the photodegradation of [beta]-carotene

Wenyue Wang
University of Dayton

Follow this and additional works at: https://ecommons.udayton.edu/graduate_theses

Recommended Citation

Wang, Wenyue, "Photochemical characterization of intensity dependence in multiphoton-reactive systems: application to the photodegradation of [beta]-carotene" (2008). *Graduate Theses and Dissertations*. 6227.

https://ecommons.udayton.edu/graduate_theses/6227

This Thesis is brought to you for free and open access by the Theses and Dissertations at eCommons. It has been accepted for inclusion in Graduate Theses and Dissertations by an authorized administrator of eCommons. For more information, please contact mschlange1@udayton.edu, ecommons@udayton.edu.

Photochemical Characterization of Intensity Dependence in Multiphoton-Reactive Systems: Application to the Photodegradation of β -Carotene

Thesis

Submitted To

The School of Arts and Sciences of the

UNIVERSITY OF DAYTON

in Partial Fulfillment of the Requirements for

The Degree

Master of Science

By

Wenyue Wang

UNIVERSITY OF DAYTON

Dayton, Ohio

December 2008

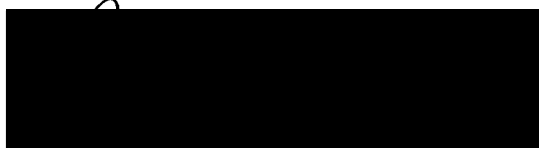
APPROVED BY:



Mark B. Masthay, Ph.D.
Director and Associate Professor
Department of Chemistry
University of Dayton
Committee Chairman



Shawn M. Swavey, Ph.D.
Assistant Professor
Department of Chemistry
University of Dayton
Committee Member



David W. Johnson, Ph.D.
Associate Professor,
Department of Chemistry
University of Dayton
Committee Member

ABSTRACT

A novel method which facilitates the characterization of the number n of photons which must be absorbed by individual molecules to initiate multiphoton-induced reactions is presented. In this method, n is characterized using longitudinally-and-temporally averaged n^{th} -order intensities $\overline{I_{x,t}^n}$ instead of (conventionally-used) incident intensities $I_{0,0}^n$. Because the intensity exponentially decreases across the optical path $0 \leq x \leq \ell$ in one-photon absorbing samples according to Beer's Law, this novel $\overline{I_{x,t}^n}$ -based method is especially suited for characterizing n in multiphoton-reactive systems with finite optical densities (Beer's Law absorbance) at the actinic wavelength. By accounting for intensity losses across the optical path originating from one-photon absorption, $\overline{I_{x,t}^n}$ approximates the actinically effective higher order intensities which induce nonlinear photochemistry more closely than $I_{0,0}^n$.

We demonstrate the utility of this $\overline{I_{x,t}^n}$ -based method by using it to characterize n for the rapid color loss of orange solutions of β -Carotene in carbon tetrachloride solvent induced by intense 532 nm laser pulses. By contrasting the rates of color loss of solutions irradiated with different intensities, we demonstrate that $2.0 \geq n_{0,0} \sim n_{x,t} \geq 1.6$ for solutions having identical initial optical densities A_{532}^{initial} , indicating the rate of color loss is proportional to both $I_{0,0}^2$ and $\overline{I_{x,t}^2}$. Essentially identical values of $n_{x,t}$ were obtained

for solutions of different $A_{532}^{initial}$ provided they were calculated using $\overline{I_{x,l}''}$. In contrast, incident intensities significantly underestimated ($n_{0,0} \sim 0.0$) or overestimated ($n_{0,0} \sim 3.5$) the intensity dependence with solutions of different $A_{532}^{initial}$. Our results thus demonstrate that n values based on incident intensities are reliable only if the solutions have identical $A_{532}^{initial}$; n values based on longitudinally-and-temporally averaged intensities are considerably more robust.

In view of the large and inconsistent optical densities characteristic of human tissue and the photolability of photodynamic dyes, we conclude our discussion by detailing the potential applications of longitudinally-and-temporally averaged intensities to the growing field of nonlinear photodynamic therapy. Our results suggest that reliable n values may be obtained for nonlinear photodynamic processes occurring under *in vivo* conditions – in which large and inconsistent optical densities are inherent and beyond the experimentalist's control – by employing longitudinally-and-temporally averaged intensities.

ACKNOWLEDGEMENTS

My special thanks are in order to Dr. Mark B. Masthay, my research advisor, for giving me the opportunity to do research in his laboratory and guiding me through. Besides his numerous help on my research work, I'm also grateful for his understanding and support at all times.

I would like to express my appreciation to everyone who has helped with my work. This includes my committee members Dr. David Johnson and Dr. Shawn Swavey; as well as my undergraduate co-worker Aaron Beach. In addition, discussions between Dr. Masthay and Drs. V.A. Benin, C.J. Cairns, H.B. Fannin, D.W. Johnson, A. Mortensen, D.A. Owen and P.E. Powers solved many of the problems we encountered during the course of this research. Additional thanks go to Ms. Kayla Miller and Ms. Sara McCrate for help in preparing the manuscript, and to Mr. C. Woods for help in preparing figures.

This research was partially funded by awards to Dr. Masthay from the National Institutes of Health, the National Science Foundation, the Ohio Board of Regents Research Incentive Program, the University of Dayton, the Christian Scholars Foundation, and to me by a University of Dayton Graduate Summer Fellowship. Additional funding was also provided by a Merck/AAAS grant to the Departments of Chemistry and Biology at the University of Dayton.

I would also like to thank everybody in the chemistry department for being so nice and kind, which makes my two years of study at the University of Dayton unforgettable. Last but not least, this work is dedicated to my family, for their love and support under all circumstances.

TABLE OF CONTENTS

INTRODUCTION.....	1
THEORY	5
A. Two-Photon Excitation in One-Photon Transparent ($A = 0$) Samples.....	5
B. Two-Photon Excitation in One-Photon Absorbing ($A > 0$) Samples	8
1. <i>Local, Instantaneous Intensities and Rates</i>	8
2. <i>Longitudinally-and-Temporally Averaged Intensities and Rates</i>	13
3. <i>Normalized Average Rates for Intensity Dependence of β-Carotene Photodegradation</i>	15
EXPERIMENTAL.....	20
A. Purification of β -Carotene	20
B. Preparation of β -Carotene Solutions	21
C. Characterization of Intensity Dependence of β -carotene Photodegradation.....	21
D. Impact of Deuterium Lamp on β -Carotene Photodegradation	25
E. Data Analysis	28
1. <i>The method of 56 pairs</i>	28
2. <i>The method of least squares</i>	28
3. <i>Rejection of bad points</i>	29
4. <i>95% confidence limits (λ_{95})</i>	32
5. <i>Full error propagation (ϵ) of n</i>	32
RESULTS AND DISCUSSION.....	36
A. Effects of Intensity Averaging on Intensity Dependence: $n_{0,0}$ and $n_{x,t}$ Contrasted.....	36
B. Effects of Irradiation Interval, Actinic Dose and Absorbance Drop on Intensity Dependence	
43	
C. Comparison between the Method of 56 Pairs and the Method of Least Squares	44
D. The β -Carotene Photodegradation Mechanism	45
1. <i>Concentration Dependence</i>	45
2. <i>Intensity Dependence</i>	49
3. <i>Wavelength Dependence</i>	50
E. Contributions of Dark and Monophotonic Reactions to the Total Photodegradation Rate	56
F. Photodegradation Quantum Yield and Two-Photon Absorptivity of β -Carotene	57
G. Implications of Intensity Averaging for Photodynamic Therapy.....	61
CONCLUSIONS AND FUTURE STUDIES	64
A. Conclusions	64
B. Future Studies	66
REFERENCES.....	67
APPENDIX.....	73

LIST OF FIGURES

Figure 1. Effects of optical density on actinic beam intensity in (a) optically transparent ($A = 0$), (b) low absorbance (LA), and (c) high absorbance (HA) samples.....	9
Figure 2. One-photon, simultaneous two-photon and sequential biphotonic photochemical processes.....	10
Figure 3. Actinically effective squared intensity $I_{x,t}^2$ (see Equation [11]) and mean actinically effective squared intensity $\overline{I_{x,t}^2}$ (see Equations [15c]) for a representative one-photon absorbing, two-photon reactive system undergoing two-photon induced photodegradation.....	12
Figure 4. Structure of β -carotene (β C).....	15
Figure 5. Proposed β -carotene-to-solvent photoinduced electron transfer (PET) mechanism.....	16
Figure 6. Schematic diagram of the intensity-controlled laser irradiation system in our laboratory.....	22
Figure 7. Spectrum of β -carotene in CCl_4 solvent.....	24
Figure 8. Conversion of β C to P_{350} photoproducts induced by 2 mJ pulse ⁻¹ , 532 nm pulses from a Nd:YAG laser operating at 10 Hz for 3600 seconds, followed by irradiation with the 313 nm line from Hg lamp for 30 seconds.....	24
Figure 9. Spectra of β C solution ($A_{532} = 1.0$) with D ₂ lamp off (top) and on (bottom)...	26
Figure 10. Spectra of β C solution ($A_{532} = 0.2$) with D ₂ lamp off (top) and on (bottom).	27
Figure 11A. Values of $\bar{n}_{0,0}$ (blue) and $\bar{n}_{x,t}$ (red) obtained with identical irradiation intervals of 45, 90 and 180 seconds contrasted.....	38
Figure 11B. Values of $\bar{n}_{0,0}$ (blue) and $\bar{n}_{x,t}$ (red) obtained with identical actinic doses of 0.9, 1.8 and 3.6J contrasted.....	39

Figure 11C. Values of $\bar{n}_{0,0}$ (blue) and $\bar{n}_{x,t}$ (red) obtained with identical absorbance drops of 5%, 10%, 20% and 50% contrasted.....	40
Figure 12. Representative plots of the logarithms of the average normalized rates $\overline{R'_{x,t}}$ of β C photodegradation in CCl_4 solvent versus the logarithms of the longitudinally-and-temporally averaged root mean square intensities.....	45
Figure 13. Dependence of β C photodegradation of rate on concentration of CCl_4	48
Figure 14. Dependence of average normalized β C photodegradation rates $\overline{R'_{0,0}}$ (see Equation [22b]) on 532 nm incident intensities $I_{0,0}$ as monitored with 20% decreases in absorbance, indicating biphotonic saturation for $I_{0,0} > 2.5 \text{ MW cm}^{-2}$ (10 mJ pulse^{-1}).....	50
Figure 15. π -molecular orbitals of β -carotene.....	51
Figure 16. One- and two-photon electronic dipole selection rules for β C.....	52
Figure 17. Proposed energetics of 532 nm one-photon-induced (bottom) and 266 nm one-photon-induced and 532 nm two-photon-induced (top) electron transfer from β C to CCl_4	54
Figure 18. Intensity dependence on 313 nm light of β C photodegradation in CCl_4	55
Figure 19. Dependence of two-photon reaction quantum yield on 532 nm incident intensities $I_{0,0}$	59

LIST OF TABLES

Table I-A. Data set of $I\Delta t = 3.6$ J, HA - HI vs. HA - LI scenario before a “bad” point rejection.....	30
Table I-B. Data set of $I\Delta t = 3.6$ J, HA - HI vs. HA - LI scenario after a “bad” point rejection.....	31
Table II-A. Intensity dependence $\bar{n}_{0,0}$ and 95% confidence limits λ_{95} obtained by the method of 56 points.....	36
Table II-B. Intensity dependence $\bar{n}_{x,t}$ and 95% confidence limits λ_{95} obtained by the method of 56 points.....	37
Table III-A. Intensity dependence $\bar{n}_{0,0}$, 95% confidence limits λ_{95} and linear least squares correlation coefficients R^2 obtained by the method of least squares.....	41
Table III-B. Intensity dependence $\bar{n}_{x,t}$, 95% confidence limits λ_{95} and linear least squares correlation coefficients R^2 obtained by the method of least squares.....	42
Table IV. Dependence of rate of 532 nm-induced photodegradation of β C on concentration of β C.....	47
Table V. Dependence of rate of 532 nm-induced photodegradation of β C on concentration of CCl_4	49
Table VI-A. Full data set of $\Delta t = 45$ s, HA - HI vs. HA - LI scenario.....	74
Table VI-B. Full data set of $\Delta t = 45$ s, LA - HI vs. LA - LI scenario.....	75
Table VI-C. Full data set of $\Delta t = 45$ s, LA - HI vs. HA - LI scenario.....	76
Table VI-D. Full data set of $\Delta t = 45$ s, HA - HI vs. LA - LI scenario.....	77
Table VII-A. Full data set of $\Delta t = 90$ s, HA - HI vs. HA - LI scenario.....	78
Table VII-B. Full data set of $\Delta t = 90$ s, LA - HI vs. LA - LI scenario.....	79

Table VII-C. Full data set of $\Delta t = 90\text{s}$, LA - HI vs. HA - LI scenario.....	80
Table VII-D. Full data set of $\Delta t = 90\text{s}$, HA - HI vs. LA - LI scenario.....	81
Table VIII-A. Full data set of $\Delta t = 180\text{s}$, HA - HI vs. HA - LI scenario.....	82
Table VIII-B. Full data set of $\Delta t = 180\text{s}$, LA - HI vs. LA - LI scenario.....	83
Table VIII-C. Full data set of $\Delta t = 180\text{s}$, LA - HI vs. HA - LI scenario.....	84
Table VIII-D. Full data set of $\Delta t = 180\text{s}$, HA - HI vs. LA - LI scenario.....	85
Table IX-A. Full data set of $I\Delta t = 0.9\text{J}$, HA - HI vs. HA - LI scenario.....	86
Table IX-B. Full data set of $I\Delta t = 0.9\text{J}$, LA - HI vs. LA - LI scenario.....	87
Table IX-C. Full data set of $I\Delta t = 0.9\text{J}$, LA - HI vs. HA - LI scenario.....	88
Table IX-D. Full data set of $I\Delta t = 0.9\text{J}$, HA - HI vs. LA - LI scenario.....	89
Table X-A. Full data set of $I\Delta t = 1.8\text{J}$, HA - HI vs. HA - LI scenario.....	90
Table X-B. Full data set of $I\Delta t = 1.8\text{J}$, LA - HI vs. LA - LI scenario.....	91
Table X-C. Full data set of $I\Delta t = 1.8\text{J}$, LA - HI vs. HA - LI scenario.....	92
Table X-D. Full data set of $I\Delta t = 1.8\text{J}$, HA - HI vs. LA - LI scenario.....	93
Table XI-A. Full data set of $I\Delta t = 3.6\text{J}$, HA - HI vs. HA - LI scenario.....	94
Table XI-B. Full data set of $I\Delta t = 3.6\text{J}$, LA - HI vs. LA - LI scenario.....	95
Table XI-C. Full data set of $I\Delta t = 3.6\text{J}$, LA - HI vs. HA - LI scenario.....	96
Table XI-D. Full data set of $I\Delta t = 3.6\text{J}$, HA - HI vs. LA - LI scenario.....	97
Table XII-A. Full data set of $\Delta A/\bar{A} = 5\%$, HA - HI vs. HA - LI scenario.....	98
Table XII-B. Full data set of $\Delta A/\bar{A} = 5\%$, LA - HI vs. LA - LI scenario.....	99
Table XII-C. Full data set of $\Delta A/\bar{A} = 5\%$, LA - HI vs. HA - LI scenario.....	100
Table XII-D. Full data set of $\Delta A/\bar{A} = 5\%$, HA - HI vs. LA - LI scenario.....	101
Table XIII-A. Full data set of $\Delta A/\bar{A} = 10\%$, HA - HI vs. HA - LI scenario.....	102

Table XIII-B. Full data set of $\Delta A/\bar{A} = 10\%$, LA - HI vs. LA - LI scenario.....	103
Table XIII-C. Full data set of $\Delta A/\bar{A} = 10\%$, LA - HI vs. HA - LI scenario.....	104
Table XIII-D. Full data set of $\Delta A/\bar{A} = 10\%$, HA - HI vs. LA - LI scenario.....	105
Table XIV-A. Full data set of $\Delta A/\bar{A} = 20\%$, HA - HI vs. HA - LI scenario.....	106
Table XIV-B. Full data set of $\Delta A/\bar{A} = 20\%$, LA - HI vs. LA - LI scenario.....	107
Table XIV-C. Full data set of $\Delta A/\bar{A} = 20\%$, LA - HI vs. HA - LI scenario.....	108
Table XIV-D. Full data set of $\Delta A/\bar{A} = 20\%$, HA - HI vs. LA - LI scenario.....	109
Table XV-A. Full data set of $\Delta A/\bar{A} = 50\%$, HA - HI vs. HA - LI scenario.....	110
Table XV-B. Full data set of $\Delta A/\bar{A} = 50\%$, LA - HI vs. LA - LI scenario.....	111
Table XV-C. Full data set of $\Delta A/\bar{A} = 50\%$, LA - HI vs. HA - LI scenario.....	112
Table XV-D. Full data set of $\Delta A/\bar{A} = 50\%$, HA - HI vs. LA - LI scenario.....	113

CHAPTER I

INTRODUCTION

While the possibility of multiphoton transitions in atoms and molecules was theoretically predicted by Maria Göppert-Mayer in the 1930's,¹ such transitions were not observed experimentally until the advent of high intensity lasers in the 1960's. Since that time, multiphoton transitions – and particularly two-photon transitions – in atomic and molecular systems have been studied extensively.^{2,3}

In most studies of two-photon processes published to date, the systems share two characteristics. First, the samples are “one-photon transparent” (molar extinction coefficient $\epsilon_\lambda = 0$) but two-photon absorbing (two-photon absorptivity $\delta_\lambda > 0$) at the actinic wavelength λ . Since the number of doubly photoexcited solute molecules is generally small compared to the total numbers of photons and solute molecules,⁴⁻⁶ the intensity is effectively uniform and equal to the incident intensity I_0 (*i.e.*, the intensity at $x = 0$) across the entire optical path of such samples. Second, the samples are not “two-photon reactive”; that is, two-photon absorption does not initiate photochemistry. Since the strength of n -photon signals is proportional to the actinic intensity I raised to the n^{th} power, two-photon absorption is confirmed when the signal depends quadratically on intensity.² Multiphoton signals in these earlier studies were obtained using a variety of techniques, including fluorescence,⁷⁻¹² thermal lensing,^{9,13-15} photothermal deflection,¹⁶ photoacoustic,^{17,18} mass spectrometric,¹⁹⁻²¹ and optical double resonance²² techniques.

Significantly less effort has been devoted to characterizing multiphoton-reactive systems, in which multiphoton absorption initiates photochemistry. The most extensive research in this regard was performed by Nikogosyan and coworkers, who characterized the two-photon-induced photodegradation of purine and pyrimidine bases²³⁻²⁸ and amino acids²⁸ by plotting the rate R (defined as $\frac{\Delta A}{A I \Delta t}$, in which \bar{A} is the average Beer's law absorbance at the actinic wavelength over an irradiation interval Δt , $\frac{\Delta A}{A}$ is the normalized change in the absorbance and $I \Delta t$ is the total actinic dose) versus the incident intensity (for optically diffuse samples, for which $I = I_0$)²³⁻²⁸ or versus an empirical average intensity I_{ave} (for optically dense samples in which both sample and solvent absorb).^{23,24,29} Since the actinic dose is proportional to the intensity, two-photon-induced reactions were confirmed when R depended linearly on I .

More recently, Chizhov, *et. al.*³⁰ and Masthay, *et. al.*³¹ have characterized the intensity dependence of photodegradation of the purple membrane protein bacteriorhodopsin (BR) induced by 532 nm laser pulses. Chizhov, *et. al.* utilized low Beer's Law absorbance ($A_{532} \leq 0.2$) samples of BR in their studies, and hence were able to utilize the method developed by Nikogosyan, *et. al.* for optically thin samples. In contrast, Masthay, *et. al.* were constrained to use more concentrated ($A_{532} \leq 0.8$) samples in their studies. These researchers noted that n values based on incident intensities could potentially be spurious because the intensity deviates significantly from I_0 across the optical path in high absorbance samples (see Figures 1 and 3). Masthay, *et. al.* also noted that $I_{x,t}$ increased at $x > 0$ during the course of their irradiation intervals due to the decrease in A_{532} with time. These authors accordingly characterized n with their optically

dense samples using a *longitudinally-and-temporally averaged squared intensity* $\overline{I_{x,t}^2}$, which accounts for modulation of the beam intensity along the beam axis over the irradiation interval (see Equations [10] and [11] below).³¹⁻³⁵

Though $\overline{I_{x,t}^2}$ was utilized in this earlier study of BR because the reaction rates from which n is characterized are not uniform across the optical path due to one-photon absorption, its derivation was not presented in detail.³¹ A complete derivation of $\overline{I_{x,t}^2}$ as well as a detailed discussion of the conditions under which it applies is accordingly presented below.³⁴⁻³⁶

We illustrate the utility of the longitudinally-and-temporally averaged intensity by applying $\overline{I_{x,t}^2}$ to the 532 nm laser-induced photodegradation of β -carotene (β C; see Figure 4) in carbon tetrachloride (CCl_4) solvent.³⁷⁻⁴⁰ β C- CCl_4 solutions were used in the present study because they undergo unidirectional photochemistry and do not scatter light, in contrast to aqueous suspensions of BR,⁴¹⁻⁴³ which undergo reversible photochemistry and are turbid.³¹ Our results demonstrate that the color loss is mediated by a biphotonic process (most likely a sequential biphotonic β C-to- CCl_4 photoinduced electron transfer process; see Figures 2 and 5) with an effective two-photon absorptivity of $\delta_{532}^{\beta C} = 1.7 \times 10^7 \text{ GM}$.⁴¹⁻⁴³ The utility of the $\overline{I_{x,t}^2}$ -based approach is enhanced by its general applicability, as it can be used to characterize not only two-photon reactive systems such as β C, but also to three-photon-reactive systems, four-photon-reactive systems, *etc.*

Our results indicate that the longitudinally-and-temporally averaged intensity dependence $n_{x,t}$ obtained using $\overline{I_{x,t}^2}$ is significantly more reliable than the incident

intensity dependence $n_{0,0}$ obtained using $I_{0,0}^{n_{0,0}}$ with high absorbance samples. The greater reliability of $n_{x,t}$ is particularly manifest when samples having different Beer's law absorbance are used in the analysis.

In light of the considerations described above, we anticipate that the $\overline{I_{x,t}^n}$ -based approach will be useful in studies of a wide variety of nonlinear photochemical and photobiological processes in which inconsistent sample-to-sample absorbances are encountered. For example, $n_{x,t}$ should offer significant advantage over $n_{0,0}$ for investigations of multiphoton-induced photochemistry under *in vivo* conditions because of the inconsistencies in optical densities inherent to biological tissue due to light scattering and the presence of endogenous absorbing chromophores. We accordingly conclude by discussing ways in which the $\overline{I_{x,t}^n}$ -based approach may provide new insights into the photochemical mechanisms underlying the growing field of nonlinear photodynamic therapy, which is increasingly used in treating cancer and other diseases due to the greater tissue penetration depths attainable with the long wavelengths used to activate two-photon photodynamic dyes.^{3,5,44-59}

CHAPTER II

THEORY

A. Two-Photon Excitation in One-Photon Transparent ($A = 0$) Samples

In one-photon transparent samples, in which the absorbance $A = 0$ at the actinic wavelength, the longitudinal intensity profile of a temporally and spatially (*i.e.*, cross-sectionally) gaussian profile the actinic beam is the same for all x and t . The number of photons absorbed via two-photon excitation of one-photon transparent solute molecules in the path of an unfocused temporally and spatially gaussian laser beam with a pulsewidth of τ_{pulse} seconds in such samples is

$${}^2N_{hv} = \frac{1}{\sqrt{2}} \frac{\ell \delta}{\pi r_b^2} C N P_0 \quad (1)$$

in which ℓ is the optical pathlength in cm, r_b is the beam radius in cm, δ is the two-photon absorptivity of the chromophore at the actinic wavelength in $\text{cm}^4 \text{ sec photon}^{-1} \text{ molecule}^{-1}$, C is the number density of the chromophore in molecules cm^{-3} , N is the number of photons per pulse, and $P_0 = N/(1.06447\tau_{pulse})$ is the number of photons per second at peak intensity.² The number N^{**} of doubly-excited reactant molecules generated per pulse is equal to one-half the number of photons ${}^2N_{hv}$ absorbed per pulse

$$N^{**} = \frac{{}^2N_{hv}}{2} = \frac{1}{2\sqrt{2}} \frac{\ell \delta}{\pi r_b^2} C N P_0 \quad , \quad (2)$$

in which the factor of 2 in the denominator has units of photons per doubly-excited

molecule. Substituting $P_0 = \frac{N}{1.06647 \tau_{pulse}}$ into Equation (2) yields

$$N^{**} = \frac{\ell \delta}{1.06647 \cdot 2\sqrt{2} \tau_{pulse} \pi r_b^2} CN^2 \quad (3)$$

The molarity c^{**} of doubly-excited molecules generated per pulse in the beam volume is then obtained by dividing N^{**} by the product of Avogadro's Number N_A and the beam

volume $\frac{\pi r_b^2 \ell}{1000 \text{ cm}^3 \text{ L}^{-1}} = V_{beam}$ in liters to yield

$$c^{**} = \frac{N^{**}}{N_A V_{beam}} = \frac{\delta}{1.06647 \cdot 2\sqrt{2} \tau_{pulse} \pi^2 r_b^4} c N^2, \quad (4)$$

in which $c = \frac{1000 \text{ cm}^3 \text{ L}^{-1}}{N_A} \times C \gg c^{**}$ is the molarity of ground state reactant molecules

in the beam volume.⁴ Substituting $N = \pi r_b^2 \tau_{pulse} I_{0,0}$ into Equation (4) yields

$$c^{**} = \frac{\tau_{pulse} \delta}{1.06647 \cdot 2\sqrt{2}} c I_{0,0}^2 = bc I_{0,0}^2, \quad (5)$$

in which

$$b = \frac{\tau_{pulse} \delta}{1.06647 \cdot 2\sqrt{2}} = 0.331518 \tau_{pulse} \delta \quad (6)$$

is a constant having units of $\text{cm}^4 \text{ sec}^2 \text{ photon}^{-2} \text{ pulse}^{-1} = 1 \text{ GM molecule sec photon}^{-1} \text{ pulse}^{-1}$ and $1 \text{ GM} = 1 \text{ Göppert-Mayer} = 1 \times 10^{-50} \text{ cm}^4 \text{ sec molecule}^{-1} \text{ photon}^{-1}$ is the standard unit of two-photon absorptivity.²

Provided the total sample volume V_{tot} is irradiated by the beam (*i.e.*, provided $V_{total} = V_{beam}$) the concentration of doubly-excited molecules c_{beam}^{**} in the beam volume will equal the concentration of doubly-excited molecules $c_{tot vol}^{**}$ for the entire sample

volume. For circular actinic sources such as the Nd:YAG laser in our laboratory, this condition would require a cylindrical sample cell with a diameter equal to that of the laser beam. More typically, samples are irradiated in rectangular cuvettes to facilitate spectrophotometric monitoring of the reaction rate. In this common experimental scenario (which was employed in the current investigation; see *Experimental* below), V_{beam} is typically less than V_{total} because the surface area of the cuvette face exceeds the cross-sectional area of the actinic beam. Hence, the *concentration* of doubly-excited molecules averaged over the total volume is less than that in the irradiated volume by a factor of $\frac{V_{beam}}{V_{total}}$:

$$c_{tot\ vol}^{**} = \frac{V_{beam}}{V_{total}} c_{beam}^{**} \quad . \quad (7)$$

Provided the fractional yield f for the conversion of doubly-excited reactant to photoproduct

$$f = \frac{N_{photoproduct}}{N^{**}} \quad . \quad (8)$$

is equal to unity,^{2,31} $c_{tot\ vol}^{**}$ can be equated with the change in the concentration of reactant molecules over the entire volume

$$-\Delta c_{tot\ vol} = c_{tot\ vol}^{**} f = \frac{\Delta A}{\epsilon \ell} f = \frac{\Delta A}{\epsilon \ell} \quad . \quad (9)$$

The assumption that $f = 1$ is not unreasonable in systems with high photodegradation quantum yields such as BR³¹ and β C.^{41,42}

B. Two-Photon Excitation in One-Photon Absorbing ($A > 0$) Samples

1. Local, Instantaneous Intensities and Rates

The *local, instantaneous intensity* $I_{x,t}$ of an actinic beam normalized to account for one-photon absorption at an optical depth $0 \leq x \leq \ell$ inside an optical cell of pathlength ℓ after t seconds of irradiation is given by

$$I_{x,t} = 10^{-\varepsilon c_{x,t} x} I_{0,0} \quad , \quad (10)$$

in which ε is the molar extinction coefficient in units of $M^{-1} \text{ cm}^{-1}$ at the actinic wavelength, $c_{x,t}$ is the local, instantaneous concentration in $M = \text{mole L}^{-1}$ at x and t , and $I_{0,0}$ is the incident initial actinic intensity in units of $\text{photon cm}^{-2} \text{ sec}^{-1}$ (see Figure 1). (In most studies, in which the absorbance $A = \varepsilon c \ell$ is constant with time, the incident intensity – which is equal to the intensity at the incident face of the optical cell is designated simply as I_0 . The additional designation for time dependence in Equation [10] is applied because our model accounts for changes in absorbance with time.)³³

The probability that a molecule will absorb two photons is proportional to the square of the actinic intensity. This quadratic dependence holds regardless of whether the second photon is absorbed by a short-lived virtual intermediate state (lifetime $\tau \leq 10^{-14}$ seconds) in a conventional “simultaneous” two-photon excitation process^{2,8,9,22} or by a long-lived ($\tau \geq 10^{-14}$ seconds) ground or excited state intermediate in a consecutive biphotonic process^{23,25-27,31,60} (see Figure 2). By squaring Equation (10) we obtain the *local, instantaneous squared intensity*

$$I_{x,t}^2 = 10^{-2\varepsilon c_{x,t} x} I_{0,0}^2 \quad , \quad (11)$$

to which the local, instantaneous rates at x and t of two-photon induced reactions are directly proportional as discussed below, in units of $\text{photon}^2 \text{ cm}^{-4} \text{ sec}^{-2}$.

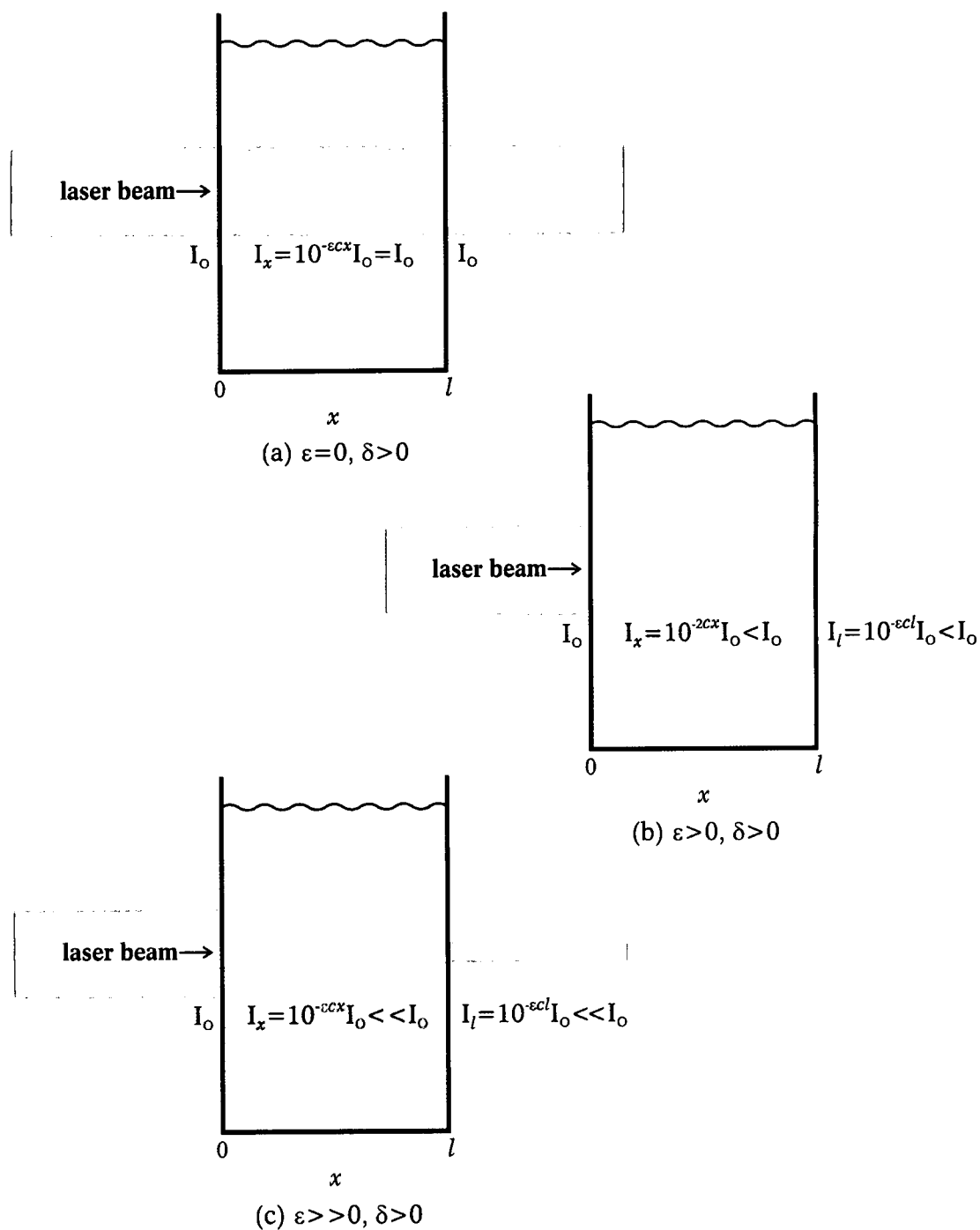


Figure 1. Effects of optical density on actinic beam intensity in (a) optically transparent ($A = 0$), (b) low absorbance (LA), and (c) high absorbance (HA) samples.

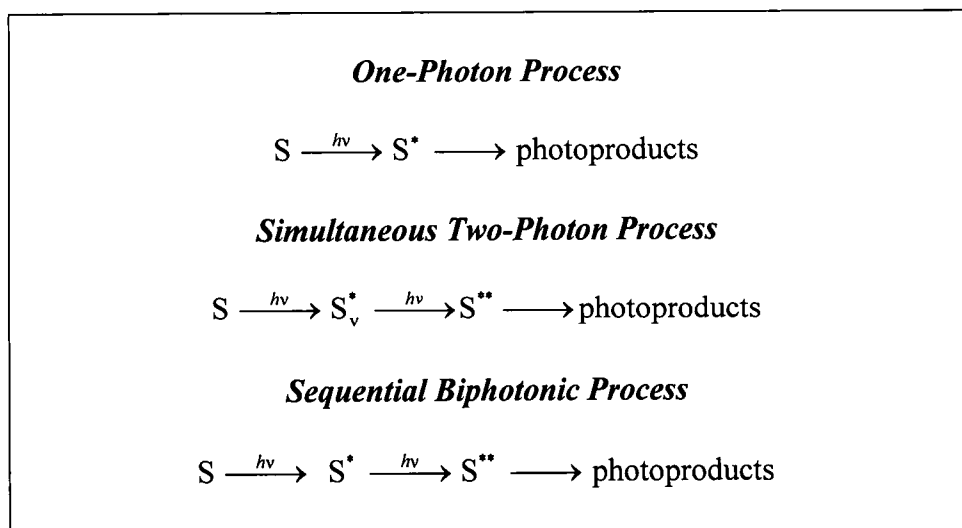


Figure 2. One-photon, simultaneous two-photon and sequential biphotonic photochemical processes. The instantaneous two-photon mechanism is mediated by $\tau \leq 10^{-14}$ second virtual intermediate states S_v^* . Sequential biphotonic processes are mediated by long lived ($\tau \geq 10^{-14}$ second) excited state intermediates S^* accessed via the absorption of the first photon (see also Reference 31).

Although the beam intensity is modulated slightly by two-photon absorption processes in two-photon absorbing samples, $I_{x,t}^2$ is corrected exclusively for one-photon (Beer's Law) absorbance in Equation (11) because two-photon absorption processes are generally many orders of magnitude less efficient than one-photon absorption processes, so that the number of solute molecules which absorb two photons is generally small compared to the number of photons in a laser pulse and to the total number of solute molecules in the beam volume.⁴⁻⁶

Through second order in intensity, the local, instantaneous rate of a photochemical process is equal to

$$R_{x,t} = -\frac{dc_{x,t}}{dt} = c_{x,t} \left(k_{0h\nu} + [k_{1h\nu} + k_{post-1h\nu}] I_{x,t}^1 + [k_{2h\nu} + k_{post-2h\nu}] I_{x,t}^2 \right) \quad (12a)$$

in which $c_{x,t}$, $I_{x,t}$, and $I_{x,t}^2$ are defined in Equations (10) and (11), $k_{0h\nu}$ is the rate constant

for dark thermal (zero-photon) reactions, $k_{1h\nu}$ and $k_{2h\nu}$ are rate constants for monophotonic and biphotonic light reactions, and $k_{post-1h\nu}$ and $k_{post-2h\nu}$ are rate constants for monophotonically-initiated and biphotonically-initiated thermal reactions which occur *between* pulses. Under conditions in which the rates of dark thermal, monophotonic, and post-monophotonic thermal reactions are negligible compared to those of biphotonic and post-biphotonic thermal reactions, Equation (12a) reduces to

$$R_{x,t} = -\frac{dc_{x,t}}{dt} = (k_{2h\nu} + k_{post-2h\nu}) c_{x,t} I_{x,t}^2 = k c_{x,t} I_{x,t}^2. \quad (12b)$$

The local instantaneous rate is effectively constant across the entire pathlength in the low concentration limit, in which $I_{x,t}^2 \rightarrow I_{0,0}^2$. In contrast, since $I_{x,t}^2 = 10^{-2\varepsilon c_{x,0}x} I_{0,0}^2$ declines rapidly with increasing optical penetration depth x , $R_{x,t}$ decreases with increasing x for optically dense samples. Hence, the bulk of two-photon induced photochemistry occurs near the incident edge of the optical path in high absorbance samples, as illustrated in Figures 1 and 3.^{4,61} Furthermore, $c_{x,t}$ decreases with increasing t in samples which undergo two-photon-induced photodegradation, so that $I_{x,t}^2$ progressively increases with time, approaching $I_{0,0}^2$ for all x as the reaction nears completion. Two-photon induced photochemistry thus becomes proportionally more efficient and rapid with time in samples which undergo decreases in absorbance – particularly at large x . These longitudinal and temporal dependencies of $I_{x,t}^2$ and $R_{x,t}$ in optically dense, two-photon-reactive samples can lead to significant errors in n values based on $I_{0,0}^2$. A more complete model which accounts for the longitudinal and temporal variations in $I_{x,t}^2$ in such samples is thus required.

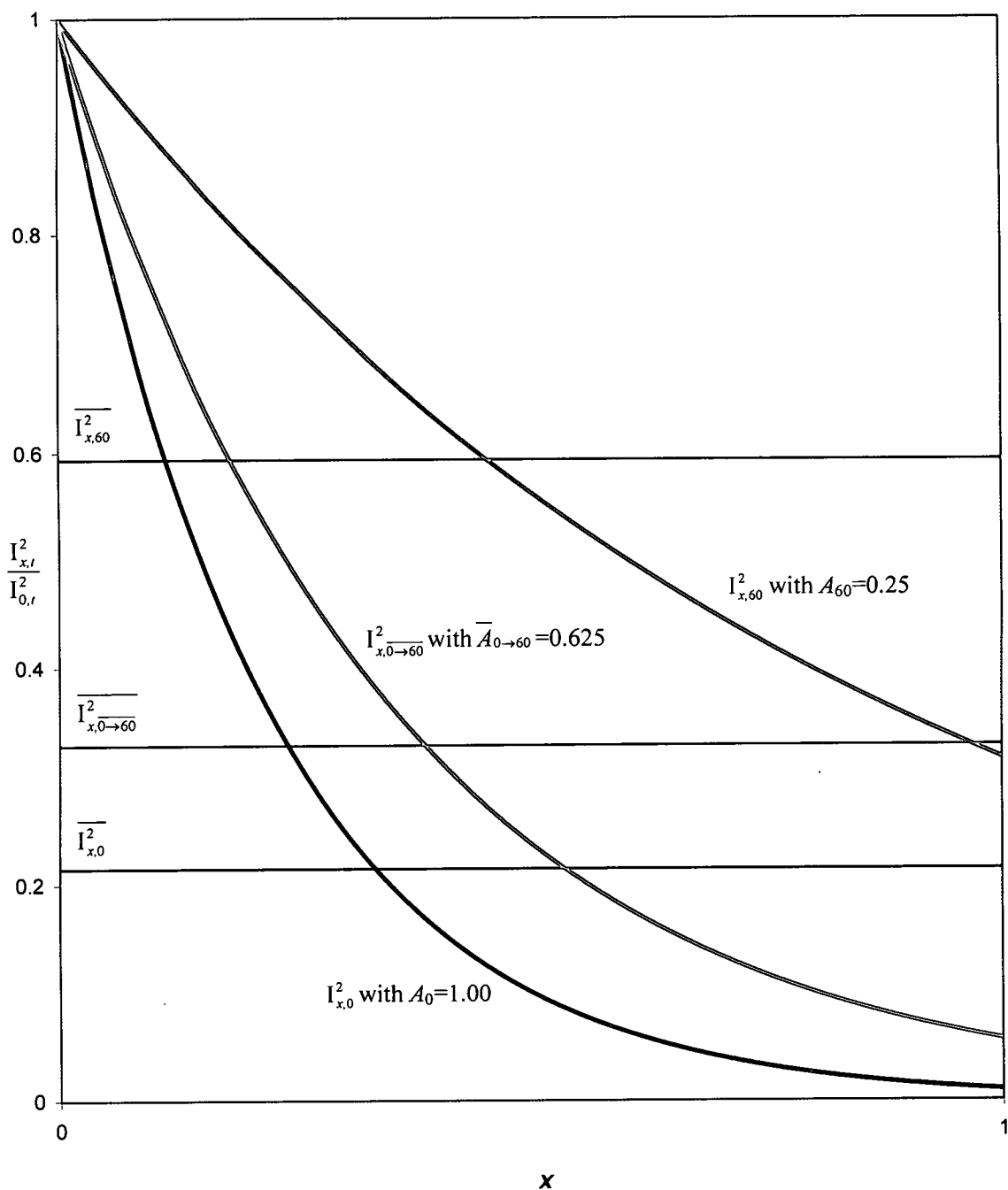


Figure 3. Actinically effective squared intensity $I_{x,t}^2$ (see Equation [11]) and mean actinically effective squared intensity $\overline{I_{x,t}^2}$ (see Equations [15c]) for a representative one-photon absorbing, two-photon reactive system undergoing two-photon induced photodegradation. Beer's law absorbances A_t after t seconds of irradiation are $A_0 = 1.00$, $A_{60} = 0.25$, and $\bar{A} = \left(\frac{A_0 + A_{60}}{2} \right) = 0.625$. Note progressive rise in $I_{x,t}^2$ and $\overline{I_{x,t}^2}$ due to progressive decrease in absorbance with time.

2. Longitudinally-and-Temporally Averaged Intensities and Rates

The longitudinally-and-temporally averaged squared intensity

$$\overline{I_{x,t}^2} = \frac{\int_0^\ell \int_0^t I_{x,t}^2 dx dt}{\int_0^\ell \int_0^t dx dt} = \frac{\int_0^\ell \int_0^t 10^{-2\epsilon c_{x,t} x} I_{0,0}^2 dx dt}{\int_0^\ell \int_0^t dx dt} \quad (13)$$

of laser pulses across the pathlength over an irradiation interval of duration $\Delta t = t$ seconds has no closed form solutions – even for samples which obey simple first order ($c_{x,t} = c_{x,0} e^{-kt}$) or second order ($c_{x,t}^{-1} = c_{x,0}^{-1} + kt$) kinetics. Fortunately, Equation (13) can be solved provided the longitudinal concentration profile is homogeneous across the pathlength. Due to limitations in stirring rates, longitudinally homogeneous concentration profiles during the $10^{-8} - 10^{-9}$ second lifetime of individual laser pulses from our Nd:YAG laser are difficult to attain when samples in rectangular cuvettes are stirred with magnetic stir bars. The assumption of rapid stirring is not unreasonable for multiple pulse irradiation intervals however, since individual pulses are separated by 0.1 second “dark” intervals for our laser, which operates at a repetition rate of 10 Hz.

Under rapid stirring conditions, in which the samples are thoroughly mixed between pulses, the concentration is equal for all x at a given t :

$$c_{x,t} = c_{0,t} \quad . \quad (14a)$$

The concentration over a multiple pulse irradiation interval (duration $\Delta t = t - 0 \gg \tau_{pulse}$) may thus be assumed to be equal to the average of the initial and final concentrations

$$\overline{c} = \frac{c_{0,0} + c_{0,t}}{2} \quad , \quad (14b)$$

and hence to be constant and longitudinally uniform. Inserting Equation (14b) for $c_{x,t}$ in Equation (13) yields

$$\overline{I_{x,t}^2} = \frac{\int_0^\ell \int_0^t 10^{-2\epsilon \bar{c} x} I_{0,0}^2 dx dt}{\int_0^\ell \int_0^t dx dt} \quad (15a)$$

Since \bar{c} is constant for a given irradiation interval, the integrals over x and t are separable so that Equation (15a) reduces to

$$\overline{I_{x,t}^2} = I_{0,0}^2 \frac{\int_0^\ell 10^{-2\epsilon \bar{c} x} dx \int_0^t dt}{\int_0^\ell dx \int_0^t dt} = I_{0,0}^2 \frac{\int_0^\ell 10^{-2\epsilon \bar{c} x} dx}{\ell} \quad (15b)$$

Substituting $e^{2.303}$ for 10 in the rightmost term of Equation (15b) and integrating yields

$$\overline{I_{x,t}^2} = I_{0,0}^2 \frac{\int_0^\ell e^{-4.606\epsilon \bar{c} x} dx}{\ell} = \frac{I_{0,0}^2}{4.606\epsilon \bar{c} \ell} (1 - e^{-4.606\epsilon \bar{c} \ell}) = \frac{(1 - 10^{-2\bar{A}})}{4.606\bar{A}} I_{0,0}^2 \quad (15c)$$

Combining Equations (5), (14), and (15c) we obtain the average concentration

$$\overline{c_{beam}^{**}}_{pulse^{-1}} = b \bar{c} \overline{I_{x,t}^2} = b \bar{c} \frac{(1 - 10^{-2\bar{A}})}{4.606\bar{A}} I_{0,0}^2, \quad (16a)$$

of doubly-excited reactant molecules generated *per pulse* in the beam volume of a one-photon absorbing, two-photon reactive sample during a multiple pulse irradiation interval. By further combining Equation (16a) with Equations (7) – (9), we obtain the average change in reactant concentration per pulse in the total volume

$$-\overline{\Delta c_{tot vol pulse^{-1}}} = \overline{c_{tot vol pulse^{-1}}^{**}} f = \frac{V_{beam}}{V_{tot}} f \overline{c_{beam}^{**}}_{pulse^{-1}} = \frac{V_{beam}}{V_{tot}} f b \bar{c} \frac{(1 - 10^{-2\bar{A}})}{4.606\bar{A}} I_{0,0}^2, \quad (16b)$$

in which f (generally assumed equal to 1; see Equation [8]) is shown for purposes of generality.

The decrease in reactant concentration over the total volume during the entire interval is equal to the product of the total number of pulses $10\Delta t$ in the interval and the average concentration change over the total volume per pulse:

$$-\Delta c_{tot\ vol\ interval^{-1}} = 10\Delta t \cdot \overline{\Delta c_{tot\ vol\ pulse^{-1}}} = 10\Delta t \cdot \frac{V_{beam}}{V_{tot}} f b \bar{c} \frac{(1 - 10^{-2\bar{A}})}{4.606\bar{A}} I_{0,0}^2 \quad (17)$$

The local, instantaneous rate $R_{x,t}$ is not amenable to characterization because the longitudinal concentration profile $c_{x,t}$ is difficult to characterize for all x and t and because infinitesimal irradiation intervals are not experimentally feasible. The intensity dependence may nevertheless be obtained from the *average* rate of photodegradation provided the samples are stirred rapidly enough that $c_{x,t} = \bar{c}$ and $I_{x,t}^2 = \overline{I_{x,t}^2}$. By combining Equations (12b) and (17), we obtain the average rate of photodegradation

$$\overline{R_{x,t}} = -\frac{\Delta c_{tot\ vol\ interval^{-1}}}{\Delta t} = k \bar{c} \overline{I_{x,t}^2} = k \bar{c} \frac{(1 - 10^{-2\bar{A}})}{4.606\bar{A}} I_{0,0}^2 \quad (18)$$

in units of $M\ sec^{-1}$ over a pathlength ℓ and irradiation interval Δt , in which

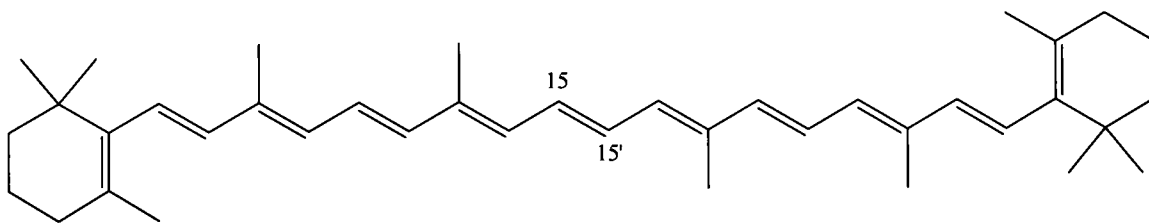
$$k = k_{2h\nu} + k_{post-2h\nu} = 10 \frac{V_{beam}}{V_{tot}} f b = 3.31518 \frac{V_{beam}}{V_{tot}} \tau_{pulse} \delta \quad (19)$$

is a rate constant with units $cm^4\ sec\ photon^{-2} = 1\ GM\ molecule\ photon^{-1}$.^{2,31}

3. Normalized Average Rates for Intensity Dependence of β -Carotene

Photodegradation

$\beta C-CCl_4$ solutions lose color rapidly upon irradiation with intense 532 nm laser pulses, but extremely slowly upon irradiation with low intensity 532 nm light and in the dark.



More specifically, we find that $k_{2h\nu} \sim 1,000 k_{post-2h\nu} \gg k_{1h\nu} \sim k_{post-1h\nu} \sim k_{0h\nu} \sim 0$ (see Equations [12]), indicating that the photodegradation originates principally from biphotonic light reactions, with small contributions from biphotonically-initiated thermal reactions and essentially no contributions from monophotonic, monophotonically-initiated thermal, or dark thermal reactions. The post- $2h\nu$ thermal reactions are probably mediated by long-lived ($\tau > \tau_{pulse}$) free radicals which originate from reactions between doubly-excited β C and solvent (see Figure 5 and *Results*). Accordingly, the photodegradation rate is given by a rate law of the form of Equation (18).

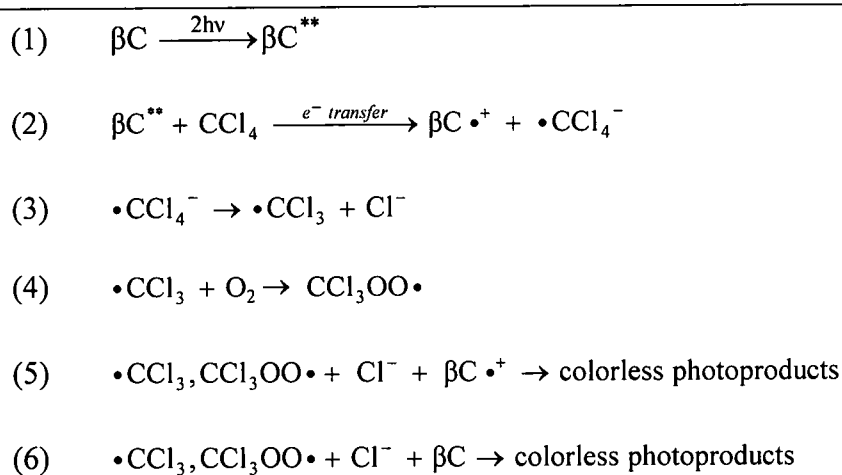


Figure 5. Proposed β -carotene-to-solvent photoinduced electron transfer (PET) mechanism. While recent studies indicate that the photodegradation of β -carotene in CCl_4 proceeds via Reactions 1-6 above, the stoichiometric and structural details of Reactions 5 and 6 are not yet known.

Because the solvent acts as a reactant (see Figure 4), the average rates of photodegradation of βC in terms of $\overline{I_{x,t}^{n_{x,t}}} = \left(\sqrt[n_{x,t}]{I_{x,t}^{n_{x,t}}} \right)^{n_{x,t}}$ and $I_{0,0}^{n_{0,0}}$ are given in units of sec^{-1}

M by

$$\overline{R_{x,t}} = - \frac{\Delta c_{\text{tot vol interval}}^{-1}}{\Delta t} = \tilde{k} c_{\text{CCl}_4} \bar{c} \left(\sqrt[n_{x,t}]{I_{x,t}^{n_{x,t}}} \right)^{n_{x,t}} \quad (20a)$$

and

$$\overline{R_{0,0}} = - \frac{\Delta c_{\text{tot vol interval}}^{-1}}{\Delta t} = \tilde{k} c_{\text{CCl}_4} \bar{c} I_{0,0}^{n_{0,0}}, \quad (20b)$$

respectively, in which \tilde{k} is an n^{th} -order rate constant with units of $\text{M}^{-1} \text{ photon}^{-n} \text{ cm}^{2n} \text{ sec}^{n-1}$, $n_{x,t} \sim n_{0,0} \sim 2$ are the numbers of photons absorbed by individual βC molecules, and $\Delta t \gg \tau_{\text{pulse}}$ is the duration in seconds of a multiple pulse irradiation interval. Since the concentration of solvent ($c_{\text{CCl}_4} = 10.3 \text{ M}$ at 25°C) vastly exceeded the maximum initial concentration of the solute ($c_{\beta\text{C}}^{\text{initial}} = 2.5 \times 10^{-4} \text{ M}$), our samples obeyed pseudo-first order kinetics. Equations (20) thus reduce to

$$\overline{R_{x,t}} = - \frac{\Delta c_{\text{tot vol interval}}^{-1}}{\Delta t} = \bar{k} \bar{c} \left(\sqrt[n_{x,t}]{I_{x,t}^{n_{x,t}}} \right)^{n_{x,t}} \quad (21a)$$

and

$$\overline{R_{0,0}} = - \frac{\Delta c_{\text{tot vol interval}}^{-1}}{\Delta t} = \bar{k} \bar{c} I_{0,0}^{n_{0,0}}, \quad (21b)$$

in which $\bar{k} = \tilde{k} c_{\text{CCl}_4}$ is a pseudo-first order rate constant accounting for the combined contributions from n^{th} -order light and post- n^{th} -order thermal reactions to the photodegradation (see Equation [19]) with units of $\text{photon}^{-n} \text{ cm}^{2n} \text{ sec}^{n-1}$.

For accurate assessment of $n_{x,t}$ and $n_{0,0}$ the rate laws must be normalized to the average concentration and to the actinic dose. Accordingly, we divide Equations (21a)

and (21b) by $\bar{c} = \frac{\overline{A_{532}}}{\varepsilon_{532} \ell}$ and by ${}^{n_{x,t}}\sqrt{I_{x,t}} \cdot \tau_{pulse} \cdot 10$ and $I_{0,0} \cdot \tau_{pulse} \cdot 10$, respectively, to

yield the average rates

$$\begin{aligned}
 \overline{R'_{x,t}} &= \frac{\overline{R_{x,t}}}{\bar{c} \cdot \left({}^{n_{x,t}}\sqrt{I_{x,t}} \cdot \tau_{pulse} \cdot 10 \right)} = - \frac{\Delta c_{tot \text{ vol interval}^{-1}}}{\bar{c} \cdot \left({}^{n_{x,t}}\sqrt{I_{x,t}} \cdot \tau_{pulse} \cdot 10 \Delta t \right)} \\
 &= - \frac{\Delta A_{532}}{\overline{A_{532}} \cdot \left({}^{n_{x,t}}\sqrt{I_{x,t}} \cdot \tau_{pulse} \cdot 10 \Delta t \right)} = \frac{\bar{k} \left({}^{n_{x,t}}\sqrt{I_{x,t}} \right)^{n_{x,t}-1}}{\tau_{pulse} \cdot 10} \\
 &= \bar{k}' \left({}^{n_{x,t}}\sqrt{I_{x,t}} \right)^{n_{x,t}-1} \tag{22a}
 \end{aligned}$$

and

$$\begin{aligned}
 \overline{R'_{0,0}} &= \frac{\overline{R_{0,0}}}{\bar{c} \cdot (I_{0,0} \cdot \tau_{pulse} \cdot 10)} = - \frac{\Delta c_{tot \text{ vol interval}^{-1}}}{\bar{c} \cdot (I_{0,0} \cdot \tau_{pulse} \cdot 10 \Delta t)} \\
 &= - \frac{\Delta A_{532}}{\overline{A_{532}} \cdot (I_{0,0} \cdot \tau_{pulse} \cdot 10 \Delta t)} = \frac{\bar{k} I_{0,0}^{n_{0,0}-1}}{\tau_{pulse} \cdot 10} \\
 &= \bar{k}' I_{0,0}^{n_{0,0}-1} \tag{22b}
 \end{aligned}$$

in units of $\text{cm}^2 \text{ photon}^{-1}$ normalized to the actinic doses²⁵ and to the changes in

concentration, in which $\Delta A_{532} = \varepsilon_{532} \ell \Delta c_{tot \text{ vol interval}^{-1}}$, the factor of 10 carries units of pulse

sec^{-1} , $\tau_{pulse} = 6.5 \times 10^{-9} \text{ sec}$, and the rate constants $\bar{k}' = 1.54 \times 10^7 \bar{k}$ have units of photon^{-n}

$\text{cm}^{2n} \text{ sec}^{n-1}$.

The intensity dependence is obtained from Equations (22a) and (22b) by plotting the logarithms of the normalized rates vs. the logarithms of the intensities, yielding lines with intercepts of $\log_{10} \bar{k}'$ and slopes of $n_{x,t} - 1$ and $n_{0,0} - 1$, respectively: *i.e.*,

$$\log_{10} \overline{R'_{x,t}} = (n_{x,t} - 1) \log_{10} \sqrt[n_{x,t}]{I_{x,t}} + \log_{10} \bar{k}' \quad (23a)$$

and

$$\log_{10} \overline{R'_{0,0}} = (n_{0,0} - 1) \log_{10} I_{0,0} + \log_{10} \bar{k}' \quad (23b)$$

Slopes of unity in Equations (23) are indicative of quadratic intensity dependence, and hence are diagnostic of simultaneous two-photon or sequential biphotonic processes.^{25,30,31}

For a two-point comparison, Equations (23) can be rearranged to

$$n_{x,t} = \frac{\log_{10} \overline{R'_{x,t,H}} - \log_{10} \overline{R'_{x,t,L}}}{\log_{10} \sqrt[n_{x,t}]{I_{x,t,H}} - \log_{10} \sqrt[n_{x,t}]{I_{x,t,L}}} + 1 \quad (24a)$$

and

$$n_{0,0} = \frac{\log_{10} \overline{R'_{0,0,H}} - \log_{10} \overline{R'_{0,0,L}}}{\log_{10} I_{0,0,H} - \log_{10} I_{0,0,L}} + 1 \quad (24b)$$

CHAPTER III

EXPERIMENTAL

A. Purification of β -Carotene

A 22 mm i.d. flash liquid chromatography column was packed with ~9 inches of flash grade silica gel (Silica Gel 60, 0.040-0.063 mm particle size, 230-400 mesh; EM Science) in benzene (Alfa Aesar, 99.0%). The column was loaded with 10 mL of a solution of benzene (Alfa Aesar, 99.0%) containing 0.15g all-*trans*- β -carotene (95%, Aldrich). A mobile phase of benzene was then pushed through the column with a positive pressure of N₂ gas sufficient to generate a collection rate of ~1-2 drops sec⁻¹. Immobile maroon impurities remained at the top of the column. Purified β C was isolated as a band with a well-defined, dark orange leading edge and a less defined, yellow-orange trailing edge. Excess solvent was removed by a stream of N₂ gas, leaving purified β C as a dark maroon powder on the bottom of the collection vessel. The β C powder was then stored in the dark in vials under nitrogen or argon at $T \leq -20^{\circ}\text{C}$.

β C purifications were performed under dim red light to minimize photodegradation which might result from exposure to the short wavelength components of ambient light. The only exposure of the samples to white light occurred when a flashlight was used to facilitate identification of the bands as they came off of the column.

B. Preparation of β -Carotene Solutions

Concentrated solutions of β C ($4.9 - 24 \times 10^{-5}$ M, for which $A_{532} = 0.2 - 1.0$ since $\epsilon_{532} = 3,630 \pm 100 \text{ M}^{-1} \text{ cm}^{-1}$)⁴² were prepared by dissolving purified β C in CCl_4 (HPLC grade, Aldrich). The photodegradation rate was obtained by monitoring the decrease in A_{532} , as the absorbance was too high to permit usage of Beer's Law at the absorption maximum ($A_{463} = 5.6 - 27.6$ for $4.9 - 24 \times 10^{-5}$ M solutions since $\epsilon_{463} = 107,000 \pm 3,550 \text{ M}^{-1} \text{ cm}^{-1}$).⁴² All spectra were obtained with a Hewlett-Packard 8453 Photodiode Array Spectrophotometer interfaced to a personal computer with Agilent Chemstation software.

C. Characterization of Intensity Dependence of β -carotene Photodegradation

Solutions of β C in CCl_4 were irradiated with 532 nm pulses from a Quanta-Ray Model INDI-40 Pulsed Nd:YAG laser (0.9 cm beam diameter; ~ 6.5 ns pulse width) operating in TEM_{00} mode at $10 \text{ pulse sec}^{-1}$ with actinic intensities ranging from $0.12 - 9.60 \text{ MW cm}^{-2}$ ($0.5 - 40 \text{ mJ pulse}^{-1}$). To ensure that the intensity was modulated without changing the temporal or cross sectional profiles of the pulses – which could lead to spurious values of n and δ_{532} – the laser was always operated at full flashlamp energy. Beam intensities below the two-photon saturation threshold of $\sim 2.5 \text{ MW cm}^{-2}$ (see Figure 6) were generated by attenuating the beam to 10% of its full intensity with a 10%-reflective beam sampler (Newport Model 10B20NC.1) which was antireflection coated on the back surface to eliminate ghosting and wedged at an angle of 30 ± 15 arc min to eliminate internal fringes. Prior to entering the sample, the 90%-attenuated beam was further attenuated to the desired intensity by rotating the angle of a $\frac{1}{2}$ -wave plate (Thorlabs Model WPMH05M-532) with respect to a Glan laser calcite polarizer (Thorlabs Model GL10-A). The intensities were characterized by inserting a Newport

Model 818P-020-12 Power Detector coupled to a Newport Model 1918-C Power Meter between the polarizer and sample cuvette holder prior to irradiation sessions. Pulses with intensities greater than 2.5 MW cm^{-2} – which were required to characterize the two-photon saturation threshold – were generated by replacing the 10%-reflective beam sampler with a 100%-reflective prism (Newport Model 10SR20). A complete schematic diagram of the intensity-controlled laser irradiation system is shown in Figure 6.

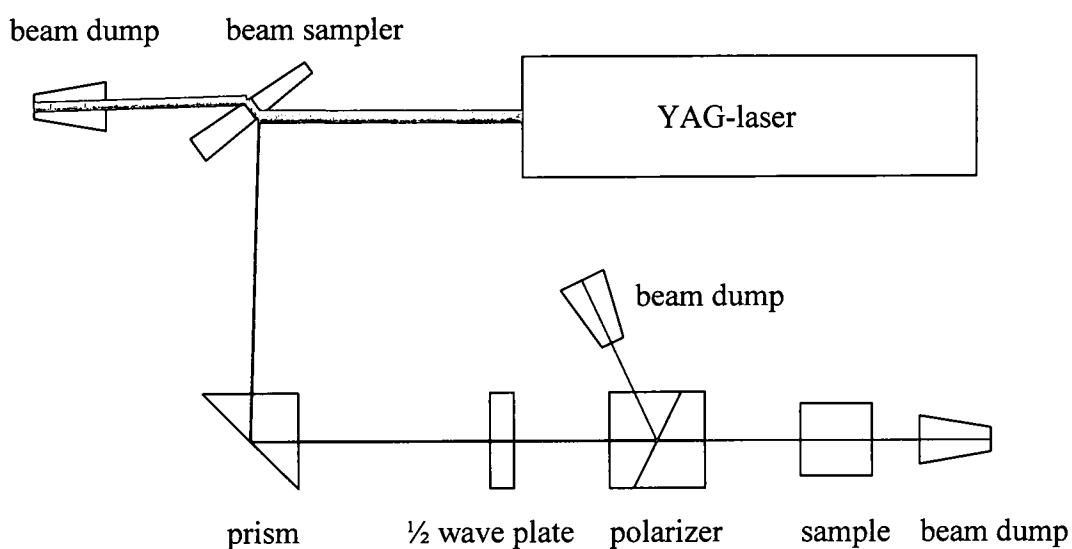


Figure 6. Schematic diagram of the intensity-controlled laser irradiation system in our laboratory.

During irradiation samples were stirred with a magnetic Starna “Spinette” stirrer, and sample temperatures were maintained at $22.5^{\circ}\pm 0.5^{\circ} \text{ C}$ with a Fisher Scientific Model 9500 constant temperature circulator; room temperatures were maintained at $22.5\pm 0.5^{\circ}\text{C}$ to prevent temperature change during transfer of the sample cuvette between the irradiation cuvette holder and the spectrophotometer cuvette holder.

For pulse energies ≥ 2 mJ, the rate of photodegradation was fast enough that A_{532} decreased from the outset of irradiation. However, induction periods of ≤ 30 seconds and ≤ 10 seconds were observed before the absorbance began to decrease when the samples were irradiated with 0.5 mJ and 1 mJ pulses, respectively. These induction periods are consistent with investigations by other researchers,⁶²⁻⁶⁴ who reported significant initial increases in absorbance for β C solutions under oxidizing conditions which Glória, *et. al.* speculatively ascribed to carotenoid oxidation products with extinction coefficients exceeding those of β C.^{62,65}

To characterize the intensity dependence of UV-induced β C photodegradation, we used a mercury arc lamp (Newport Model 6281) with a 313 nm filter (Newport Model O017-06). The mercury lamp was operated at 100 W and gave intensity at 313 nm of 0.012 W (measured with the same power meter we used for laser intensity measurement). Attenuation was obtained by placing different numbers of microscope slides (VWR Model 48312-002) in front of the cuvette. Each slide has a 69.7% transmittance at 313 nm.

The absorption spectrum of β C in CCl_4 is shown in Figure 7. Overlaid spectra illustrating the photodegradation of β C (*i.e.*, the decrease in intensity of the visible band with the concomitant generation of a broad band centered near 350 nm) induced by intense 532 nm laser pulses and low intensity ultraviolet light (UV light, $\lambda < 400$ nm) from a 100 watt Hg lamp are presented in Figure 8.

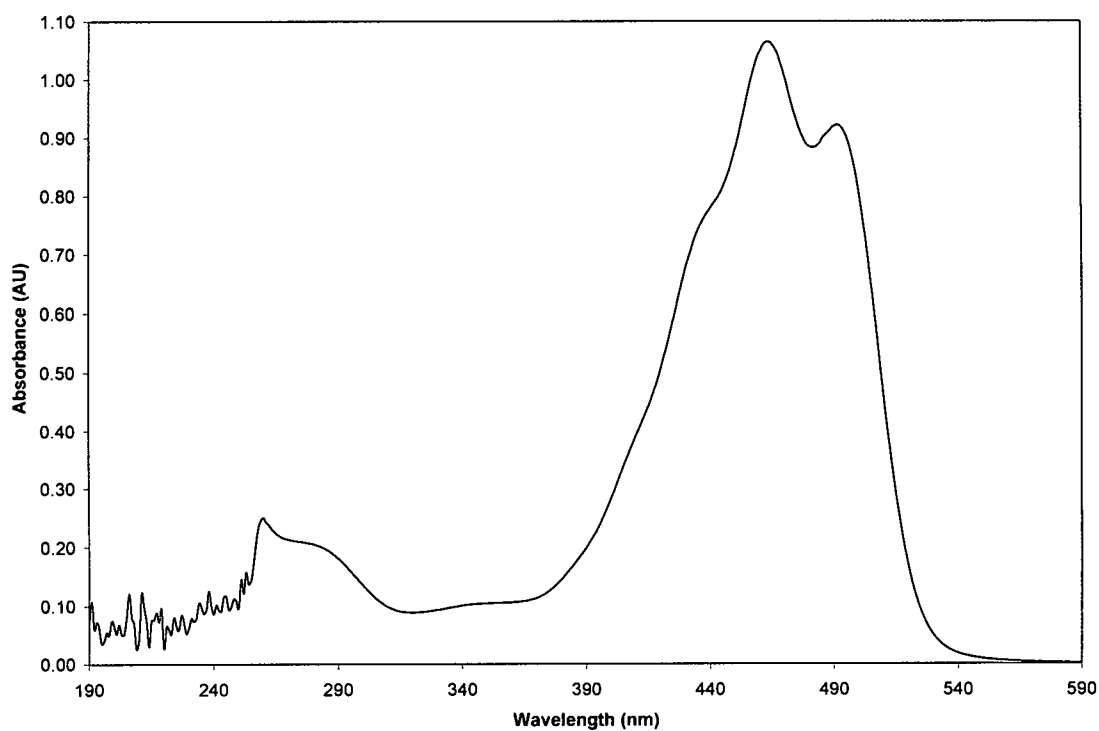


Figure 7. Spectrum of β -carotene in CCl_4 solvent.

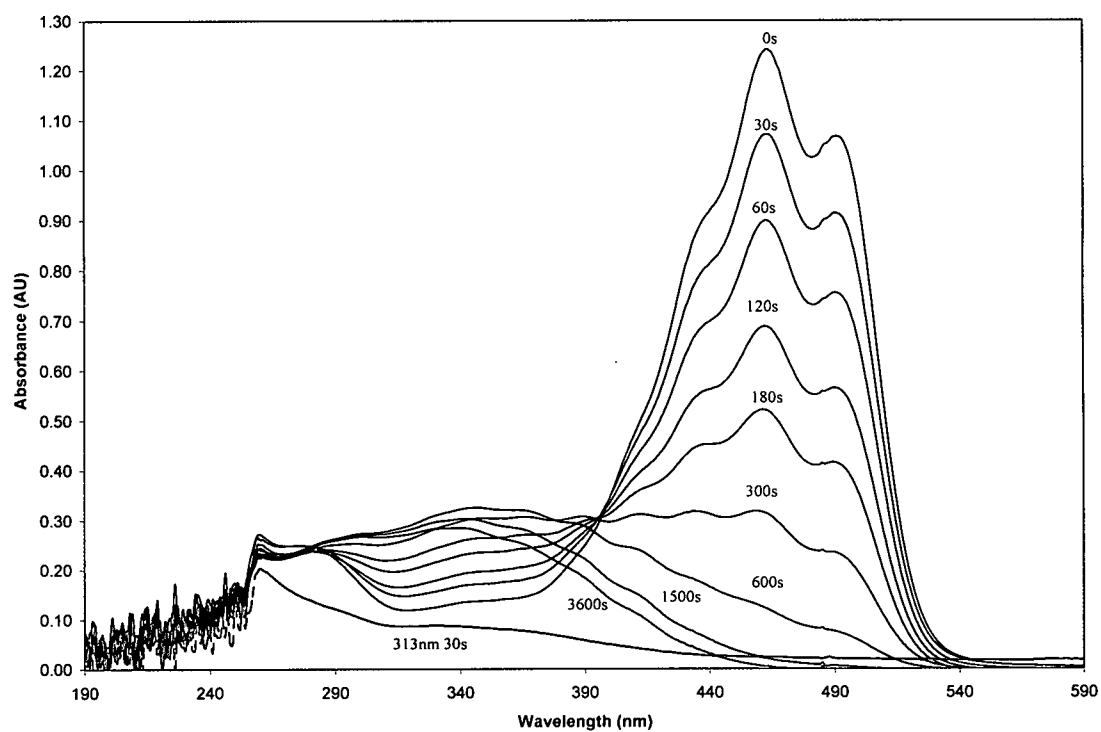


Figure 8. Conversion of βC to P_{350} photoproducts induced by 2 mJ pulse^{-1} , 532 nm pulses from a Nd:YAG laser operating at 10 Hz for 3600 seconds , followed by irradiation with the 313 nm line from Hg lamp for 30 seconds .

D. Impact of Deuterium Lamp on β -Carotene Photodegradation

Since β C photodegrades under diffuse UV light, we were concerned that it would be degraded by the UV light coming out of the deuterium (D_2) lamp on the photodiode array spectrophotometer when we measured its absorbance. To test this, we prepared β C solutions of two different concentrations, $A_{532} = 1.0$ and $A_{532} = 0.2$, and took spectra of these solutions every 30 seconds for 10 minutes with the D_2 lamp on and off respectively. Overlaid spectra are shown in Figures 9 and 10. As is clearly seen, the absorption spectra of neither the $A_{532} = 1.0$ sample nor the $A_{532} = 0.2$ samples are changed when D_2 lamp is off. On the other hand, when the D_2 lamp is on, their absorbance rises in the range from 300 nm to 380 nm, corresponding to the formation of " P_{350} " β C photoproducts (see Results and Discussion). Although the absorbance drops ΔA_{532} caused by the D_2 lamp were small (0.26% per measurement for $A_{532} = 1.0$ sample and 0.69% per measurement for $A_{532} = 0.2$ sample), we obtained spectra with the D_2 lamp off when measuring absorbance at wavelengths longer than 400 nm, since the tungsten lamp alone was intense enough to give accurate measurements in the visible region.

Note the isosbestic point near 400 nm in the bottom one of Figure 10, suggesting that only one photoproduct (the pentaene-like " P_{350} " product; see Results and Discussion) is generated during the early stages of photodegradation.

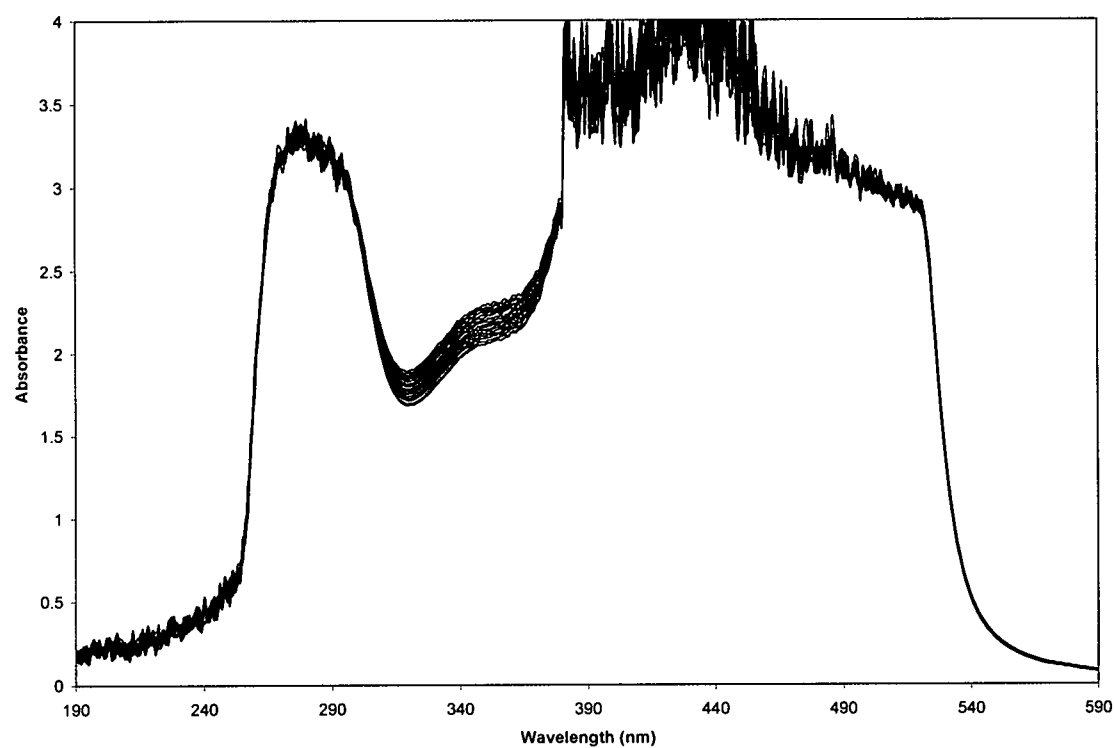
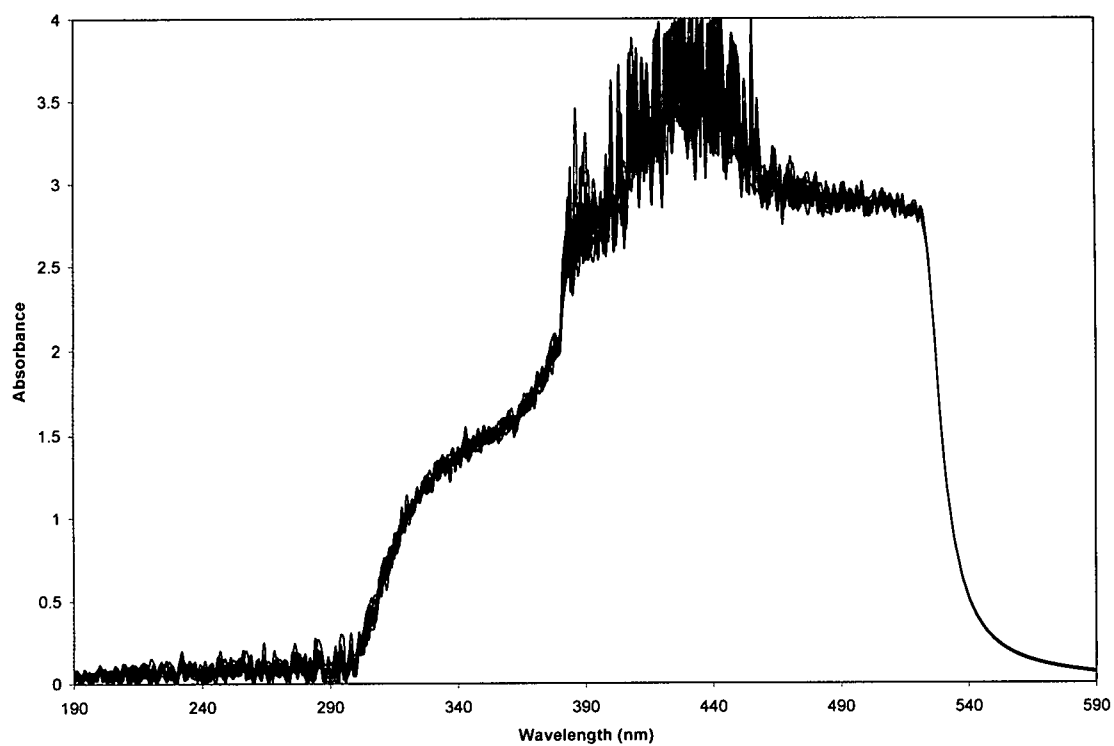


Figure 9. Spectra of β C solution ($A_{532} = 1.0$) with D₂ lamp off (top) and on (bottom).

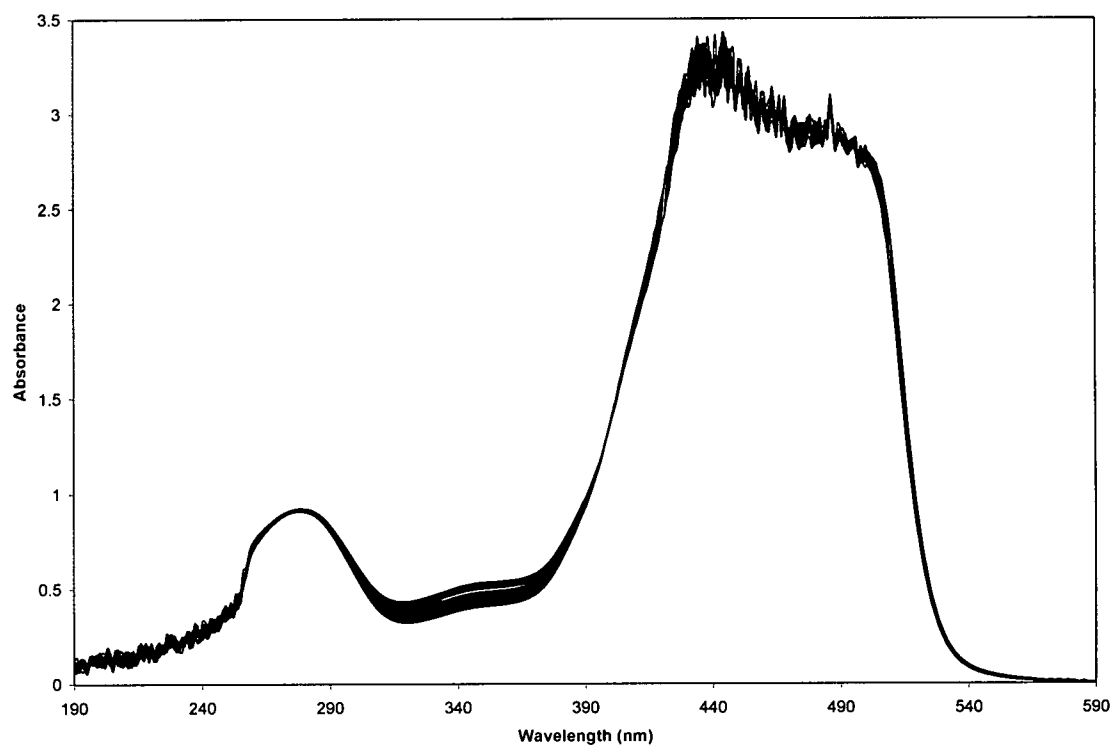
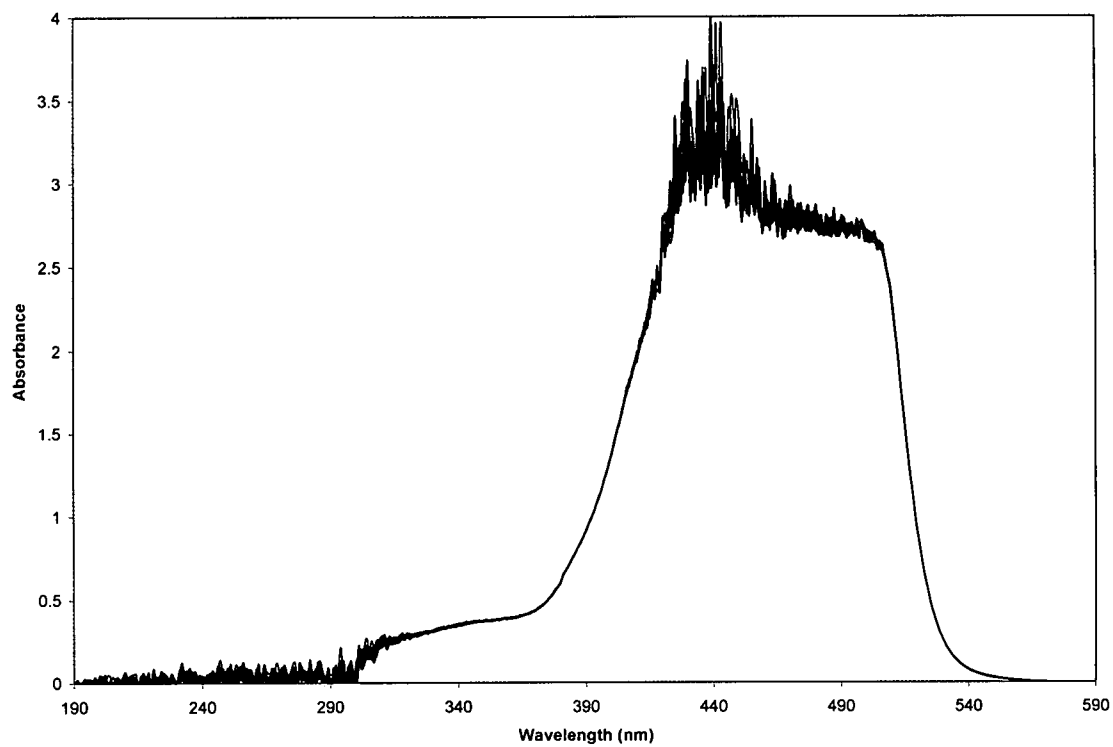


Figure 10. Spectra of β C solution ($A_{532} = 0.2$) with D₂ lamp off (top) and on (bottom).

E. Data Analysis

1. The method of 56 pairs

According to Equations (23) and (24), we always compared the reaction rate of two or more different intensities (HI vs. LI). It would be unreasonable to just randomly pick two reactions to compare, therefore, we divided all of our irradiation runs into three groups and ten subgroups: identical irradiation intervals ($\Delta t = 45\text{s}$, $\Delta t = 90\text{s}$, $\Delta t = 180\text{s}$), identical actinic doses ($I\Delta t = 0.9\text{J}$, $I\Delta t = 1.8\text{J}$, $I\Delta t = 3.6\text{J}$) and identical absorbance drop percentages ($\Delta A/\bar{A} = 5\%$, $\Delta A/\bar{A} = 10\%$, $\Delta A/\bar{A} = 20\%$, $\Delta A/\bar{A} = 50\%$). Only the reactions that fell into the same subgroups were compared. Since we used solutions with two different initial absorbance ($A_{532}^{\text{initial}} \sim 1.0$ and $A_{532}^{\text{initial}} \sim 0.20$, which we designated as HA and LA respectively), there were 4 different scenarios: HA – HI vs. HA – LI, LA – HI vs. LA – LI, LA – HI vs. HA – LI and HA – HI vs. LA – LI. Eight different laser intensities were utilized in our intensity dependence experiments: 0.121, 0.242, 0.363, 0.484, 0.605, 0.725, 0.967 and 1.21 MW cm⁻² (0.5, 1.0, 1.5, 2.0, 2.5, 3.0, 4.0 and 5.0 mJ pulse⁻¹); hence there were 28 pairs of individual HI-LI comparison (binomial coefficient $C_8^2 = 28$) of each scenario and a total of 56 pairs from two successive days. For each pair, we used Equations (22) and (24) to calculate n values, took the average of 56 n values (see Appendix) and reported in Tables II.

2. The method of least squares

In addition to the method of 56 pairs we stated above, we also used the method of least squares on the identical initial absorbance scenarios (HA – HI vs. HA – LI and LA – HI vs. LA – LI). For each scenario, we performed the least squares fit on 16 points (8

points on each day) of $\log_{10} \overline{R'_{0,0}}$ vs. $\log_{10} I_{0,0}$ and $\log_{10} \overline{R'_{x,t}}$ vs. $\log_{10} \sqrt[n_{x,t}]{I_{x,t}}$ (see Equations [23]) in *Excel* spreadsheet. Slopes ($n_{x,t} - 1$ and $n_{0,0} - 1$) and their standard deviations s_m were automatically generated by *Excel* (see Tables III).

3. Rejection of bad points

We rejected “bad” points – which were more than 3 standard deviations from the mean on the results of the method of 56 pairs. HA - HI vs. HA - LI scenario of $I\Delta t = 3.6$ J is shown below as a step-by-step example. As in the standard statistical analysis, we calculated average n value $\bar{n}_{pre-rejection}$ and standard deviation $s_{pre-rejection}$ for the full data set prior to the rejection of any data points.

HA - HI vs. HA - LI	$n_{0,0}$		$n_{x,t}$	
HA - 0.242 vs. HA - 0.121	2.138	1.779	1.990	1.819
HA - 0.363 vs. HA - 0.121	1.790	1.789	1.747	1.736
HA - 0.363 vs. HA - 0.242	1.196	1.807	1.272	1.612
HA - 0.484 vs. HA - 0.121	1.941	1.820	1.908	1.783
HA - 0.484 vs. HA - 0.242	1.743	1.861	1.816	1.750
HA - 0.484 vs. HA - 0.363	2.515	1.938	2.544	1.972
HA - 0.605 vs. HA - 0.121	1.854	1.743	1.810	1.693
HA - 0.605 vs. HA - 0.242	1.639	1.715	1.662	1.605
HA - 0.605 vs. HA - 0.363	1.990	1.643	1.946	1.599
HA - 0.605 vs. HA - 0.484	1.315	1.263	1.232	1.164
HA - 0.725 vs. HA - 0.121	1.900	1.736	1.832	1.701
HA - 0.725 vs. HA - 0.242	1.751	1.709	1.727	1.631
HA - 0.725 vs. HA - 0.363	2.075	1.652	1.964	1.644
HA - 0.725 vs. HA - 0.484	1.763	1.449	1.595	1.419
HA - 0.725 vs. HA - 0.605	2.311	1.676	2.008	1.779
HA - 0.967 vs. HA - 0.121	1.881	1.820	1.802	1.763
HA - 0.967 vs. HA - 0.242	1.753	1.840	1.704	1.737
HA - 0.967 vs. HA - 0.363	1.983	1.854	1.861	1.792
HA - 0.967 vs. HA - 0.484	1.763	1.819	1.606	1.723
HA - 0.967 vs. HA - 0.605	1.975	2.084	1.776	1.999
HA - 0.967 vs. HA - 0.725	1.763	2.342	1.620	2.118
HA - 1.21 vs. HA - 0.121	1.858	1.799	1.788	1.743
HA - 1.21 vs. HA - 0.242	1.738	1.808	1.697	1.713
HA - 1.21 vs. HA - 0.363	1.920	1.808	1.825	1.750
HA - 1.21 vs. HA - 0.484	1.734	1.767	1.617	1.685
HA - 1.21 vs. HA - 0.605	1.869	1.929	1.740	1.860
HA - 1.21 vs. HA - 0.725	1.711	2.020	1.635	1.885
HA - 1.21 vs. HA - 0.967	1.644	1.605	1.656	1.562
$\bar{n}_{pre-rejection}$	1.814		1.743	
$s_{pre-rejection}$	0.226		0.208	

Table I-A. Data set of $I\Delta t = 3.6$ J, HA - HI vs. HA - LI scenario before a “bad” point rejection.

Points that lay $3s_{pre-rejection}$ or more away from $\bar{n}_{pre-rejection}$ were rejected (the rejected points are designated by a strikethrough) and $N_{post-rejection}$ is the number of data points remaining after rejection. Generally no more than 3 of the original 56 data points

were rejected (i.e., $56 \geq N_{\text{post-rejection}} \geq 53$). A new average $\bar{n}_{\text{post-rejection}}$ and a new standard deviation $s_{\text{post-rejection}}$ were calculated.

HA - HI vs. HA - LI	$n_{0,0}$		$n_{x,t}$	
HA - 0.242 vs. HA - 0.121	2.138	1.779	1.990	1.819
HA - 0.363 vs. HA - 0.121	1.790	1.789	1.747	1.736
HA - 0.363 vs. HA - 0.242	1.196	1.807	1.272	1.612
HA - 0.484 vs. HA - 0.121	1.941	1.820	1.908	1.783
HA - 0.484 vs. HA - 0.242	1.743	1.861	1.816	1.750
HA - 0.484 vs. HA - 0.363	2.515	1.938	2.544	1.972
HA - 0.605 vs. HA - 0.121	1.854	1.743	1.810	1.693
HA - 0.605 vs. HA - 0.242	1.639	1.715	1.662	1.605
HA - 0.605 vs. HA - 0.363	1.990	1.643	1.946	1.599
HA - 0.605 vs. HA - 0.484	1.315	1.263	1.232	1.164
HA - 0.725 vs. HA - 0.121	1.900	1.736	1.832	1.701
HA - 0.725 vs. HA - 0.242	1.751	1.709	1.727	1.631
HA - 0.725 vs. HA - 0.363	2.075	1.652	1.964	1.644
HA - 0.725 vs. HA - 0.484	1.763	1.449	1.595	1.419
HA - 0.725 vs. HA - 0.605	2.311	1.676	2.008	1.779
HA - 0.967 vs. HA - 0.121	1.881	1.820	1.802	1.763
HA - 0.967 vs. HA - 0.242	1.753	1.840	1.704	1.737
HA - 0.967 vs. HA - 0.363	1.983	1.854	1.861	1.792
HA - 0.967 vs. HA - 0.484	1.763	1.819	1.606	1.723
HA - 0.967 vs. HA - 0.605	1.975	2.084	1.776	1.999
HA - 0.967 vs. HA - 0.725	1.763	2.342	1.620	2.118
HA - 1.21 vs. HA - 0.121	1.858	1.799	1.788	1.743
HA - 1.21 vs. HA - 0.242	1.738	1.808	1.697	1.713
HA - 1.21 vs. HA - 0.363	1.920	1.808	1.825	1.750
HA - 1.21 vs. HA - 0.484	1.734	1.767	1.617	1.685
HA - 1.21 vs. HA - 0.605	1.869	1.929	1.740	1.860
HA - 1.21 vs. HA - 0.725	1.711	2.020	1.635	1.885
HA - 1.21 vs. HA - 0.967	1.644	1.605	1.656	1.562
$\bar{n}_{\text{pre-rejection}}$	1.814		1.743	
$s_{\text{pre-rejection}}$	0.226		0.208	
$\bar{n}_{\text{post-rejection}}$	1.801		1.729	
$s_{\text{post-rejection}}$	0.206		0.179	

Table I-B. Data set of $I\Delta t = 3.6$ J, HA - HI vs. HA - LI scenario after a “bad” point rejection.

4. 95% confidence limits (λ_{95})

For both methods, we obtained a statistical property 95% confidence limits (λ_{95}) to evaluate the n values we got. For the method of 56 points,

$$\lambda_{95} = \frac{t_{95\%}(55 \text{ degrees of freedom}) \times s_{\text{post-rejection}}}{\sqrt{N_{\text{post-rejection}}}} = \frac{2.00 \times s_{\text{post-rejection}}}{\sqrt{N_{\text{post-rejection}}}}. \quad (25a)$$

For the method of least squares,

$$\lambda_{95} = t_{95\%}(15 \text{ degrees of freedom}) \times s_m = 2.13 \times s_m. \quad (25b)$$

The difference between the two equations originates from the fact that the inverse dependence on the number of data points is already implicit in s_m .

5. Full error propagation (ϵ) of n

a. Experimental sources of errors

Errors lie in our measurements of absorbance, time and intensity. To determine errors in absorbance $\epsilon(A)$, we prepared one high absorbance β C solution ($A_{532} = 1.0$) and one low absorbance β C solution ($A_{532} = 0.2$), took 20 measurements of each solution, and calculated their average absorbance and standard deviation. The standard deviation to average ratio was 0.35% for high A_{532} solutions and 0.46% for low A_{532} solutions. We defined the error in absorbance as follows: for each high A_{532} run, $\epsilon(A_H) = \bar{A}_H * \pm 0.35\%$ and for each low A_{532} run, $\epsilon(A_L) = \bar{A}_L * \pm 0.46\%$. For our time measurements, we operated the laser and the stopwatch simultaneously to the best of our ability; all errors in time, $\epsilon(t)$ originated from the lack of perfect synchronization between stopping and starting the laser and stopwatch and were assumed to be equal to ± 0.2 s. Errors in entry intensity $\epsilon(I_{0,0})$ were assumed to be equal to the minimum scale of the power meter: 0.001 W.

b. Full Error propagation (ε).

Let the desired result be designated by F , and let the directly measured quantities be designated by $x, y, z \dots$. The formula for F will be written as $F = f(x, y, z \dots)$. Then random errors in F are equal to

$$\varepsilon(F)^2 = \left(\frac{\partial F}{\partial x}\right)^2 \varepsilon(x)^2 + \left(\frac{\partial F}{\partial y}\right)^2 \varepsilon(y)^2 + \left(\frac{\partial F}{\partial z}\right)^2 \varepsilon(z)^2 + \dots \quad (26)$$

assuming that x, y, z are independent variables.

From Equations (22b) and (24b), we obtained

$$n_{0,0} - 1 = \frac{\log \frac{\frac{\Delta A_H}{A_H} \frac{I_{0,0L}}{I_{0,0H}} \frac{\Delta t_L}{\Delta t_H}}{\frac{\Delta A_L}{A_L}}}{\log \frac{I_{0,0H}}{I_{0,0L}}} = \frac{\log \frac{\Delta A_H \overline{A_L} I_{0,0L} \Delta t_L}{\Delta A_L A_H I_{0,0H} \Delta t_H}}{\log \frac{I_{0,0H}}{I_{0,0L}}} \quad (27)$$

Taking the derivatives of $n_{0,0}-1$ with respect to each of the independent variables, we obtained

$$\frac{\partial(n_{0,0} - 1)}{\partial A_{iH}} = \frac{1}{2.303 \log \frac{I_{0,0H}}{I_{0,0L}}} \left(\frac{1}{\Delta A_H} - \frac{1}{2A_H} \right) \quad (28a)$$

$$\frac{\partial(n_{0,0} - 1)}{\partial A_{fH}} = \frac{-1}{2.303 \log \frac{I_{0,0H}}{I_{0,0L}}} \left(\frac{1}{\Delta A_H} + \frac{1}{2A_H} \right) \quad (28b)$$

$$\frac{\partial(n_{0,0} - 1)}{\partial A_{iL}} = \frac{-1}{2.303 \log \frac{I_{0,0H}}{I_{0,0L}}} \left(\frac{1}{\Delta A_L} - \frac{1}{2A_L} \right) \quad (28c)$$

$$\frac{\partial(n_{0,0} - 1)}{\partial A_{fL}} = \frac{1}{2.303 \log \frac{I_{0,0H}}{I_{0,0L}}} \left(\frac{1}{\Delta A_L} + \frac{1}{2A_L} \right) \quad (28d)$$

$$\frac{\partial(n_{0,0} - 1)}{\partial I_{0,0H}} = \frac{1}{2.303 I_{0,0H} \log^2 \frac{I_{0,0H}}{I_{0,0L}}} \log \frac{\Delta A_H \overline{A_L} \Delta t_L}{\Delta A_L \overline{A_H} \Delta t_H} \quad (29a)$$

$$\frac{\partial(n_{0,0} - 1)}{\partial I_{0,0L}} = \frac{-1}{2.303 I_{0,0L} \log^2 \frac{I_{0,0H}}{I_{0,0L}}} \log \frac{\Delta A_H \overline{A_L} \Delta t_L}{\Delta A_L \overline{A_H} \Delta t_H} \quad (29b)$$

$$\frac{\partial(n_{0,0} - 1)}{\partial \Delta t_H} = \frac{-1}{2.303 \Delta t_H \log \frac{I_{0,0H}}{I_{0,0L}}} \quad (30a)$$

$$\frac{\partial(n_{0,0} - 1)}{\partial \Delta t_L} = \frac{1}{2.303 \Delta t_L \log \frac{I_{0,0H}}{I_{0,0L}}} \quad (30b)$$

Noting that

$$\begin{aligned} \varepsilon(n_{0,0}) &= \varepsilon(n_{0,0} - 1) \\ &= \left[\left(\frac{\partial(n_{0,0} - 1)}{\partial A_{iH}} \right)^2 \varepsilon(A_{iH})^2 + \left(\frac{\partial(n_{0,0} - 1)}{\partial A_{fH}} \right)^2 \varepsilon(A_{fH})^2 + \left(\frac{\partial(n_{0,0} - 1)}{\partial A_{iL}} \right)^2 \varepsilon(A_{iL})^2 \right. \\ &\quad + \left(\frac{\partial(n_{0,0} - 1)}{\partial A_{fL}} \right)^2 \varepsilon(A_{fL})^2 + \left(\frac{\partial(n_{0,0} - 1)}{\partial I_{0,0H}} \right)^2 \varepsilon(I_{0,0H})^2 + \left(\frac{\partial(n_{0,0} - 1)}{\partial I_{0,0L}} \right)^2 \varepsilon(I_{0,0L})^2 \\ &\quad \left. + \left(\frac{\partial(n_{0,0} - 1)}{\partial \Delta t_H} \right)^2 \varepsilon(\Delta t_H)^2 + \left(\frac{\partial(n_{0,0} - 1)}{\partial \Delta t_L} \right)^2 \varepsilon(\Delta t_L)^2 \right]^{\frac{1}{2}} \\ &= \left\{ \left[\left(\frac{\partial(n_{0,0} - 1)}{\partial A_{iH}} \right)^2 + \left(\frac{\partial(n_{0,0} - 1)}{\partial A_{fH}} \right)^2 \right] \varepsilon(A_H)^2 + \left[\left(\frac{\partial(n_{0,0} - 1)}{\partial A_{iL}} \right)^2 + \left(\frac{\partial(n_{0,0} - 1)}{\partial A_{fL}} \right)^2 \right] \varepsilon(A_L)^2 \right. \\ &\quad + \left[\left(\frac{\partial(n_{0,0} - 1)}{\partial I_{0,0H}} \right)^2 + \left(\frac{\partial(n_{0,0} - 1)}{\partial I_{0,0L}} \right)^2 \right] \varepsilon(I_{0,0})^2 \\ &\quad \left. + \left[\left(\frac{\partial(n_{0,0} - 1)}{\partial \Delta t_H} \right)^2 + \left(\frac{\partial(n_{0,0} - 1)}{\partial \Delta t_L} \right)^2 \right] \varepsilon(\Delta t)^2 \right\}^{\frac{1}{2}}, \quad (31) \end{aligned}$$

we obtained

$$\begin{aligned}
\varepsilon(n_{0,0}) = & \left\{ 2 \left(\frac{\varepsilon(A_H)}{2.303 \log^2 \frac{I_{0,0H}}{I_{0,0L}}} \right)^2 \left[\left(\frac{1}{\Delta A_H} \right)^2 + \left(\frac{1}{2\overline{A_H}} \right)^2 \right] \right. \\
& + 2 \left(\frac{\varepsilon(A_L)}{2.303 \log^2 \frac{I_{0,0H}}{I_{0,0L}}} \right)^2 \left[\left(\frac{1}{\Delta A_L} \right)^2 + \left(\frac{1}{2\overline{A_L}} \right)^2 \right] \\
& + \left(\frac{\varepsilon(I_{0,0})}{2.303 \log^2 \frac{I_{0,0H}}{I_{0,0L}}} \log \frac{\Delta A_H \overline{A_L} \Delta t_L}{\Delta A_L \overline{A_H} \Delta t_H} \right)^2 \left[\left(\frac{1}{I_{0,0H}} \right)^2 + \left(\frac{1}{I_{0,0L}} \right)^2 \right] \\
& \left. + \left(\frac{\varepsilon(\Delta t)}{2.303 \log \frac{I_{0,0H}}{I_{0,0L}}} \right)^2 \left[\left(\frac{1}{\Delta t_H} \right)^2 + \left(\frac{1}{\Delta t_L} \right)^2 \right] \right\}^{\frac{1}{2}}. \tag{32}
\end{aligned}$$

A full table of $\varepsilon(n_{0,0})$ is provided in Appendix. Only $\varepsilon(n_{0,0})$ is presented because the full error propagation of $n_{x,t}$ contains an intractably large number of terms. Significantly, $\varepsilon(n_{0,0})$ and $\lambda_{95}(n_{0,0})$ are comparable in magnitude. By way of analogy, we also expect $\varepsilon(n_{x,t})$ and $\lambda_{95}(n_{x,t})$ to be comparable in magnitude. Therefore, we report λ_{95} values believing them provide reasonable estimates of errors for both $n_{0,0}$ and $n_{x,t}$.

CHAPTER IV

RESULTS AND DISCUSSION

A. Effects of Intensity Averaging on Intensity Dependence: $n_{0,0}$ and $n_{x,t}$ Contrasted

The tables below are a summary of the averaged $n_{0,0}$ and $n_{x,t}$ values we obtained.

A full table of n values can be found in Appendix.

	HA-HI vs HA-LI		LA-HI vs LA-LI		LA-HI vs HA-LI		HA-HI vs LA-LI	
	$\bar{n}_{0,0}$	λ_{95}	$\bar{n}_{0,0}$	λ_{95}	$\bar{n}_{0,0}$	λ_{95}	$\bar{n}_{0,0}$	λ_{95}
$\Delta t = 45s$	1.892	0.094	1.883	0.078	3.75	0.56	0.06	0.39
$\Delta t = 90s$	1.876	0.065	1.734	0.052	3.47	0.34	0.08	0.36
$\Delta t = 180s$	1.911	0.066	1.50 ^a	0.11 ^a	3.09	0.30	0.21	0.32
$I\Delta t = 0.9J$	1.77	0.11	1.768	0.068	3.67	0.40	-0.09	0.38
$I\Delta t = 1.8J$	1.801	0.072	1.754	0.059	3.67	0.38	-0.08	0.37
$I\Delta t = 3.6J$	1.801	0.056	1.676	0.056	3.48	0.34	0.02	0.34
$\Delta A/\bar{A} = 5\%$	1.752	0.089	1.596	0.084	3.18	0.27	0.06	0.32
$\Delta A/\bar{A} = 10\%$	1.707	0.065	1.665	0.060	3.30	0.32	0.04	0.33
$\Delta A/\bar{A} = 20\%$	1.691	0.050	1.683	0.061	3.38	0.34	0.02	0.33
$\Delta A/\bar{A} = 50\%$	1.658	0.039	1.698	0.059	3.26	0.33	0.12	0.31

Table II-A. Intensity dependence $\bar{n}_{0,0}$ and 95% confidence limits λ_{95} obtained by the method of 56 points.

^a Although this $\bar{n}_{0,0}$ value is somewhat small, with rather large λ_{95} value, $\bar{n}_{0,0}$ rises to 1.703 and λ_{95} drops to 0.081 when the two highest intensity runs ($I_{0,0} = 1.21$ and 0.967 MW cm⁻²) are eliminated from the data analysis.

	HA-HI vs HA-LI		LA-HI vs LA-LI		LA-HI vs HA-LI		HA-HI vs LA-LI	
	$\bar{n}_{x,t}$	λ_{95}	$\bar{n}_{x,t}$	λ_{95}	$\bar{n}_{x,t}$	λ_{95}	$\bar{n}_{x,t}$	λ_{95}
$\Delta t = 45\text{s}$	1.81	0.10	1.826	0.074	1.842	0.036	1.96	0.34
$\Delta t = 90\text{s}$	1.739	0.064	1.661	0.052	1.740	0.029	1.83	0.26
$\Delta t = 180\text{s}$	1.684	0.057	1.43 ^a	0.10 ^a	1.588	0.069	1.66	0.22
$I\Delta t = 0.9\text{J}$	1.75	0.11	1.765	0.070	1.816	0.038	1.84	0.27
$I\Delta t = 1.8\text{J}$	1.765	0.069	1.735	0.061	1.826	0.030	1.83	0.24
$I\Delta t = 3.6\text{J}$	1.729	0.048	1.635	0.051	1.741	0.026	1.3 ^b	1.0 ^b
$\Delta A/\bar{A} = 5\%$	1.78	0.10	1.596	0.081	1.690	0.041	1.59	0.26
$\Delta A/\bar{A} = 10\%$	1.701	0.066	1.681	0.055	1.720	0.028	1.66	0.17
$\Delta A/\bar{A} = 20\%$	1.695	0.050	1.682	0.061	1.741	0.026	1.67	0.26
$\Delta A/\bar{A} = 50\%$	1.666	0.038	1.700	0.058	1.739	0.025	1.56	0.31

Table II-B. Intensity dependence $\bar{n}_{x,t}$ and 95% confidence limits λ_{95} obtained by the method of 56 points.

^a See Footnote *a* of Table II-A. Although this $\bar{n}_{x,t}$ value is somewhat small, with rather large λ_{95} values, $\bar{n}_{x,t}$ rises to 1.625 and λ_{95} drops to 0.078 when the two highest intensity runs ($I_{0,0} = 1.21$ and 0.967 MW cm^{-2}) are eliminated from the data analysis.

^b $\bar{n}_{x,t}$ is unusually small and λ_{95} is unusually large for the $I\Delta t = 3.6 \text{ J}$, HA-HI vs. LA-LI data set because of a negative slope of spuriously large magnitude ($n_{x,t} = -25.429$; see Appendix) obtained with the [$A_{532}^{\text{initial}} \sim 1.0$, $I_{0,0} = 1.21 \text{ MW cm}^{-2}$] vs. [$A_{532}^{\text{initial}} \sim 0.2$, $I_{0,0} = 0.725 \text{ MW cm}^{-2}$] comparison, which did not lie $3s_{\text{pre-rejection}}$ away from $\bar{n}_{x,t}$. More reasonable values ($\bar{n}_{x,t} = 1.84$, $\lambda_{95} = 0.33$) are obtained when all points lying more than $2s_{\text{pre-rejection}}$ from $\bar{n}_{x,t}$ are rejected. This relaxation of the rejection standard does not seriously compromise the quality of the incident intensity data ($\bar{n}_{0,0} = 0.28$, $\lambda_{95} = 0.26$; compare with Table II-A) in this case. (The spurious negative slope originates from the very small difference in $\sqrt{I_{x,t}^2}$ values for the [$A_{532}^{\text{initial}} \sim 1.0$, $I_{0,0} = 1.21 \text{ MW cm}^{-2}$] vs. [$A_{532}^{\text{initial}} \sim 0.2$, $I_{0,0} = 0.725 \text{ MW cm}^{-2}$] runs, for which $\sqrt{I_{x,t}^2} = 0.6193$ and $0.6208 \text{ MW cm}^{-2}$, respectively.)

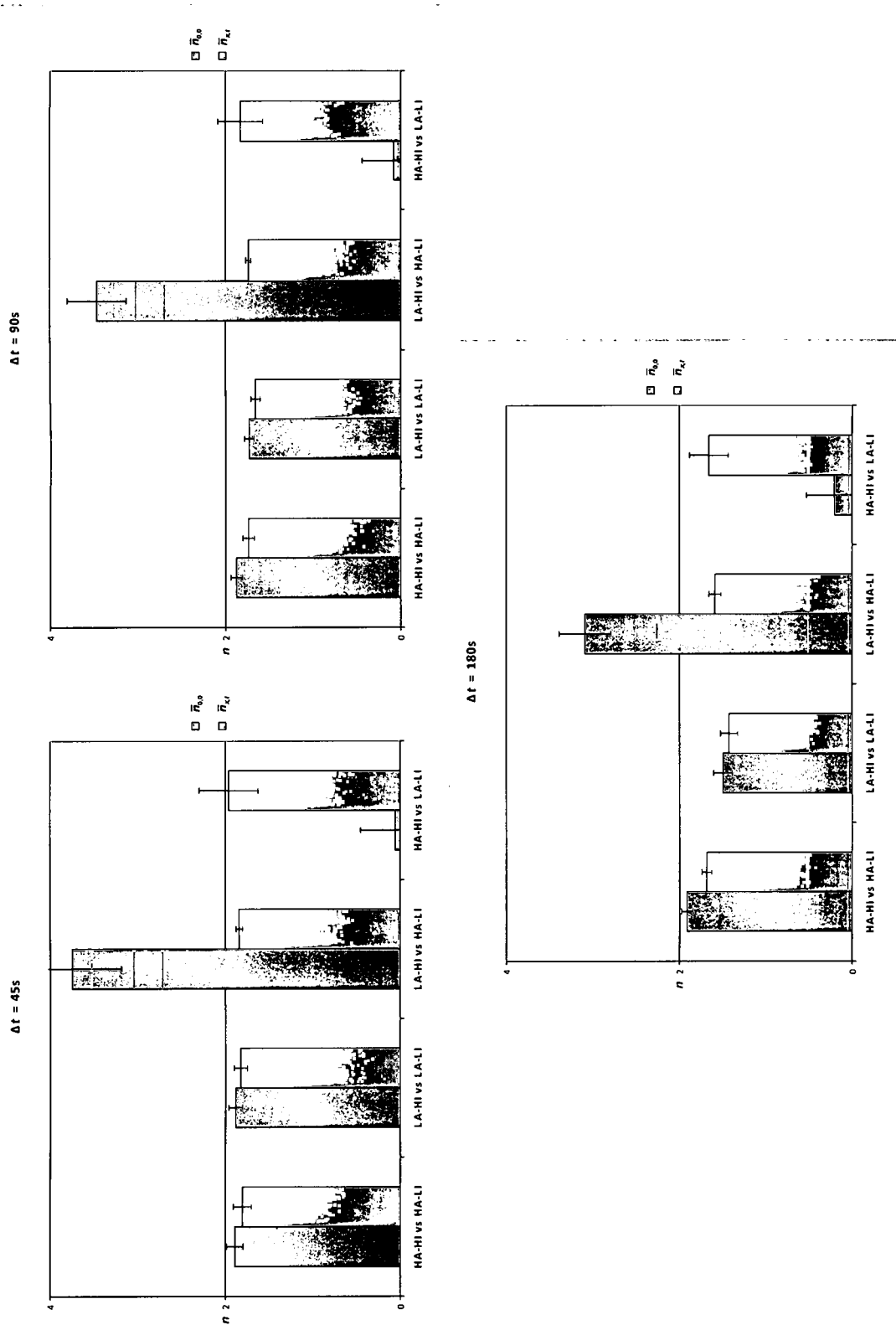


Figure 11A. Values of $\bar{n}_{0,0}$ (blue) and $\bar{n}_{x,x}$ (red) obtained with identical irradiation intervals of 45, 90 and 180 seconds contrasted. Error bars show $\pm \lambda_{95}$.

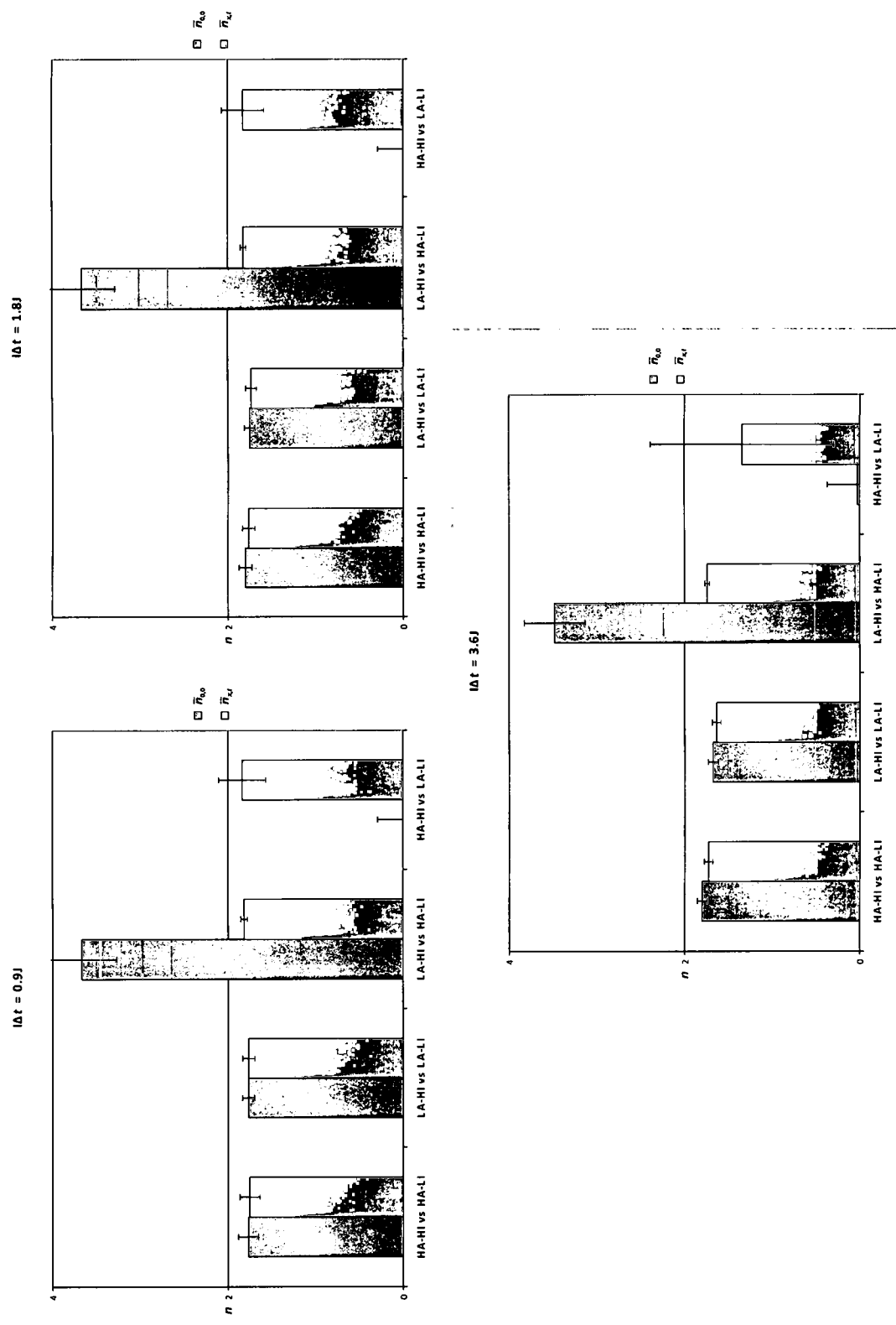


Figure 11B. Values of $\bar{n}_{0,0}$ (blue) and $\bar{n}_{x,i}$ (red) obtained with identical actinic doses of 0.9, 1.8 and 3.6 J contrasted. Error bars show $\pm \lambda_{95}$.

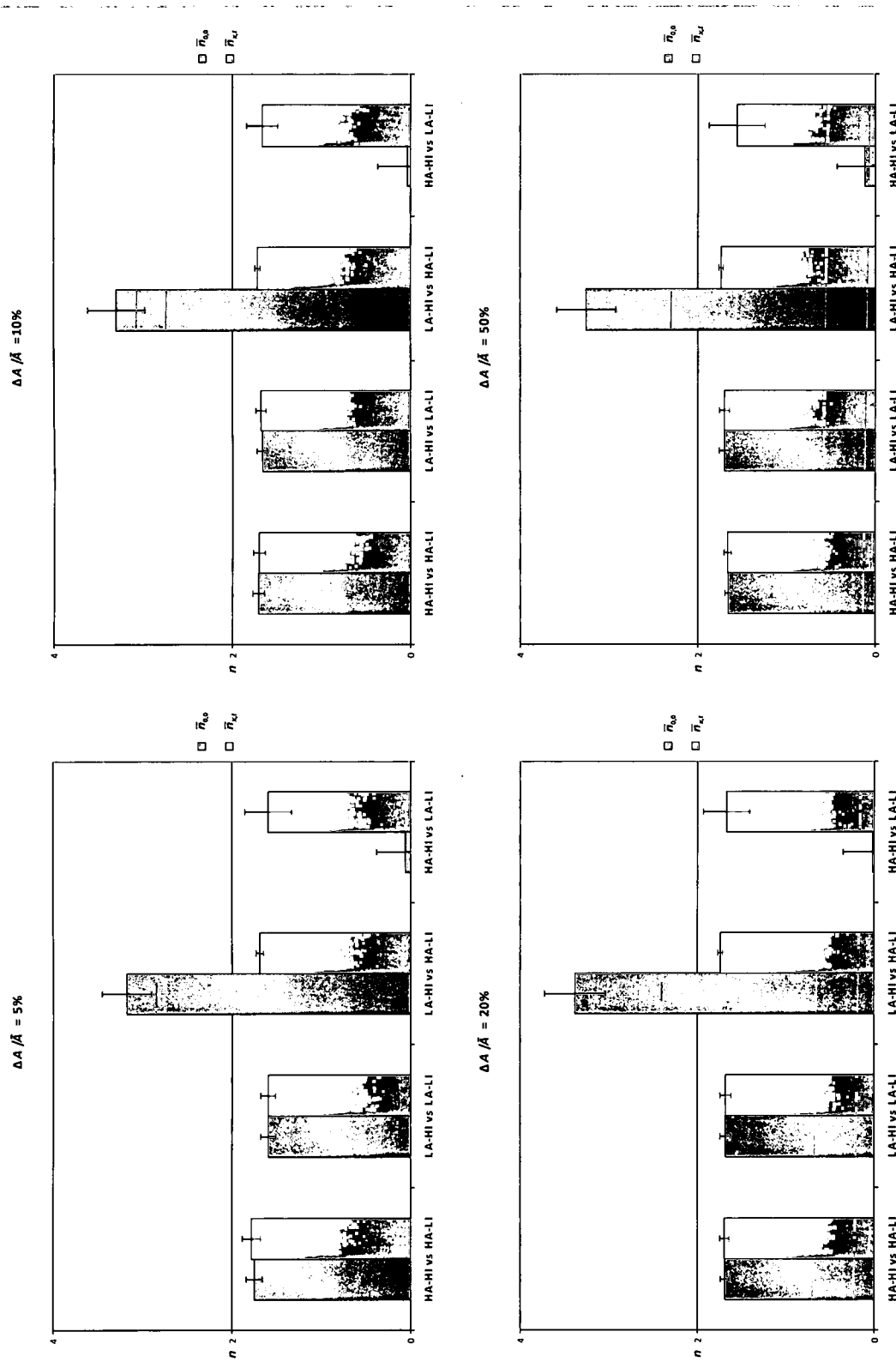


Figure 11C. Values of $\bar{n}_{0,0}$ (blue) and $\bar{n}_{x,l}$ (red) obtained with identical absorbance drops of 5%, 10%, 20% and 50% contrasted. Error bars show $\pm \lambda_{95}$.

	HA-HI vs HA-LI			LA-HI vs LA-LI		
	$\bar{n}_{0,0}$	λ_{95}	R^2	$\bar{n}_{0,0}$	λ_{95}	R^2
$\Delta t = 45\text{s}$	1.87	0.11	0.952	1.97	0.17	0.918
$\Delta t = 90\text{s}$	1.849	0.079	0.974	1.787	0.075	0.972
$\Delta t = 180\text{s}$	1.926	0.064	0.987	1.60 ^a	0.16 ^a	0.812 ^a
$I\Delta t = 0.9\text{J}$	1.77	0.10	0.949	1.789	0.089	0.962
$I\Delta t = 1.8\text{J}$	1.829	0.070	0.978	1.774	0.081	0.967
$I\Delta t = 3.6\text{J}$	1.820	0.055	0.986	1.703	0.068	0.972
$\Delta A/\bar{A} = 5\%$	1.757	0.087	0.960	1.64	0.10	0.927
$\Delta A/\bar{A} = 10\%$	1.720	0.060	0.979	1.681	0.070	0.967
$\Delta A/\bar{A} = 20\%$	1.689	0.047	0.986	1.690	0.072	0.968
$\Delta A/\bar{A} = 50\%$	1.641	0.047	0.983	1.689	0.068	0.971

Table III-A. Intensity dependence $\bar{n}_{0,0}$, 95% confidence limits λ_{95} and linear least squares correlation coefficients R^2 obtained by the method of least squares.

^a See Footnote *a* of Table II-A. Although these $\bar{n}_{0,0}$ and R^2 values are somewhat small, they rise to 1.81 and 0.938, respectively, while λ_{95} remains relatively unchanged (0.14), when the two highest intensity runs ($I_{0,0} = 1.21$ and 0.967 MW cm^{-2}) are eliminated from the data analysis.

	HA-HI vs HA-LI			LA-HI vs LA-LI		
	$\bar{n}_{x,t}$	λ_{95}	R^2	$\bar{n}_{x,t}$	λ_{95}	R^2
$\Delta t = 45s$	1.82	0.11	0.950	1.93	0.16	0.913
$\Delta t = 90s$	1.760	0.068	0.976	1.722	0.079	0.964
$\Delta t = 180s$	1.80	0.11	0.978	1.53 ^a	0.16 ^a	0.783 ^a
$I\Delta t = 0.9J$	1.76	0.10	0.947	1.772	0.085	0.964
$I\Delta t = 1.8J$	1.798	0.068	0.978	1.743	0.077	0.968
$I\Delta t = 3.6J$	1.756	0.051	0.987	1.662	0.064	0.973
$\Delta A/\bar{A} = 5\%$	1.758	0.089	0.959	1.641	0.098	0.932
$\Delta A/\bar{A} = 10\%$	1.723	0.062	0.979	1.680	0.070	0.968
$\Delta A/\bar{A} = 20\%$	1.691	0.049	0.984	1.689	0.070	0.969
$\Delta A/\bar{A} = 50\%$	1.652	0.051	0.982	1.688	0.068	0.971

Table III-B. Intensity dependence $\bar{n}_{x,t}$, 95% confidence limits λ_{95} and linear least squares correlation coefficients R^2 obtained by the method of least squares.

^a See Footnote *a* of Table III-A. Although these $\bar{n}_{x,t}$ and R^2 values are somewhat small, they rise to 1.74 and 0.930, respectively, while λ_{95} remains relatively unchanged (0.14), when the two highest intensity runs ($I_{0,0} = 1.21$ and 0.967 MW cm^{-2}) are eliminated from the data analysis.

From Tables II and III and Figures 11 above, we can draw a conclusion that the intensity dependence may be calculated reliably with both the longitudinally-and-

temporally averaged n^{th} order intensity $\sqrt[n_{x,t}]{I_{x,t}^{n_{x,t}}}$ and the (conventionally used) incident

intensity $I_{0,0}$ provided that samples which are irradiated with different intensities have the

same the initial absorbance $A_{\lambda}^{\text{initial}}$ at the actinic wavelength λ . That is, both $n_{0,0}$ and $n_{x,t}$

are reliable for HA–HI vs HA-LI and LA–HI vs LA-LI runs. There is no real advantage of

$\sqrt[n_{x,t}]{I_{x,t}^{n_{x,t}}}$ over $I_{0,0}$ in this case.

When it came to different $A_{\lambda}^{initial}$ on the other hand, only $\sqrt[n_{x,t}]{I_{x,t}^{n_{x,t}}}$ gave consistently reasonable results. This is because beam intensities in HA samples are attenuated to a greater extent than those in LA samples (see Equation [15c]), so that the actual beam intensities to which β C solutions are exposed are disproportionately smaller than the incident actinic intensity $I_{0,0}$. For the LA-HI vs. HA-LI comparison, $I_{0,0_L}$ in Equation (24b) is larger than the actual effective intensity, hence $n_{0,0}$ is spuriously large. For the HA-HI vs. LA-LI comparison on the other hand, $I_{0,0_H}$ in equation (24b) is larger, hence making $n_{0,0}$ spuriously small. And in the cases of identical $A_{\lambda}^{initial}$, the effects of absorbance on $I_{0,0_H}$ and $I_{0,0_L}$ are the same, so we were able to get reasonable $n_{0,0}$. Since the longitudinally-and-temporally averaged n^{th} order intensity $\sqrt[n_{x,t}]{I_{x,t}^{n_{x,t}}}$ accounts for the beam attenuation across the path length, $n_{x,t}$ values are consistently good.

B. Effects of Irradiation Interval, Actinic Dose and Absorbance Drop on Intensity

Dependence

Based on the results in Tables II, for the same initial absorbance scenarios, all three methods (identical irradiation intervals, actinic doses and absorbance drops) gave good intensity dependence and 95% confidence limits ($\bar{n}_{x,t} \sim \bar{n}_{0,0} \geq 1.6$ with $\lambda_{95} < 0.10$), with one exception. The one exception to this rule occurred with identical long intervals ($\Delta t = 180$ sec) for LA runs, which yielded $\bar{n}_{0,0} \pm \lambda_{95} = 1.50 \pm 0.11$ and $\bar{n}_{x,t} \pm \lambda_{95} = 1.43 \pm$

0.10. This is because when low absorbance samples were irradiated with high intensities ($I_{0,0} = 0.967$ and 1.21 MW cm^{-2}) for a long period of time, the βC concentration was knocked down so far that the reaction rate was very slow. These extremely slow rates at high intensities lead to very small numerators in Equations (24a) and (24b), hence leading to small $n_{x,t}$ and $n_{0,0}$ values, respectively, as illustrated in the point-by-point results presented in Appendix. Even so, when the two highest intensity runs were eliminated from the data set, $\bar{n}_{x,t}$ and $\bar{n}_{0,0}$ were both greater than 1.6 and the λ_{95} values dropped to 0.078 and 0.081, respectively. The same effect was also observed when we used the method of least squares (see Tables III). However, this doesn't necessarily make identical intervals method less reliable than the other two, because the choice of irradiation intervals, actinic doses and absorbance drops is somewhat random. We believe if we had chosen only short irradiation intervals, we wouldn't see these bad results; or if we had chosen a much bigger dose or absorbance drop, we would see this in the other two methods as well. In general the identical actinic doses is the best approach since it is more easily carried out experimentally than identical absorbance drops, and also makes more sense physically than identical irradiation intervals.

C. Comparison between the Method of 56 Pairs and the Method of Least Squares

From Tables II and III, we can see that the method of 56 points and the method of least squares gave roughly identical results, for n values and for λ_{95} . Despite this, we believe that the least squares method is a better approach when possible for these reasons. First, the correlation coefficient R^2 obtained with the least squares method allows for easy evaluation of data quality. Second, when there's a bad point in the data set, the n value obtained with the least squares method (slope of best fit line) is less affected than the n

value obtained with the 56 pairs method (simple averaging). Third, we can easily plot the points and more easily identify the trend and any bad data points with the method of least squares than the method of 56 pairs.

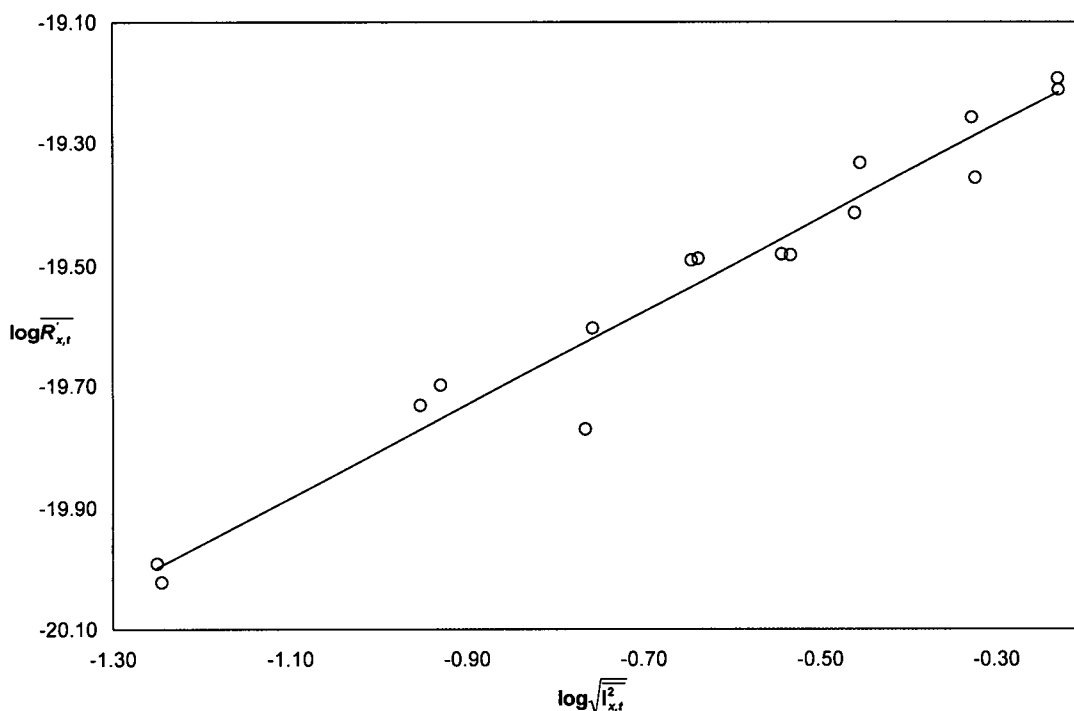


Figure 12. Representative plots of the logarithms of the average normalized rates $\overline{R'_{x,t}}$ of β C photodegradation in CCl_4 solvent versus the logarithms of the longitudinally-and-temporally averaged root mean square intensities (see Equations [22a] and [23a]). For the $I\Delta t = 1.8\text{J}$, HA-HI vs HA-LI run shown in the figure, we obtained a slope of 0.798, indicating quadratic intensity dependence ($n_{x,t} = 1.798$) with a correlation coefficient $R^2 = 0.978$.

D. The β -Carotene Photodegradation Mechanism

1. Concentration Dependence

According to the mechanism proposed in Figure 5, the photodegradation rate should be first order in both $c_{\beta\text{C}}$ and c_{CCl_4} . To corroborate the proposed mechanism, the effects of $c_{\beta\text{C}}$ and c_{CCl_4} on the photodegradation rate were characterized in both neat CCl_4 and dilute CCl_4 : hexane solutions, as described below.

a. Photodegradation of β C in Neat CCl_4

Because the concentration of neat CCl_4 solvent exceeds that of β C in our solutions by many orders of magnitude, it should be effectively constant throughout the course of a reaction, yielding rates of β C photodegradation which are independent of c_{CCl_4} and first order in $c_{\beta\text{C}}$ (see Figure 5). To confirm these expectations, HA and LA solutions were irradiated with 532 nm pulses with identical incident intensities ranging from $0.121 - 1.21 \text{ MW cm}^{-2}$, corresponding to longitudinally-and-temporally averaged root mean square intensities ranging from $0.0559 - 0.702 \text{ MW cm}^{-2}$ and $0.0970 - 1.08 \text{ MW cm}^{-2}$ for HA and LA samples, respectively. We observed a fivefold enhancement of reaction rate in the high initial absorbance samples as compared to the low initial absorbance samples, hence confirming the first order dependence of the reaction rate on $c_{\beta\text{C}}$ (see Table IV). Significantly however, the fivefold enhancement was observed only when rates were calculated using longitudinally-and-temporally averaged intensities in accord with Equation (22a); the enhancement was only twofold when the rates were calculated using incident intensities according to Equation (22b). The diminished concentration dependence for the $I_{0,0}$ -based rates originates from the greater diminution of intensity across the pathlength in high absorbance samples, giving rise to a decrease in reaction rate in the high absorbance samples with respect to that of low absorbance samples. This interesting and significant result confirms that $\overline{I_{x,t}^2}$ more closely approximates the actinically-effective squared intensity than $I_{0,0}^2$, and highlights the importance of using $\overline{I_{x,t}^2}$ to calculate reaction rates in optically dense – multiphoton reactive samples.

$I_{0,0}$ (MW cm ⁻²)	$\frac{\overline{A}_{532}(HA)^a}{\overline{A}_{532}(LA)}$	$\frac{\overline{R}_{0,0}(HA)}{\overline{R}_{0,0}(LA)}$	$\frac{\overline{R}_{x,t}(HA)}{\overline{R}_{x,t}(LA)}$
0.121	5.04	1.80	5.26
0.242	4.78	1.85	5.06
0.363	4.84	1.68	4.71
0.484	5.08	1.92	5.68
0.605	5.16	1.97	5.79
0.725	4.83	2.12	5.98
0.967	4.87	2.00	5.70
1.21	5.22	1.89	5.57
AVERAGE	4.98	1.90	5.47

Table IV. Dependence of rate of 532 nm-induced β C photodegradation on concentration of β C.

^a Ratio of mean absorbance $\overline{A}_{532} = \frac{A_{532}^{initial} + A_{532}^{final}}{2}$ over irradiation intervals which induced ~20% absorbance drops.

b. Photodegradation of β C in Dilute CCl₄

Solutions of β C in hydrocarbon solvents are photochemically inert upon irradiation with 532 nm laser pulses, allowing for the characterization of the effects of c_{CCl₄} on the reaction rate in dilute CCl₄: hydrocarbon solvent mixtures. Upon irradiating $A_{450}^{initial} \sim 1.0$ solutions of β C in dilute CCl₄: hexane mixtures ($c_{\beta C}^{initial} \sim 6.5 \times 10^{-6}$ M; c_{CCl₄} $\sim 0.01 - 0.0005$ M) with $I_{0,0} = 2$ mJ pulse⁻¹ = 0.484 MW cm⁻² laser pulses for 600 seconds we find that the rate increases linearly with c_{CCl₄} for a given c _{β C} (see Figure 13 and Table V) and that it is twice as fast in the $A_{450}^{initial} \sim 1.0$ as in $A_{450}^{initial} \sim 0.5$ for a given c_{CCl₄} (data not shown). Rates were characterized using changes in A_{450} in these experiments because this is the wavelength at which β C maximally absorbs in hexanes solvent. In combination with the results presented in Section IV.A.1.a above, these

results confirm that the photodegradation is first order in both $c_{\beta\text{C}}$ and c_{CCl_4} in dilute CCl_4 but depends exclusively on $c_{\beta\text{C}}$ in neat CCl_4 , consistent with Equations (20)-(21) and Figure 5.

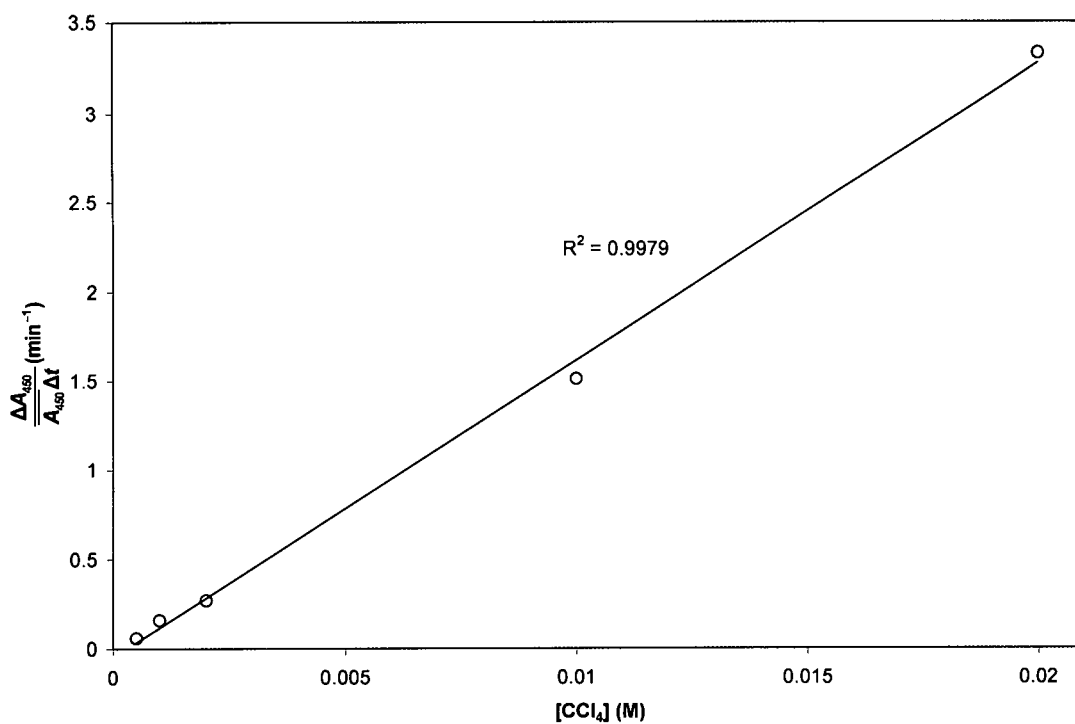


Figure 13. Dependence of rate of 532 nm-induced βC photodegradation on concentration of CCl_4 .

Data Set i	c_{CCl_4} (M)	$R_i = \frac{\Delta A_{450}}{\bar{A}_{450} \Delta t}$ (min ⁻¹)	$\frac{[\text{CCl}_4]_i}{[\text{CCl}_4]_{i+1}}$	$\frac{R_i}{R_{i+1}}$	Order p_i^f
1	2.00×10^{-2}	3.33	2.00	2.20	1.10
2	1.00×10^{-2}	1.51			
3	2.00×10^{-3}	0.272	5.00	5.56	1.11
4	1.00×10^{-3}	0.136	2.00	2.00	1.00
5	5.00×10^{-4}	0.0596	2.00	2.28	1.14

Table V. Dependence of rate of 532 nm-induced photodegradation of βC on concentration of CCl_4 .

^a Order of reaction rate p with respect to c_{CCl_4} calculated by comparing R_i and R_{i+1} assuming $R = k c_{\text{CCl}_4}^p I_{532}^n = K c_{\text{CCl}_4}^p$, in which $K = k I_{532}^n$ is a pseudo-first order rate constant with units of sec^{-1} (assumes reaction is first order in $c_{\beta\text{C}}$ and second order in intensity).

2. Intensity Dependence

Solutions of βC in CCl_4 are effectively inert in the dark and upon irradiation with diffuse green light (532 nm laser light from Nd:YAG lasers operating in the $\tau_{\text{pulse}} \sim 10^{-6}$ second “long-pulse” mode). In contrast, these solutions turn colorless within minutes upon irradiation with intense ($\geq 0.1 \text{ MW cm}^{-2}$) 532 nm laser pulses,⁶⁶ yielding photoproducts P_{350}^{laser} with absorption maxima near 350 nm, as Mortensen and Skibsted,³⁷⁻³⁹ and our group⁴¹⁻⁴³ have demonstrated (see Figure 8). The rate of color loss depends quadratically on the intensity provided the 532 nm laser pulse intensities are kept below the two-photon saturation threshold of $I_{0,0} \sim 10 \text{ mJ pulse}^{-1} = 2.4 \text{ MW cm}^{-2}$,⁴¹⁻⁴³ above which the intensity dependence becomes linear (see Figure 14)⁴¹⁻⁴³. $\beta\text{C-CCl}_4$ solutions

are thus ideal systems for testing the utility of $\overline{I_{x,t}^2}$ -based measurements of n at intensities below the biphotonic saturation threshold.

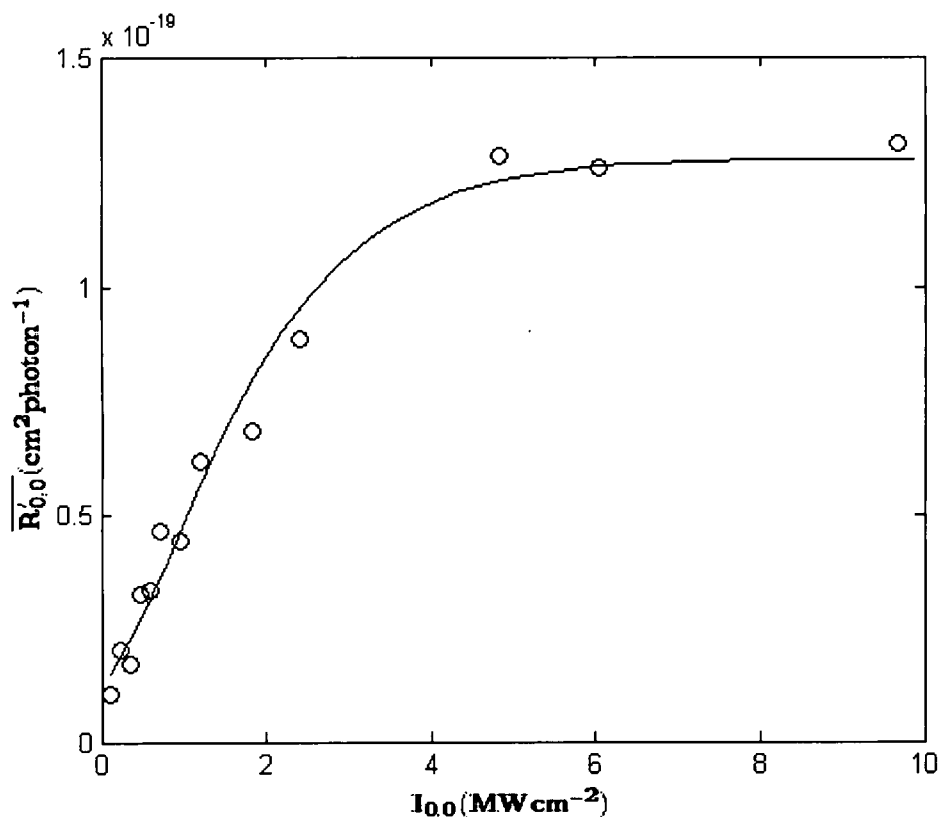


Figure 14. Dependence of average normalized β C photodegradation rates $\overline{R'_{0,0}}$ (see Equation [22b]) on 532 nm incident intensities $I_{0,0}$ as monitored with 20% decreases in absorbance, indicating biphotonic saturation for $I_{0,0} > 2.5 \text{ MW cm}^{-2}$ (10 mJ pulse^{-1}).

3. Wavelength Dependence

Solutions of β C in CCl_4 rapidly become colorless upon irradiation with diffuse 254, 313, and 365 lines from a 100W Hg lamp in a fashion analogous to the color loss induced by intense 532 nm laser pulses while they are effectively inert upon irradiation with diffuse green light. These results are rationalized in terms of the electronic structure of β C below.

a. Electronic Structure and Selection Rules of β C

Like other all-*trans* linear polyenes, β C belongs to the C_{2h} point group, with π -molecular orbitals (π -MOs) of a_u and b_g symmetries which alternate with increasing energy (see Figure 15). The closed shell ground electronic singlet state, with all π -MOs through the highest occupied molecular orbital (HOMO = 11 = a_u) doubly occupied, has A_g symmetry.

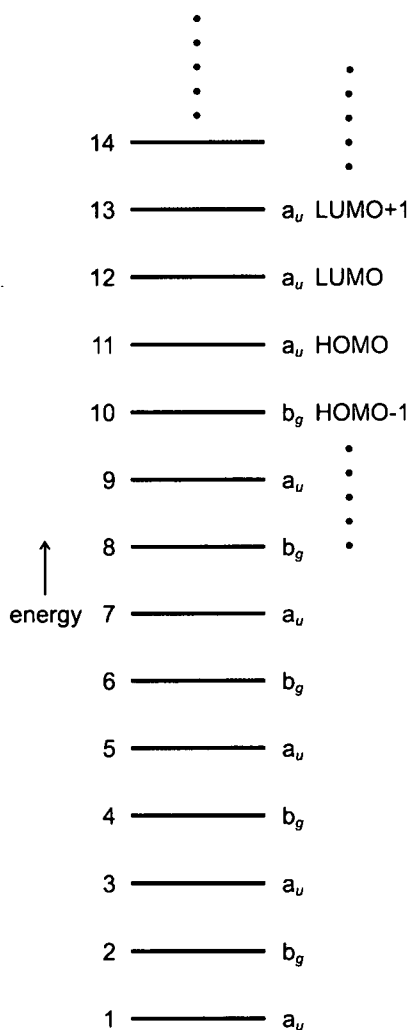


Figure 15. π -molecular orbitals of β -carotene.

Excited electronic states have symmetries equivalent to that of the symmetry products of the singly occupied MOs. The excited states thus have either $A_g = a_u \otimes a_u$, $A_g = b_g \otimes b_g$ or $B_u = a_u \otimes b_g$. In accord with Pariser's notation,⁶⁷ The electronic states are additionally labeled with alternancy "+" or "-" labels, depending on whether their wavefunctions consist of sums or differences of degenerate excited configurations.^{41,68-70} The one-photon and two-photon selection rules – which ultimately govern the photochemistry of β C – are given in Figure 16.

<i>One-Photon Allowed, Two-Photon Forbidden</i>			
$g \leftrightarrow u$		$+$	$\leftrightarrow -$
<i>Two-Photon Allowed, One-Photon Forbidden</i>			
$g \leftrightarrow g$	$u \leftrightarrow u$	$+$	$\leftrightarrow +$ $- \leftrightarrow -$

Figure 16. One- and two-photon electronic dipole selection rules for β C.

Since all electronic transitions originate from the ground ($1^1A_g^-$) electronic state, excited states of $^1B_u^+$ ($^1A_g^-$) states are accessed via one (two) photon excitation, with $^1B_u^-$ and $^1A_g^+$ states both one- and two-photon forbidden. Hence, all one-photon (two-photon) induced photochemistry of β C originates either directly from $^1B_u^+$ ($^1A_g^-$) excited states (provided the rate of β C-to- CCl_4 PET exceeds the rate of thermal relaxation⁷¹⁻⁷⁵) or from a potentially common lower-lying excited state of unspecified symmetry to which $^1B_u^+$ and $^1A_g^-$ states relax thermally. The most recent MO calculations suggest that the ordering of electronic states of β C is (in order of increasing energy) $S_1 = \text{ground} = 1^1A_g^-$,

$S_2 = 2^1A_g^-$, $S_3 = 1^1B_u^-$, $S_4 = 3^1A_g^-$ and $S_5 = 1^1B_u^+$.^{41,68-70} To our knowledge, the symmetries of states higher in energy than S_5 have not been reported.

b. Wavelength Dependence of β C Photodegradation

Because only excited states of $1^1B_u^{*+}$ symmetry are electric dipole-allowed from the $S_1 = 1^1A_g^-$ ground singlet state, the complexity of the electronic structure of β C is somewhat masked in the absorption spectrum. For example, the intense visible band extending from 400-550 nm – which is responsible for the orange color of β C – is comprised of three vibronic peaks with absorption maxima at 440, 463, and 491. Each of these vibronic peaks originate from the $S_1 \rightarrow S_5$ ($1^1A_g^- \rightarrow 1^1B_u^{*+}$) electronic transition, which is principally HOMO \rightarrow LUMO in character.^{41,42} The dipole-forbidden $S_2 = 2^1A_g^-$, $S_3 = 1^1B_u^-$, and $S_4 = 3^1A_g^-$ states which lie between the ground state and the $1^1B_u^+$ state are not manifest in the one-photon absorption spectrum.^{69,70} The weaker absorption bands centered near 350 nm and 280 nm originate from higher energy $S_0 \rightarrow S_{m>5}$ electronic transitions, the wavefunctions of which contain significant contributions from higher energy (the HOMO \rightarrow LUMO + 1, HOMO \rightarrow LUMO + 2, *etc.*) configurations. The fact that β C photodegrades upon irradiation with diffuse UV light and intense 532 nm laser light but not with diffuse green light suggests that the β C-to-CCl₄ PET process which gives rise to the photodegradation of β C is mediated principally by these higher-lying $S_{m>5}$ states.^{37-39,61,71-73,76-88}; the S_2 , S_3 , S_4 , and S_5 states contribute minimally to the photodegradation.^{37-40,61,71,88-90}, since the S_5 state is accessed by diffuse 532 nm light via one-photon excitation (see Figure 17).

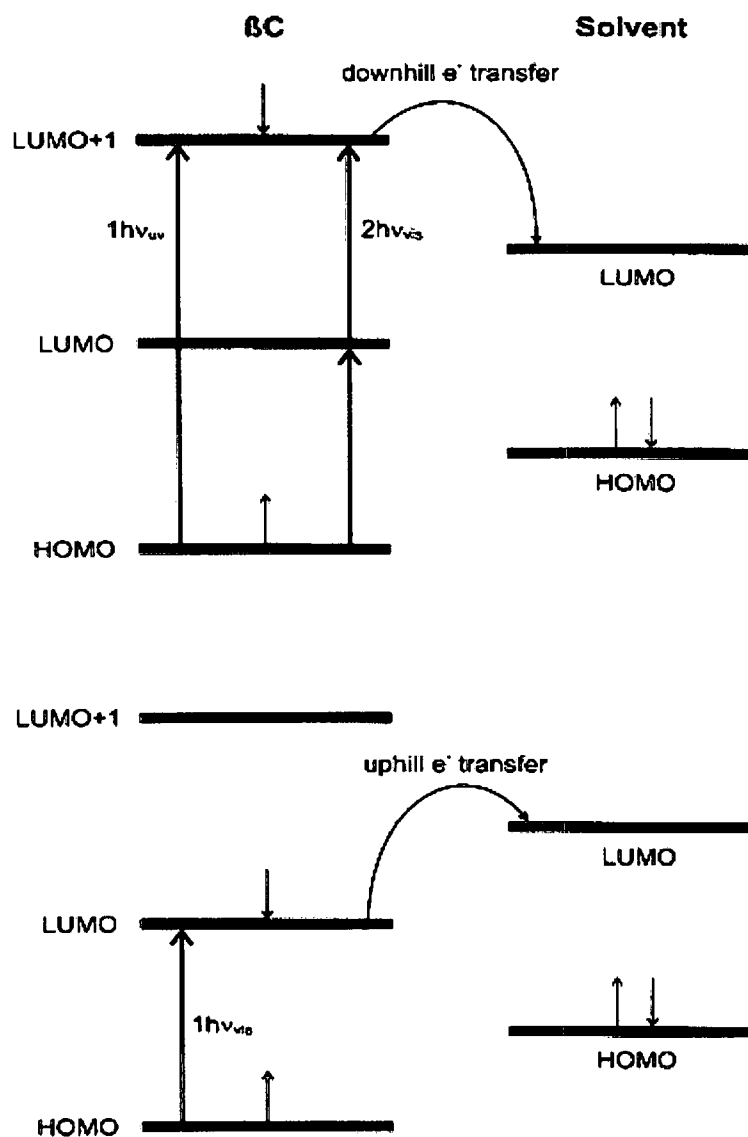


Figure 17. Proposed energetics of 532 nm one-photon-induced (bottom) and 266 nm one-photon-induced and 532 nm two-photon-induced (top) electron transfer from β C to CCl_4 . Based on reaction rates, the processes appear to be thermodynamically uphill (bottom) and thermodynamically downhill (top), respectively.

We also characterized the intensity dependence of β C photodegradation induced by 313 nm light and analyzed it in the same way as Equation (23b), see Figure 18.

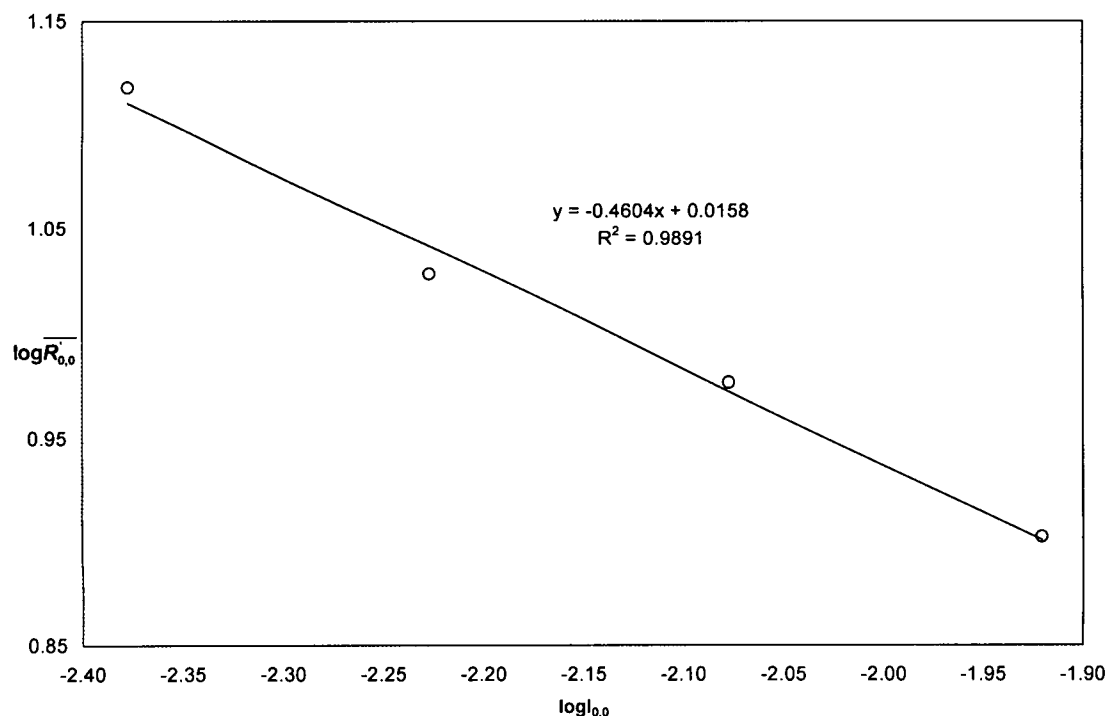


Figure 18. Intensity dependence of 313 nm-induced β C photodegradation in CCl_4 solvent.

The data in Figure 18 yield $n = -0.460 + 1.000 = 0.540$, indicating a one-photon process. This is consistent with the results of Gurzadyan and Steenken, who report linear power dependence for the β C photodegradation in chloromethane solvents at 355 nm up to very high ($> 1 \text{ GW cm}^{-2}$) intensities.⁴⁰

The colorless P_{350}^{UV} photoproducts generated upon UV irradiation are spectroscopically similar to the P_{350}^{laser} photoproducts generated with 532 nm laser pulses.^{41-43,91} Significantly, while P_{350}^{laser} is photochemically inert under 532 nm pulsed laser irradiation, it converts to “ $P_{<260}$ ” photoproducts upon further irradiation with UV light (see Figure 8, in which the absorption of P_{350}^{laser} didn’t change much from 25 minutes

of 532 nm laser irradiation to 60 minutes of 532 nm laser irradiation, but was readily knocked down after 30 seconds of 313 nm Hg lamp irradiation). Earlier UV-visible, fluorescence, and FTIR spectra, thin layer chromatograms, and gravimetric properties of the P_{350}^{UV} photoproducts suggest that they consist of pentaene moieties resulting from cleavage of and/or addition across the 15,15' double bond of β C.⁴²

E. Contributions of Dark and Monophotonic Reactions to the Total Photodegradation Rate

Essentially no degradation of β C was observed when $A_{532}^{initial} \sim 1.0$ solutions were incubated in the dark for one hour at ambient temperature. In fact, the absorbance increased by $\sim 2\%$ during the first 10 minutes of incubation, after which it became effectively constant, consistent with the initial increases in the absorbance of β C solutions during the initial stages of oxidation reported by other researchers.⁶²⁻⁶⁴ Likewise, essentially no degradation was observed when β C solutions were irradiated with the 532 nm output of the Nd:YAG laser operating in the long pulse ($\tau_{pulse} \sim 10^{-6}$ sec) mode. In contrast, A_{532} steadily declined at a post-2h ν thermal reaction rate of 0.00042 a.u. min⁻¹ when an $A_{532}^{initial} = 1.03720$ solution was irradiated with 1.20 MW cm⁻² pulses until the absorbance dropped to 0.49185 (a 53% decrease following irradiation with 900 pulses, during which the rate of absorbance loss was 0.3636 a.u. min⁻¹) and subsequently incubated in the dark for one hour. Contributions to the photodegradation from biphotonic light reactions are thus nearly 1,000-fold greater than those from post-2h ν thermal reactions indicating that the photodegradation of β C originates almost exclusively from biphotonic light reactions, with negligible contributions from post-2h ν

thermal reactions and no contributions from dark thermal reactions, monophotonic light reactions, or post-1h ν thermal reactions (see Equations [12] and [19]).

F. Photodegradation Quantum Yield and Two-Photon Absorptivity of β -Carotene

For computational efficiency, Equation (3) may be rewritten as

$$N_{\beta C}^{**} = \frac{\ell \delta}{1.06647 \cdot 2\sqrt{2} \tau_{pulse} \pi r_b^2} \times \bar{C} N^2 \quad (33a)$$

in which the first term in the product contains factors common to all irradiation intervals for a given laser, actinic wavelength, optical cell, and solute, the second term contains all factors specific to a given irradiation interval, and the initial concentration C of solute βC in molecule cm^{-3} in Equation (3) has been replaced by the average concentration $\bar{C} =$

$\frac{\bar{A} N_A}{1000 \varepsilon \ell}$ over the interval.^{2,22} Noting that the number N of photons in a pulse of energy E

Joules is equal to $\frac{E\lambda}{hc}$, we obtain

$$N_{\beta C}^{**} = \frac{0.331518 \delta \bar{A} N_A E^2}{1000 \varepsilon \cdot \left(\frac{hc}{\lambda}\right)^2 \tau_{pulse} \pi r_b^2} = \frac{\Delta A V_{tot} N_A}{1000 \varepsilon \ell \cdot 10 \Delta t} \quad (33b)$$

in which the rightmost term gives $N_{\beta C}^{**}$ as experimentally determined from the change in absorbance, total sample volume, and length of irradiation interval.

Cancelling common terms in Equation (33b) and solving for δ yields

$$\delta = \frac{\left(\frac{hc}{\lambda}\right)^2 \tau_{pulse} \pi r_b^2 \Delta A V_{tot}}{3.31518 \bar{A} E^2 \ell \Delta t} \quad (34)$$

Applying this to our experimental conditions (532 nm laser pulses of 6.5 ns duration with laser operating at 10 pulse sec^{-1} ; typical sample volumes of 1.7 cm^3) we obtain the

general expression

$$\delta_{532} = \left(2.9557 \times 10^4 \frac{\text{GMJ}^2 \text{ sec}}{\text{pulse}^2} \right) \times \frac{\Delta A_{532}}{A E^2 \Delta t} = \left(2.9557 \times 10^3 \frac{\text{GMJ}^2}{\text{pulse}} \right) \times \frac{\Phi_{532}^{\%}}{E^2}, \quad (35)$$

in which we assume that each doubly-excited βC molecule converts to colorless photoproducts (*i.e.*, $f=1$; see Equation [8]) so that the percentage of doubly-excited molecules in the beam volume will equal the percentage decrease in absorbance per pulse and

$$\Phi_{532}^{\%} = 100 \times \left(\frac{N_{\beta\text{C}}^{**}}{N_{\text{TOT}}} \right) = 100 \times \frac{\Delta A_{532}}{A_{532} \cdot 10 \Delta t} \quad (36)$$

is the quantum yield of photodegradation of βC expressed in units of % absorbance drop per pulse.

In terms of the number of βC molecules destroyed per photon of light absorbed, the quantum yield of photodegradation is

$$\begin{aligned} \Phi_{532} &= \frac{\Delta N_{\beta\text{C}}}{N_{532}^{\text{absorbed}}} = \frac{\Delta N_{\beta\text{C}}}{N_{\beta\text{C} \rightarrow \beta\text{C}^{\bullet}} + N_{\beta\text{C}^{\bullet} \rightarrow \beta\text{C}^{**}}} = \frac{\Delta N_{\beta\text{C}}}{N_{\beta\text{C} \rightarrow \beta\text{C}^{\bullet}} + \Delta N_{\beta\text{C}}} \\ &= \frac{\frac{\Delta A_{532}}{\epsilon_{532} \cdot l} \cdot V_{\text{tot}} \cdot N_A}{I_{532} \cdot \Delta t \cdot \pi r_b^2 \cdot (1 - 10^{-\overline{A}_{532}}) + \frac{\Delta A_{532}}{\epsilon_{532} \cdot l} \cdot V_{\text{tot}} \cdot N_A} \end{aligned} \quad (37)$$

in which $\Delta N_{\beta\text{C}}$ is the number of βC molecules destroyed, $N_{532}^{\text{absorbed}}$ is the sum of the number of photons absorbed via excitation from the ground to the intermediate state ($N_{\beta\text{C} \rightarrow \beta\text{C}^{\bullet}}$) and via excitation from the singly excited to the doubly excited state

($N_{\beta\text{C}^{\bullet} \rightarrow \beta\text{C}^{**}} = \Delta N_{\beta\text{C}}$), I_{532} is the intensity of the actinic light in units of photons $\text{cm}^{-2} \text{ sec}^{-1}$,

h is Planck's constant, \overline{A}_{532} is the average absorbance at 532 nm over the irradiation

interval. The quantum yields ($\Phi_{0,0}$ using $I_{0,0}$ and $\Phi_{x,t}$ using $\sqrt{I_{x,t}^2}$ for I_{532} , respectively) in molecule photon⁻¹ are plotted as functions of $I_{0,0}$ for low ($I_{0,0} < 1.3 \text{ MW cm}^{-2}$) and high ($I_{0,0} < 10 \text{ MW cm}^{-2}$) intensity ranges in Figure 19.

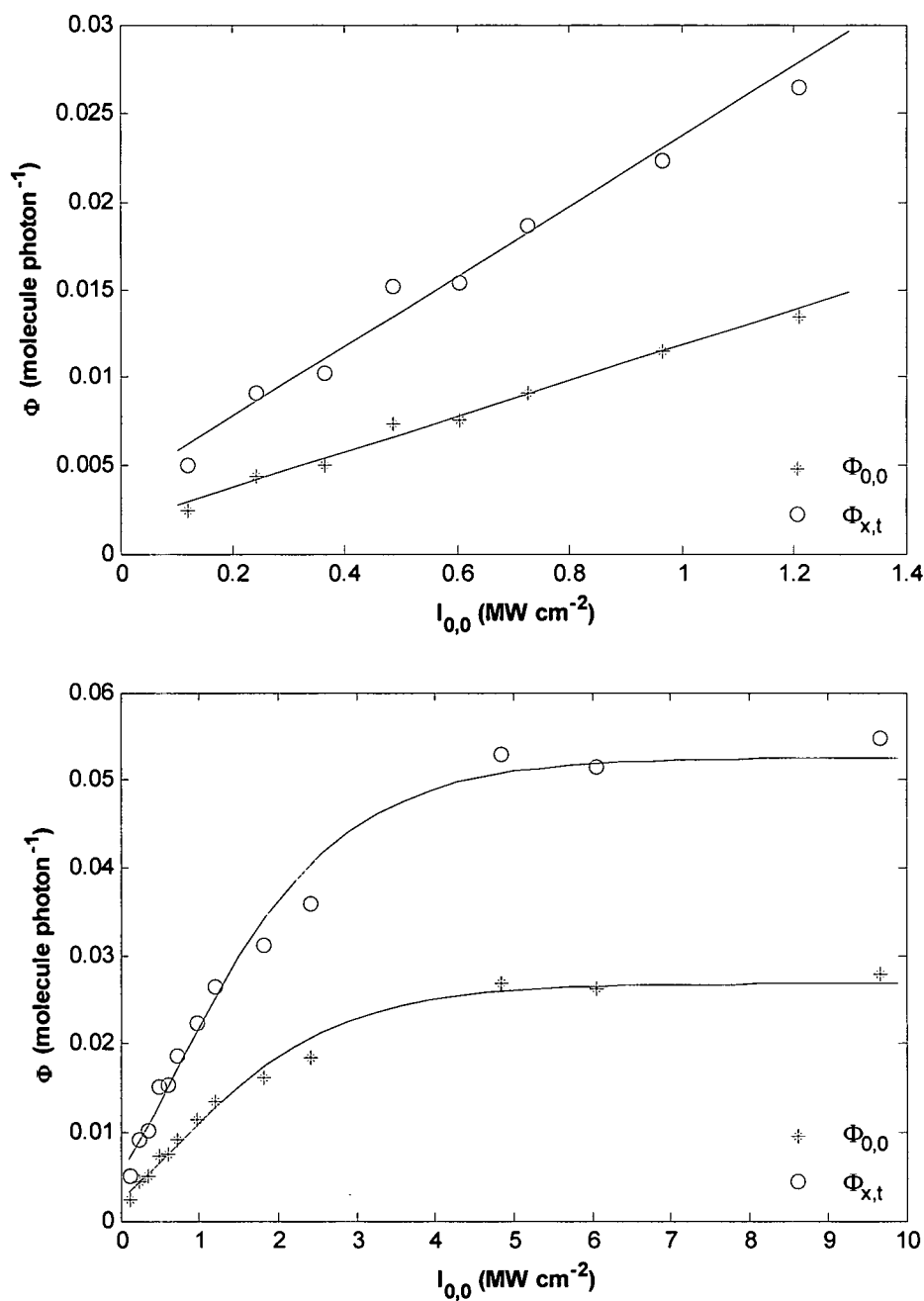


Figure 19. Dependence of two-photon reaction quantum yield on 532 nm incident intensities $I_{0,0}$.

As we can see from Figure 19, the quantum yield depends linearly on low intensities (top) before saturation occurs for $I_{0,0} > 2.5 \text{ MW cm}^{-2}$ (bottom) which corresponds with the saturation point of photodegradation rate (see Figure 14).

The average two-photon cross section is $\delta_{532} = (1.71 \pm 0.88) \times 10^7 \text{ GM}$ when calculated as though the sample is one-photon transparent (*i.e.*, as though the squared intensity is equal to $I_{0,0}^2$ across the entire optical path). Since the longitudinally-and-temporally averaged intensity $\overline{I_{x,t}^2}$ is less than $I_{0,0}^2$ in our one-photon absorbing samples, the true two-photon cross section is expected to be greater than the incident-intensity based value. In accord with this expectation, the two-photon cross section calculated using $\overline{I_{x,t}^2}$ is equal to $\delta_{532} = (3.87 \pm 0.99) \times 10^7 \text{ GM}$.

The two-photon absorptivity of βC is exceptionally large, exceeding by more than an order of magnitude the largest two-photon absorptivity reported to date for chromophores which are one-photon transparent at the actinic wavelength ($\delta_{780} = 90,600 \text{ GM}$ for core modified aromatic octaphyrins).⁹² The two-photon absorptivities of one-photon transparent chromophores are typically less than 10^4 GM since the second photon must be absorbed by short-lived virtual intermediate states of these molecules.^{2,22,93-98} Accordingly, we attribute the exceptional magnitude of δ_{532} to resonance enhancement via excitation into the optically-allowed $S_5 = 1^1B_u^+$ state of βC since (i) the 463 nm absorption band of βC – which originates from the $S_0 \rightarrow S_5$ transition – has appreciable absorbance at 532 nm ($\epsilon_{532} = 3,630 \text{ M}^{-1} \text{ cm}^{-1}$; see Figure [8]), (ii) the lifetime of the S_5 state is on the order of 0.1 ps,⁹⁹ or 1-3 orders of magnitude larger than that of typical virtual states,^{2,31} giving ample opportunity for the absorption of a second photon prior to

thermal relaxation, and (iii) our δ_{532} values are of roughly the same order of magnitude as those of the retinyl protein bacteriorhodopsin ($\delta_{532} \sim 10^6$ GM) which is resonance-enhanced due to intense one-photon absorption at 532 nm,³¹ and of chlorophyll *a* ($\delta_{694.3} \sim 10^7$ GM), which is resonance-enhanced due to the overlap of the actinic 694.3 ruby laser line with the visible $S_0 \rightarrow S_1$ “Q” absorption band of chlorophyll *a*.^{97,98,100}

G. Implications of Intensity Averaging for Photodynamic Therapy

Photodynamic therapy (PDT) is the use of drugs (photosensitizers) that are activated by light. Photosensitizers generally act as singlet oxygen (1O_2) sensitizers, though some may be directly phototoxic (*i.e.*, oxygen-independent). Since biological tissues scatter light strongly and frequently contain endogenous chromophores which absorb light at photodynamically useful wavelengths, PDT is typically relegated to treating disorders of tissues which can be accessed with light via fiber-optic devices directly (bladder, lung, esophagus, nasopharyngeal, skin, and eye), surgically via fiber optic devices (prostate, liver, and pancreas) or other light sources (brain), and via other special procedures (bone marrow).¹⁰¹ Nevertheless, because the depth of radiative penetration in highly scattering media increases with increasing wavelength, the longer (generally near IR) wavelengths used to induce two-photon excitation of photodynamic dyes in principle allows for treatment of tumors at greater tissue depths than conventional linear PDT.¹⁰¹⁻¹⁰⁴ Such “nonlinear PDT” mediated by multi-photon-absorbing dyes has accordingly received a great deal of attention.

To date, effective two-photon induced cell killing at a depth of 4 cm has been attained in a model system in which human breast cancer cells dosed with a porphyrin-based PDT agent are embedded in a breast tissue phantom which models the optical

properties of human breast tissue with 150-200 fs, 790 nm pulses from a Ti: Sapphire laser.¹⁰² The killing depth under these conditions is reduced to 1 cm in mice containing implanted tumors in which the radiation passes through the skin.¹⁰² Greater penetration depths are attainable if dyes which absorb at longer wavelengths can be developed.

In light of the considerations described above, it is noteworthy that – though two-photon activated photodynamic dyes show promise for increasing penetration depth – their effectiveness is still likely to be limited due to the reasonably small two-photon cross sections of dyes which absorb via an instantaneous two-photon absorption mechanism. Though instantaneous two-photon absorbing porphyrin PDT agents with large (1.7×10^4 GM) two photon cross sections have been developed,¹⁰⁵ these cross sections are still much smaller than those obtained for sequential biphotonic absorbers such as β C, as we have demonstrated. Our results thus suggest that greater clinical effectiveness will be achieved with photodynamic dyes which are activated by sequential biphotonic absorption. This strategy is employed with a small number of PDT dyes used to date.^{55,101}

Our results also suggest that longitudinally-and-temporally averaged intensities may facilitate improvements in nonlinear PDT for at least three reasons. First, they may be used to characterize the intensity dependence of photodynamic effects under *in vitro* conditions using solutions in cuvettes, in accord with the methodology presented in this paper. In similar fashion, $\sqrt{I_{x,t}^{pk,t}}$ may also be applied to tissue sections under *ex vivo* conditions, provided absorption and scattering coefficients of the tissue are known.¹⁰¹

Second, as has been noted elsewhere, substantiation of quadratic intensity dependence for photodynamic effects *in vivo* is important for advancing nonlinear PDT

research and clinical practice, but presents a substantial experimental challenge.^{101,106,107}

Our results suggest that longitudinally-and-temporally averaged intensities may constitute an important step forward for PDT researchers in this regard, as they can be used to characterize the mode of action and therapeutic efficiency of nonlinear photodynamic dyes under *in vivo* conditions. For example, the rate of photodynamically-induced shrinkage of deep tumors in animal models may be more accurately characterized with $\sqrt[n_{x,t}]{I_{x,t}^{n_{x,t}}}$ than with $I_{0,0}$.

Third, since $\sqrt[n_{x,t}]{I_{x,t}^{n_{x,t}}}$ more closely approximates the actual actinic intensity than $I_{0,0}$ at x and t , our model may facilitate improvements in the calculations of actinic dose, which are frequently problematic.¹⁰¹ Our model may prove especially useful for calculating doses for photodynamic dyes which are both one- and two-photon absorbing. For example, our model also clearly predicts that the actinic incident sides of tumors receive greater photodynamic doses than the actinic exit sides, and two-photon photolabile dyes will provide more uniform photodynamic doses throughout tumors than photostable dyes because photolabile dyes degrade more rapidly on the incident side of the tumor, providing for greater penetration depth by subsequent laser pulses.^{44,45}

CHAPTER IV

CONCLUSIONS AND FUTURE STUDIES

A. Conclusions

The rates of simultaneous two-photon and sequential biphotonic processes – which are proportional to the square of the intensity $I_{x,t}^2$ – decline rapidly across the optical path of one-photon absorbing, two-photon reactive samples such as β -carotene, because one-photon absorption in such samples leads to severe attenuation of $I_{x,t} = 10^{\varepsilon C_{x,t} x} I_{0,0}$ with increasing x . The extent of this attenuation also changes with time in samples which undergo photoinduced changes in absorbance. The principal objective of this paper is to test the hypothesis that in samples with high Beer's Law absorbance the intensity dependence $n_{x,t}$ calculated with the longitudinally-and-temporally averaged n^{th} -order intensity $\sqrt[n_{x,t}]{I_{x,t}^{n_{x,t}}}$ is more accurate than the intensity dependence $n_{0,0}$ calculated with incident intensities $I_{0,0}$. As a test of our hypothesis, we utilized longitudinally-and-temporally averaged n^{th} order intensities to characterize the dependence of the rate of the two-photon-induced photodegradation of β -carotene on actinic intensity. Our results confirm our hypothesis and lead to the following conclusions, which should apply not only to β -carotene but to one-photon absorbing, multiphoton reactive samples in general.

1. Provided the initial absorbance $A_{\lambda}^{initial}$ at the actinic wavelength λ is the same for samples irradiated at different intensities, the intensity dependence n may be reliably calculated with incident intensity $I_{0,0}$ (*i.e.*, $n_{0,0} \sim n_{x,t} \sim 2.0$). If $A_{\lambda}^{initial}$ is not identical for samples irradiated with different intensities, the longitudinally-and-temporally averaged n^{th} order intensity $\sqrt[n_{x,t}]{I_{x,t}^{n_{x,t}}}$ yields for more realistic n values than $I_{0,0}$ (*i.e.*, $n_{x,t} \sim 2.0$ whereas $n_{0,0} \sim 3.5$ or 0.0).
2. Reliable n values may be obtained by exposing samples to different intensities for (i) identical irradiation intervals, (ii) identical actinic doses, or (iii) identical normalized changes in absorbance. In general the identical actinic doses is the best approach since it is more easily carried out experimentally than identical absorbance drops, and also makes more sense physically than identical irradiation intervals.
3. Upon irradiation with intense 532 nm laser pulses, solutions of βC ($\lambda_{\text{max}} = 463 \text{ nm}$) in CCl_4 rapidly converts to a mixture of photoproducts with absorption maxima near 350 nm and $< 260 \text{ nm}$. The spectroscopic evidence does not indicate unequivally whether the 350 nm and $< 260 \text{ nm}$ –absorbing products are generated sequentially or simultaneously.
4. The two-photon cross section of β -carotene associated with the color loss is exceptionally large ($\delta_{532} = 1.71 \pm 0.88 \times 10^{-43} \text{ cm}^4 \text{ sec molecule}^{-1} \text{ photon}^{-1}$), indicating that the photodegradation is mediated by a sequential biphotonic process rather than a simultaneous two-photon process.

B. Future Studies

We are mostly interested in the mechanism(s) which mediate(s) the photodegradation of βC and the structures of its products. Acquisition of the action spectra for the one-photon and two-photon photodegradation of βC should provide significant insights into the nature of the electronic states of βC which mediate its photodegradation. Such studies are currently ongoing in our laboratory. The structures of the βC products also remain to be characterized. This involves the products of βC photodegradation induced by both 532 nm laser beam and UV beam from the Hg lamp. We are currently trying to generate the products in a quantity large enough for elemental analysis. Complete chromatographic separation of the product mixture and characterization of individual component will be pursued in our laboratory in the future.

REFERENCES

- (1) Göppert-Mayer, M. Über Elementarakte mit zwei Quantenssprüngen. *Ann. Phys. (Leipzig)* **1931**, *401*, 273-294.
- (2) Birge, R. R. One-photon and two-photon excitation spectroscopy. *Ultrasensitive Laser Spectroscopy*; Academic Press: New York, 1983; pp 109-175.
- (3) Leupold, D.; Kochevar, I. E. Multiphoton photochemistry in biological systems. *Photochem. Photobiol.* **1997**, *66*, 562-565.
- (4) The decrease in intensity due to two-photon absorption can generally be ignored because the number of two-photon absorption events is small compared to the total number of photons in a laser pulse, even with exceptionally strong two-photon absorbers. For example, only 0.90% of the 532 nm photons in a 1.0 MW cm^{-2} (4.14 mJ , 6.5 ns , 0.64 cm^{-2} area) laser pulse are absorbed by $5.0 \times 10^{-5} \text{ M}$ solutions of β -carotene in CCl_4 across a 1 cm pathlength in spite of the exceptionally large two-photon absorptivity of this compound ($\delta_{532} = 1.7 \times 10^7 \text{ GM}$; see text). In contrast, 34.16% of the 532 nm photons are absorbed via one-photon excitation under the same conditions, even though the molar extinction coefficient β -carotene in CCl_4 is relatively small ($\epsilon_{532} = 3,630 \text{ M}^{-1} \text{ cm}^{-1}$).
- (5) Stiel, H.; Teuchner, K.; Leupold, D.; Oberländer, S.; Ehlert, J. et al. Computer aided laser-spectroscopic characterization and handling of molecular excited states. *Intelligent Instruments & Computers* **1991**, *9*, 79-88.
- (6) Ehlert, J. A numerical solver for rate equations and photon transport equations in nonlinear laser spectroscopy. *Comp. Phys. Comm.* **2000**, *124*, 330.
- (7) Denk, W.; Strickler, J. N.; Webb, W. W. Two-photon laser scanning fluorescence microscopy. *Science* **1990**, *248*, 73-76.
- (8) Bennett, J. A.; Birge, R. R. Two-photon spectroscopy of diphenylbutadiene. The nature of the lowest-lying $1\text{Ag}^*-\pi\pi^*$ state. *J. Chem. Phys.* **1980**, *73*, 4234-4246.
- (9) Birge, R. R.; Murray, L. P.; Zidovetzki, R.; Knapp, H. M. Two-photon, ^{13}C and two dimensional ^1H NMR spectroscopic studies of retinyl Schiff bases, protonated Schiff bases, and Schiff base salts: Evidence for a protonated induced $\pi\pi^*$ excited state level ordering reversal. *J. Am. Chem. Soc.* **1987**, *109*, 2090-2101.
- (10) Krikunova, M. A.; Leupold, D.; Rini, M.; Voigt, B.; Moskalenko, A. A. et al. The two-photon fluorescence excitation spectrum of the light-harvesting complex LH2 from *Chromatium minutissimum* in the 650-745 nm range is determined by the two-photon absorption of bacteriochlorophyll, rather than carotenoids. *Biophysics* **2002**, *47*, 940-945.
- (11) Krikunova, M. A.; Kummrow, A.; Voigt, B.; Rini, M.; Lokstein, H. et al. Fluorescence of native and carotenoid-depleted LH2 from *Chromatium minutissimum*, originating from simultaneous two-photon absorption in the spectral range of the presumed (optically "dark") S_1 state of carotenoids. *FEBS Lett.* **2002**, *528*, 227-230.
- (12) Sipior, J.; Sulkes, M.; Auerbach, R.; Boivineau, M. Lifetimes of individual conformational bands of jet-cooled tryptophan analogues implications for nonexponential fluorescence decay of tryptophan and its analogues in solution. *J. Phys. Chem.* **1986**, *91*, 2016-2018.
- (13) Rice, J. K.; Anderson, R. W. Two-photon, thermal lensing spectroscopy of monosubstituted benzenes in the $^1\text{B}_{2u}(^1\text{L}_b) \rightarrow ^1\text{A}_{1g}(^1\text{A})$ and $^1\text{B}_{1u}(^1\text{L}_a) \rightarrow ^1\text{A}_{1g}(^1\text{A})$ transition regions. *J. Phys. Chem.* **1986**, *90*, 6793-6800.

- (14) Kurian, A.; Lee, S. T.; Unnikrishnan, K. P.; George, D. S.; Nampoory, V. P. N. et al. Studies on two-photon absorption of aniline using thermal lens effect. *J. Nonlinear Opt. Phys. Mater.* **2003**, *12*, 75-80.
- (15) Fang, H. L.; Swofford, R. L. The Thermal Lens in Absorption Spectroscopy. *Ultrasensitive Laser Spectroscopy*; Academic Press: New York, 1983; pp 172-232.
- (16) Al-Ahmed, Z.; Li, Y. J.; Gupta, R. Two-photon photothermal deflection spectroscopy of atomic sodium. *Rev. Scient. Instr.* **2003**, *74*, 349.
- (17) Braslavsky, S. E.; Heibel, G. E. Time-resolved photothermal and photoacoustic methods applied to photoinduced processes in solution. *Chem. Rev.* **1991**, *92*, 1381-1410.
- (18) Lee, J. M.; Kyu, S.; Park, S. M. Photoacoustic detection of multiphoton dissociation of molecular chlorine by probe beam deflection. *Bull. Korean Chem. Soc.* **1997**, *18*, 547-548.
- (19) Rizzo, T. R.; Park, Y. D.; Peteanu, L. A.; Levy, D. H. The electronic spectrum of the amino acid tryptophan in the gas phase. *J. Chem. Phys.* **1985**, *84*, 2534-2541.
- (20) Weinkauff, R.; Aicher, P.; Wesley, G.; Grottemeyer, J.; Schlag, E. W. Femtosecond versus nanosecond multiphoton ionization and dissociation of large molecules. *J. Phys. Chem.* **1994**, *98*, 8381-8391.
- (21) Weinkauff, R.; Schanen, R.; Metsala, A.; Schlag, E. W. Charge transfer in peptide-cations in the gas phase: Mechanism and new results. *J. Phys. Chem.* **1996**, *100*, 18567.
- (22) Birge, R. R.; Zhang, C.-F. Two-photon double resonance spectroscopy of bacteriorhodopsin. Assignment of the electronic and dipolar properties of the low-lying $^1A_g^{*-}$ -like and $^1B_u^{*-}$ -like π, π^* states. *J. Chem. Phys.* **1990**, *92*, 7178-7195.
- (23) Nikogosyan, D. N.; Letokhov, V. S. Nonlinear laser photophysics, photochemistry, and photobiology of nucleic acids. *Riv. Nuovo cimento* **1983**, *6*, 1-72.
- (24) Nikogosyan, D. N.; Angelov, D. A.; Oraevsky, A. A. Determination of parameters of excited states of DNA and RNA bases by laser UV photolysis. *Photochem. Photobiol.* **1982**, *35*, 627-635.
- (25) Angelov, D. A.; Kryukov, P. G.; Letokhov, V. S.; Nikogosyan, D. N.; Oraevskii, A. A. Selective interaction of ultrashort ultraviolet laser pulses with components of macromolecules. *Sov. J. Quant. Electron.* **1980**, *10*, 746-753.
- (26) Angelov, D. A.; Kryukov, P. G.; Letokhov, V. S.; Nikogosyan, D. N.; Oraevsky, A. A. Selective action on nucleic acids components by picosecond light pulses. *Appl. Phys.* **1980**, *21*, 391-395.
- (27) Kryukov, P. G.; Letokhov, V. S.; Nikogosyan, D. N.; Borodavkin, A. V.; Budowsky, E. I. et al. Multiquantum photoreactions of nucleic acid components in aqueous solution by powerful ultraviolet picosecond radiation. *Chem. Phys. Lett.* **1979**, *61*, 375-379.
- (28) Gurzadyan, G. G.; Nikogosyan, D. N.; Belogurov, A. A. Photochemical stability of aromatic amino acids on picosecond laser ultraviolet irradiation. *Biofizika* **1981**, *26*, 991-994.
- (29) The empirical average intensity of Nikogosyan, *et. al.* is equal to $I_{ave} = (1 - 10^{-D^*})/2.3D^*$ I_0 , in which D^* is the effective Beer's Law optical density of the solution which incorporates all beam attenuation effects, including those originating from biphotonic absorption by the chromophores of interest (DNA bases) and solvent (water). In short then, I_{ave} is an empirically determined longitudinally-and-temporally averaged first order intensity, and is similar in spirit to the spatio-temporally averaged mean squared intensities which we derive in Equations (16).
- (30) Chizhov, I. V.; Engelhard, M.; Sharkov, A. V.; Hess, B. Two quantum absorption of ultrashort laser pulses by the bacteriorhodopsin chromophore. *Structures and Functions of Retinal Proteins*; John Libbey Eurotext, Ltd.: Paris, 1992; pp 171-173.
- (31) Masthay, M. B.; Sammeth, D. M.; Helvenston, M. C.; Buckman, C. B.; Li, W. et al. The laser-induced blue state of bacteriorhodopsin: Mechanistic and color regulatory roles of protein-protein and protein-lipid interactions, and metal ions. *J. Am. Chem. Soc.* **2002**, *124*, 3418-3430.
- (32) Because BR is a strong one-photon absorber at the actinic wavelength ($\epsilon_{532} = 49,000 \text{ M}^{-1} \text{ cm}^{-1}$) the actinic intensity declines appreciably across the optical pathlength in accord with Beer's Law. According to Equations (15), the mean squared actinic intensity $I_{x,0}^2$ over a 1 cm pathlength is 3.7 times smaller than the squared incident intensity $I_{0,0}^2$ for typical ($A_{532} \sim 0.78$ at $t = 0$) samples. The number of BR molecules which absorbed two photons during the earliest stages of irradiation was thus more than 3 times smaller than that calculated in Reference 31, in which $I_{x,0}^2$ was assumed to be equal to $I_{0,0}^2$. The actual two photon absorptivity of BR must thus be significantly larger than that reported in Reference 31.

- (33) $I_{0,0}$ is most properly designated as the *incident initial intensity* since $I_{x,t}$ depends on both x and t in reactive samples. For simplicity and clarity we designate $I_{0,0}$ as the *incident intensity* throughout the remainder of this paper since $I_{0,t} = I_{0,0}$ are equal to the conventional, time-independent initial intensity I_0 used in Beer's Law I_0 for all t .
- (34) Longitudinally-and-temporally averaged intensities were anticipated in earlier work by Noyes and Leighton (Ref. 34) and Calvert and Pitts (see pp. 640-642 of Ref. 35).
- (35) Noyes, W. A.; P.A., L. *The Photochemistry of Gases*; Reinhold Publishing Co.: New York, 1941.
- (36) Calvert, J. G.; Pitts, J. N. J. *Photochemistry*; John Wiley & Sons.: New York, 1966.
- (37) Mortensen, A.; Skibsted, L. H. Free radical transients in photobleaching of xanthophylls and carotenes. *Free Rad. Res.* **1997**, *26*, 549-563.
- (38) Mortensen, A.; Skibsted, L. H. Kinetics of photobleaching of β -carotene in chloroform and formation of transient carotenoid species absorbing in the near infrared. *Free Rad. Res.* **1996**, *25*, 355-368.
- (39) Nielsen, B. R.; Mortensen, A.; Jørgensen, K.; Skibsted, L. H. Singlet versus triplet reactivity in photodegradation of C_{40} carotenoids. *J. Agr. Food Chem.* **1996**, *44*, 2106-2113.
- (40) Gurzadyan, G. G.; Steenken, S. Photoionization of β -carotene via electron transfer from excited states to chlorinated hydrocarbon solvents. A picosecond transient absorption study. *Phys. Chem. Chem. Phys.* **2002**, *4*, 2983-2988.
- (41) Limphong, P. Photodegradation of β -carotene in chloromethane solvents: Characterization of mechanism and products. In *Chemistry*; M.S. Thesis, Murray State University: Murray, KY, 2004.
- (42) Begum, F. Photodegradation of β -Carotene in Chloromethane Solvents: Effects of Molecular Oxygen and Nature of the Photoproducts. In *Chemistry*; M.S. Thesis, Murray State University: Murray, KY, 2006.
- (43) Jones, R. E.; McGregor, J.; Limphong, P.; Spencer, W. C.; Sveum, N. et al. Two-photon induced electron transfer between β -carotene and carbon tetrachloride. *56th Southeast Regional Meeting of the American Chemical Society*: Raleigh, NC, 11/13/04, 2004; pp Presentation #737.
- (44) Kogan, B. Nonlinear photodynamic therapy. Saturation of a photochemical dose by photosensitizer bleaching. *Photochem. Photobiol. Sci.* **2003**, *2*, 673-676.
- (45) Kogan, B. Nonlinear photodynamic therapy. Photochemical dose levelling within a tumor by saturating a photosensitizer's triplet states. *Photochem. Photobiol. Sci.* **2004**, *3*, 360-365.
- (46) Fournier, M. Ultrafast studies of the excited-state dynamics of copper and nickel phthalocyanine tetrasulfonates: Potential sensitizers for the two-photon photodynamic therapy of tumors. *Photochem. Photobiol. Sci.* **2004**, *3*, 120-126.
- (47) Bhawalkar, J. Two-photon photodynamic therapy. *SPIE Milestone Series* **2003**, *175*, 633-636.
- (48) Liu, J.; Zhao, Y. W.; Zhao, J. Q.; Xia, A. D.; Jiang, L. J. et al. Two-photon excitation studies of hypocrellins for photodynamic therapy. *J. Photochem. Photobiol. B. Biology* **2002**, *68*, 156-164.
- (49) Freyer, W.; Stiel, H.; Hild, M.; Teuchner, K.; Leupold, D. One- and two-photon-induced photochemistry of modified palladium porphyrazines involving molecular oxygen. *Photochem. Photobiol.* **1997**, *66*, 596-604.
- (50) Fisher, W. G.; Partridge, J., W. P.; Dees, C.; Wachter, E. A. Simultaneous two-photon activation of type-1 photodynamic therapy agents. *Photochem. Photobiol.* **1997**, *66*, 141-155.
- (51) Lambert, C. R.; Stiel, H.; Leupold, D.; Lynch, M. C.; Kochevar, I. E. Intensity-dependent enzyme photosensitization using 532 nm nanosecond laser pulses. *Photochem. Photobiol.* **1996**, *63*, 154-160.
- (52) Stiel, H.; Teuchner, K.; Paul, A.; Freyer, W.; Leupold, D. Two photon excitation of alkyl substituted magnesium phthalocyanine: Radical formation via higher excited states. *J. Photochem. Photobiol. A Chem.* **1994**, *80*, 289-298.
- (53) Oh, D. H.; Stanley, R. J.; Lin, M.; Hoeffler, W. K.; Boxer, S. G. et al. Two-photon excitation of 4'-hydroxymethyl-4,5',8-trimethylpsoralen. *Photochem. Photobiol.* **1997**, *65*, 91-95.
- (54) Freyer, W.; Stiel, H.; Teuchner, K.; Leupold, D. Photophysics and photochemistry of tetraanthraporphyrazines; attempts to obtain a new generation of photosensitizers. *J. Photochem. Photobiol. A: Chemistry* **1994**, *80*, 161-167.
- (55) Smith, G.; McGimpsey, W. G.; Lynch, M. C.; Kochevar, I. E.; Redmond, R. W. An efficient oxygen independent two-photon photosensitization mechanism. *Photochem. Photobiol.* **1994**, *59*, 135-139.

- (56) Teuchner, K.; Pfarrherr, A.; Stiel, H.; Freyer, W.; Leupold, D. Spectroscopic properties of potential sensitizers for new photodynamic therapy start mechanisms via two-step excited electronic states. *Photochem. Photobiol.* **1993**, *57*, 465-471.
- (57) Andreoni, A. Two-step photoactivation of hematoporphyrin by excimer-pumped dye laser pulses. *J. Photochem. Photobiol. B. Biol.* **1987**, *1*, 187-193.
- (58) Rückmann, I.; Zeug, A.; Herter, R.; Roder, B. On the influence of higher excited states on the ISC quantum yield of octa-*a*-alkyloxy-substituted Zn-phthalocyanine molecules studied by nonlinear absorption. *Photochem. Photobiol.* **1997**, *66*, 576-584.
- (59) Leupold, D. Proposal of modified mechanisms for photodynamic therapy. *J. Photochem. Photobiol.* **1992**, *12*, 311-314.
- (60) Simultaneous two-photon and sequential biphotonic processes both involve the absorption of two photons and hence both depend quadratically on actinic power. A *simultaneous two-photon process* is characterized by two effectively simultaneous (within 10 fs) resonant or non-resonant electric dipole transitions in which the second photon is absorbed by a short-lived virtual state intermediate comprised of a linear combination of eigenstates which lie within the energy uncertainty envelope $h/4\pi\tau_{int}$ of the excitation energy $h\nu$, in which τ_{int} is the intermediate state lifetime. A *sequential biphotonic process* is characterized by two *sequential* resonant electric dipole transitions in which the second photon is absorbed by an intermediate which is either a long-lived excited state or a long-lived ground state photoproduct.
- (61) Jones, R. E.; McGregor, J.; Limphong, P.; Spencer, W. C.; Sveum, N. et al. The photodegradation of β -carotene in chloromethane solvents. *55th Southeast Regional Meeting of the American Chemical Society*: Atlanta, GA, 2003; pp Poster #772.
- (62) Glória, M. B. A.; Grulke, E. A.; Gray, J. I. Effect of type of oxidation on beta-carotene loss and volatile products formation in model systems. *Food Chem.* **1993**, *46*, 401-406.
- (63) Hunter, R. F.; Krakenberger, R. M. The oxidation of beta-carotene in solution by oxygen. *J. Chem. Soc.* **1947**, 554-556.
- (64) Seely, G. R.; Meyer, T. H. The photosensitized oxidation of β -carotene. *Photochem. Photobiol.* **1971**, *13*, 27-32.
- (65) Foppen, F. H. Tables for the identification of carotenoid pigments. *Chromatogr. Rev.* **1971**, *14*, 133-298.
- (66) The lower limit for quadratic intensity dependence was not determined due to the limitations of the power meter in our laboratory, but quadratic behavior was clearly observed at intensities as low as 0.12 MW cm^{-2} .
- (67) Pariser, R. Theory of the electronic spectra and structure of the polyacenes and of alternant hydrocarbons. *J. Chem. Phys.* **1956**, *24*, 250-268.
- (68) Christensen, R. L.; Barney, E. A.; Broene, R. D.; Galinato, M. G. I.; Frank, H. A. Linear polyenes: models for the spectroscopy and photophysics of carotenoids. *Arch. Biochem. Biophys.* **2004**, *430*, 30-36.
- (69) Fujii, R.; Inaba, T.; Watanabe, Y.; Koyama, Y.; Zhang, J.-P. Two different pathways of internal conversion in carotenoids depending on the length of the conjugated chain. *Chem. Phys. Lett.* **2003**, *369*, 165-172.
- (70) Furuichi, K.; Sashima, T.; Koyama, Y. The first detection of the $3^1A_g^-$ state in carotenoids using resonance-Raman excitation profiles. *Chem. Phys. Lett.* **2002**, *356*, 547-555.
- (71) Christophersen, A. G.; Jun, H.; Jørgensen, K.; Skibsted, L. H. Photobleaching of astaxanthin and canthaxanthin. Quantum-yields dependence of solvent, temperature, and wavelength of irradiation in relation to packaging and storage of carotenoid pigmented salmonoids. *Zeit. Lebens. Unters. Forsch.* **1991**, *192*, 433-439.
- (72) Fujii, R.; Koyama, Y.; Mortensen, A.; Skibsted, L. H. Generation of radical cation of β -carotene in chloroform via the triplet state as revealed by time-resolved absorption spectroscopy. *Chem. Phys. Lett.* **2000**, *326*, 33-38.
- (73) Jørgensen, K.; Skibsted, L. H. Light sensitivity of carotenoids used as food colours. *Z. Lebens. Unters. Forsch.* **1990**, *190*, 306-313.
- (74) Langford, C. H.; Moralejo, C. Wavelength dependence of photochemical electron transfer reactions. *Photoinduced Electron Transfer*; Elsevier, 1988; pp 420-451.
- (75) Turro, N. J.; Ramamurthy, V.; Cherry, W.; Farneth, W. The effect of wavelength on organic photoreactions in solution. Reactions from upper excited states. *Chem. Rev.* **1978**, *78*, 125-145.

- (76) Jeevarajan, A. S.; Kispert, L. D.; Avdievich, N. I.; Forbes, M. D. E. Role of excited singlet state in the photooxidation of carotenoids: A time-resolved Q-band EPR study. *J. Phys. Chem.* **1996**, *100*, 669-671.
- (77) Kononova, T. A.; Kispert, L. D.; Kononov, V. V. Photoinduced electron transfer between carotenoids and solvent molecules. *J. Phys. Chem. B* **1997**, *101*, 7858-7862.
- (78) Fujii, R.; Fujino, T.; Inaba, T.; Nagae, H.; Koyama, Y. Internal conversion of $^1B_u^+$ \rightarrow $^1B_u^-$ \rightarrow $2^1A_g^-$ and fluorescence from the $^1B_u^-$ state in all-*trans*-neurosporene as probed by up-conversion spectroscopy. *Chem. Phys. Lett.* **2004**, *384*, 9-16.
- (79) Nishimura, K.; Rondonuwu, F. S.; Fujii, R.; Akahane, J.; Koyama, Y. et al. Sequential singlet internal conversion of $1^1B_u^+$ \rightarrow $3^1A_g^-$ \rightarrow $1^1B_u^-$ \rightarrow $2^1A_g^-$ \rightarrow ($1^1A_g^-$ ground) in all-*trans*-spirilloxanthin revealed by two-dimensional sub-5-fs spectroscopy. *Chem. Phys. Lett.* **2004**, *392*, 68-72.
- (80) Onaka, K.; Fujii, R.; Nagae, H.; Kuki, M.; Koyama, Y. et al. The state energy and the displacement of the potential minima of the $2A_g^-$ state in all-*trans*- β -carotene as determined by fluorescence spectroscopy. *Chem. Phys. Lett.* **1999**, *315*, 75-81.
- (81) Polivka, T.; Zigmantas, D.; Frank, H. A.; Bautista, J. A.; Herck, J. L. et al. Near-infrared time resolved study of the S_1 state dynamics of the carotenoid spheroidene. *J. Phys. Chem. B* **2001**, *105*, 1072-1080.
- (82) Rondonuwu, F. S.; Watanabe, Y.; Zhang, J.-P.; Furuichi, K.; Koyama, Y. Internal-conversion and radiative-transition processes among the $1B_u^+$ and $2A_g^-$ states of all-*trans*-neurosporene as revealed by subpicosecond time-resolved Raman spectroscopy. *Chem. Phys. Lett.* **2002**, *347*, 376-384.
- (83) Sashima, T.; Koyama, Y.; Yamada, T.; Hashimoto, H. The $1B_u^+$, $1B_u^-$, and $2A_g^-$ energies of crystalline lycopene, β -carotene, and mini-9- β -carotene as determined by resonance-Raman excitation profiles: Dependence of the $1B_u^-$ state energy on the conjugation length. *J. Phys. Chem. B* **2000**, *104*, 5011-5019.
- (84) Watanabe, Y.; Kameyama, T.; Miki, Y.; Kuki, M.; Koyama, Y. The $2^1A_g^-$ state and two additional low-lying electronic states of spheroidene newly identified by fluorescence and fluorescence-excitation spectroscopy at 170 K. *Chem. Phys. Lett.* **1993**, *206*, 62-68.
- (85) Zhang, J.-P.; Inaba, T.; Watanabe, Y.; Koyama, Y. Excited-state dynamics among the $1B_u^+$, $1B_u^-$ and $2A_g^-$ states of all-*trans*-neurosporene as revealed by near-infrared time-resolved absorption spectroscopy. *Chem. Phys. Lett.* **2000**, *332*, 351-358.
- (86) Zhang, J.-P.; Chen, C.-H.; Koyama, Y. Vibrational relaxation and redistribution in the $2A_g^-$ state of all-*trans*-lycopene as revealed by picosecond time-resolved absorption spectroscopy. *J. Phys. Chem. B* **1998**, *102*, 1632-1640.
- (87) Gurinovich, V. V.; Sagun, Y. I.; Tsvirko, M. P. Photochemical reactions of beta-carotene in carbon tetrachloride. *Biophysics* **1988**, *32*, 609-613.
- (88) Jones, R. E.; McGregor, J.; Limphong, P.; Spencer, W. C.; Sveum, N. et al. The photodegradation of β -carotene in chloromethane solvents. *Gordon Research Conference on Carotenoids*; Ventura, CA, 2004.
- (89) Zhang, J.-P.; Skibsted, L. H.; Fujii, R.; Koyama, Y. Transient absorption from the $^1B_u^+$ state of all-*trans*- β -carotene newly identified in the near-infrared region. *Photochem. Photobiol.* **2001**, *73*, 219-222.
- (90) Zhang, J.-P.; Fujii, R.; Koyama, Y.; Rondonuwu, F. S.; Watanabe, Y. et al. The $1B_u^-$ -type singlet state of β -carotene as a precursor of the radical cation found in chloroform solution by sub-picosecond time-resolved absorption spectroscopy. *Chem. Phys. Lett.* **2001**, *348*, 235-241.
- (91) Lyons, E. H., Jr.; Dickinson, R. G. The photo-oxidation of liquid carbon tetrachloride. *J. Am. Chem. Soc.* **1935**, *57*, 443-446.
- (92) Rath, H.; Sankar, J.; PrabhuRaja, P.; Chandrashekar, T. K.; Nag, A. et al. Core-modified expanded porphyrins with large third-order nonlinear optical response. *J. Am. Chem. Soc.* **2005**, *127*, 11608-11609.
- (93) Frederiksen, P. K.; McIlroy, S. P.; Nielsen, C. B.; Nikolajsen, L.; Skovsen, E. et al. Two-photon photosensitized production of singlet oxygen in water. *JACS* **2004**, *127*, 255-269.
- (94) McIlroy, S. P.; Clo, E.; Nikolajsen, L.; Frederiksen, P. K.; Nielsen, C. B. et al. Two-photon photosensitized production of singlet oxygen: Sensitizers with phenylene-ethynylene-based chromophores. *J. Org. Chem.* **2004**, *70*, 1134-1146.

- (95) Woo, H. Y.; Hong, J. W.; Liu, B.; Mikhailovsky, A.; Korystov, D. et al. Water-soluble [2.2]paracyclophane chromophores with large two-photon action cross sections. *J. Am. Chem. Soc.* **2004**, *127*, 820-821.
- (96) Collini, E.; Ferrante, C.; Bozio, R. Strong enhancement of the two-photon absorption of tetrakis(4-sulfonatophenyl)porphyrin diacid in water upon aggregation. *J. Phys. Chem. B Lett.* **2004**.
- (97) Geacintov, N. E.; Breton, J. Exciton annihilation and other nonlinear high-intensity excitation effects. *Biological Events Probed by Ultrafast Laser Spectroscopy*; Academic: New York, 1982; pp 157-191.
- (98) Arsenault, R.; Denariez-Roberge, M. M. Non-linear absorption and fluorescence of chlorophyll *a* excited by a ruby laser. *Chem. Phys. Lett.* **1976**, *63*, 84-87.
- (99) Macpherson, A. N.; Gillbro, T. Solvent dependence of the ultrafast S₂-S₁ internal conversion rate of B-carotene. *J. Phys. Chem. A.* **1998**, *102*, 5049-5058.
- (100) Chlorophyll *a* in diethyl ether has a two-photon absorptivity of $\delta \sim 10^7$ GM upon excitation with a pulsed ruby laser (see Refs. 74-75 and references cited therein). These authors ascribed the large δ value to "resonance phenomena" since the 694.3 nm ruby line overlaps with the intense S₁ absorption band of chlorophyll *a*. The lifetime of the S₁ state of chlorophyll *a* is 15.2 ns, indicating that the large δ value originates from a sequential biphotonic process which is not mediated by a virtual intermediate state.
- (101) Wilson, B. C.; Patterson, M. S. The physics, biophysics, and technology of photodynamic therapy. *Phys. Med. Biol.* **2008**, *53*, R61-R109 and references cited therein.
- (102) Spangler, C. W.; Starkey, J. R.; Rebane, A.; F., M.; Gong, A. et al. Synthesis, characterization, and preclinical studies of two-photon-activated targeted PDT therapeutic triads. *Proc. SPIE* **2006**, *6139*, 61390X-61391-61390X-61310.
- (103) Meerovich, G. A.; Vakoulovskaya, E. G.; Chental, V. V.; Misin, V. V.; Kogan, B. Y. et al. Possibility of deep photodynamic action on tumor tissues using aluminum phthalocyanine. *Proc. SPIE-Int. Soc. Opt. Eng.* **1996**, *2924*, 230-232.
- (104) Pogue, B. W.; Redmond, R. W.; Hasan, T. A study of dosimetry for pulsed-laser photodynamic therapy. *SPIE* **1996**, *2681*, 130-139.
- (105) Collins, H. A.; Khurana, M.; Moriyama, E. H.; Mariampillai, A.; Dahlstedt, E. et al. Blood-vessel closure using photosensitizers engineered for two-photon excitation. *Nature Photonics* **2008**, *2*, 420-424.
- (106) Samkoe, K. S.; Clancy, A. A.; Karotki, A.; Wilson, B. C.; Cramb, D. T. Complete blood vessel occlusion in the chick chorioallantoic membrane using two-photon excitation therapy: Implications for treatment of wet age-related macular degeneration. *J. Biomed. Opt.* **2007**, *12*, 034025.
- (107) Khurana, M.; Collins, H. A.; Karotki, A.; Anderson, H. L.; Cramb, D. T. et al. Quantitative *in vitro* demonstration of two-photon photodynamic therapy using Photofrin® and Visudyne®. *Photochem. Photobiol.* **2007**, *83*, 1441-1448.

APPENDIX

In Appendix, we provide a full table of n values obtained by the method of 56 points, as well as ϵ values obtained by full error propagation. n values greater than 2.7 are marked in red while those less than 1.3 are marked in blue. Rejected points are designated by a strikethrough (see text).

$\Delta t = 45s$

HA - HI vs. HA - LI	$n_{0,0,1}$	$\epsilon_{0,0,1}$	$n_{0,0,2}$	$\epsilon_{0,0,2}$	$n_{x,t,1}$	$n_{x,t,2}$
HA - 0.242 vs. HA - 0.121	2.105	2.039	1.981	1.911	2.000	2.057
HA - 0.363 vs. HA - 0.121	1.489	1.235	1.770	1.148	1.476	1.746
HA - 0.363 vs. HA - 0.242	0.435	1.088	1.409	1.012	0.466	1.281
HA - 0.484 vs. HA - 0.121	1.940	0.969	1.903	0.904	1.947	1.898
HA - 0.484 vs. HA - 0.242	1.775	0.531	1.825	0.548	1.887	1.751
HA - 0.484 vs. HA - 0.363	3.662	1.432	2.411	0.992	3.854	2.509
HA - 0.605 vs. HA - 0.121	1.840	0.829	1.752	0.771	1.829	1.728
HA - 0.605 vs. HA - 0.242	1.640	0.381	1.578	0.390	1.688	1.500
HA - 0.605 vs. HA - 0.363	2.597	0.654	1.712	0.459	2.591	1.688
HA - 0.605 vs. HA - 0.484	1.223	0.657	0.812	0.611	1.144	0.749
HA - 0.725 vs. HA - 0.121	1.951	0.747	1.798	0.692	1.913	1.786
HA - 0.725 vs. HA - 0.242	1.854	0.320	1.683	0.323	1.856	1.627
HA - 0.725 vs. HA - 0.363	2.683	0.470	1.843	0.327	2.588	1.851
HA - 0.725 vs. HA - 0.484	1.989	0.387	1.441	0.337	1.811	1.412
HA - 0.725 vs. HA - 0.605	2.926	0.956	2.210	0.817	2.579	2.343
HA - 0.967 vs. HA - 0.121	1.870	0.641	1.869	0.598	1.820	1.837
HA - 0.967 vs. HA - 0.242	1.753	0.246	1.813	0.256	1.726	1.735
HA - 0.967 vs. HA - 0.363	2.297	0.308	1.979	0.227	2.190	1.937
HA - 0.967 vs. HA - 0.484	1.731	0.195	1.800	0.196	1.588	1.719
HA - 0.967 vs. HA - 0.605	1.972	0.255	2.269	0.282	1.793	2.204
HA - 0.967 vs. HA - 0.725	1.367	0.270	2.307	0.389	1.269	2.127
HA - 1.21 vs. HA - 0.121	1.891	0.579	1.864	0.540	1.839	1.822
HA - 1.21 vs. HA - 0.242	1.799	0.212	1.814	0.220	1.767	1.728
HA - 1.21 vs. HA - 0.363	2.259	0.247	1.950	0.181	2.157	1.889
HA - 1.21 vs. HA - 0.484	1.818	0.145	1.805	0.143	1.687	1.712
HA - 1.21 vs. HA - 0.605	2.010	0.165	2.125	0.174	1.861	2.033
HA - 1.21 vs. HA - 0.725	1.683	0.156	2.094	0.190	1.586	1.937
HA - 1.21 vs. HA - 0.967	2.090	0.339	1.821	0.301	2.011	1.689

$\bar{n}_{pre-rejection}$	1.898	1.843
$S_{pre-rejection}$	0.459	0.468
$\bar{n}_{post-rejection}$	1.892	1.807
$S_{post-rejection}$	0.346	0.383
λ_{95}	0.094	0.103
$\bar{\epsilon}$	0.561	

Table VI-A. Full data set of $\Delta t = 45s$, HA - HI vs. HA - LI scenario.

$\Delta t = 45s$

LA - HI vs. LA - LI	$n_{0,0,1}$	$\epsilon_{0,0,1}$	$n_{0,0,2}$	$\epsilon_{0,0,2}$	$n_{x,t,1}$	$n_{x,t,2}$
LA - 0.242 vs. LA - 0.121	2.087	1.079	3.352	2.172	2.068	3.285
LA - 0.363 vs. LA - 0.121	1.911	0.641	2.520	1.282	1.907	2.474
LA - 0.363 vs. LA - 0.242	1.609	0.598	1.098	0.478	1.627	1.080
LA - 0.484 vs. LA - 0.121	1.926	0.505	2.457	1.008	1.914	2.419
LA - 0.484 vs. LA - 0.242	1.765	0.348	1.563	0.316	1.760	1.546
LA - 0.484 vs. LA - 0.363	1.985	0.634	2.218	0.712	1.941	2.209
LA - 0.605 vs. LA - 0.121	1.873	0.429	2.306	0.860	1.848	2.266
LA - 0.605 vs. LA - 0.242	1.711	0.251	1.515	0.228	1.683	1.491
LA - 0.605 vs. LA - 0.363	1.791	0.309	1.846	0.327	1.726	1.817
LA - 0.605 vs. LA - 0.484	1.541	0.488	1.365	0.451	1.458	1.325
LA - 0.725 vs. LA - 0.121	1.858	0.384	2.283	0.771	1.837	2.243
LA - 0.725 vs. LA - 0.242	1.714	0.206	1.609	0.194	1.692	1.582
LA - 0.725 vs. LA - 0.363	1.775	0.218	1.908	0.238	1.729	1.876
LA - 0.725 vs. LA - 0.484	1.626	0.264	1.688	0.275	1.579	1.644
LA - 0.725 vs. LA - 0.605	1.731	0.527	2.083	0.628	1.735	2.039
LA - 0.967 vs. LA - 0.121	1.809	0.328	2.269	0.664	1.777	2.214
LA - 0.967 vs. LA - 0.242	1.670	0.158	1.727	0.158	1.633	1.681
LA - 0.967 vs. LA - 0.363	1.696	0.143	1.988	0.167	1.636	1.926
LA - 0.967 vs. LA - 0.484	1.575	0.141	1.892	0.166	1.512	1.813
LA - 0.967 vs. LA - 0.605	1.592	0.173	2.142	0.227	1.538	2.041
LA - 0.967 vs. LA - 0.725	1.503	0.233	2.179	0.327	1.420	2.042
LA - 1.21 vs. LA - 0.121	1.886	0.299	2.250	0.599	1.834	2.189
LA - 1.21 vs. LA - 0.242	1.799	0.142	1.776	0.138	1.736	1.722
LA - 1.21 vs. LA - 0.363	1.863	0.123	2.005	0.134	1.770	1.934
LA - 1.21 vs. LA - 0.484	1.825	0.116	1.937	0.124	1.719	1.851
LA - 1.21 vs. LA - 0.605	1.916	0.131	2.122	0.145	1.802	2.017
LA - 1.21 vs. LA - 0.725	1.982	0.157	2.136	0.169	1.824	2.010
LA - 1.21 vs. LA - 0.967	2.599	0.380	2.079	0.306	2.315	1.968
$\bar{n}_{pre-rejection}$		1.909				1.852
$S_{pre-rejection}$		0.347				0.333
$\bar{n}_{post-rejection}$		1.883				1.826
$S_{post-rejection}$		0.289				0.273
λ_{95}		0.078				0.074
$\bar{\epsilon}$		0.405				

Table VI-B. Full data set of $\Delta t = 45s$, LA - HI vs. LA - LI scenario.

$\Delta t = 45s$

LA - HI vs. HA - LI	$n_{0,0,1}$	$\epsilon_{0,0,1}$	$n_{0,0,2}$	$\epsilon_{0,0,2}$	$n_{x,t,1}$	$n_{x,t,2}$
LA - 0.242 vs. HA - 0.121	3.643	2.195	3.609	2.076	2.004	2.006
LA - 0.363 vs. HA - 0.121	2.892	1.290	2.682	1.197	1.913	1.776
LA - 0.363 vs. HA - 0.242	4.238	1.454	3.881	1.384	1.845	1.587
LA - 0.484 vs. HA - 0.121	2.704	1.006	2.586	0.937	1.917	1.840
LA - 0.484 vs. HA - 0.242	3.303	0.678	3.191	0.676	1.868	1.666
LA - 0.484 vs. HA - 0.363	7.345	2.306	5.702	1.761	2.495	1.859
LA - 0.605 vs. HA - 0.121	2.543	0.857	2.417	0.797	1.868	1.786
LA - 0.605 vs. HA - 0.242	2.874	0.462	2.746	0.462	1.802	1.666
LA - 0.605 vs. HA - 0.363	4.810	0.884	3.808	0.671	2.269	1.827
LA - 0.605 vs. HA - 0.484	6.289	1.852	5.609	1.661	1.734	1.588
LA - 0.725 vs. HA - 0.121	2.460	0.766	2.383	0.714	1.858	1.806
LA - 0.725 vs. HA - 0.242	2.684	0.368	2.636	0.373	1.795	1.707
LA - 0.725 vs. HA - 0.363	4.000	0.564	3.354	0.437	2.192	1.859
LA - 0.725 vs. HA - 0.484	4.239	0.667	4.023	0.635	1.734	1.674
LA - 0.725 vs. HA - 0.605	7.931	2.299	7.954	2.309	1.921	1.980
LA - 0.967 vs. HA - 0.121	2.328	0.655	2.355	0.614	1.808	1.833
LA - 0.967 vs. HA - 0.242	2.439	0.276	2.541	0.288	1.736	1.758
LA - 0.967 vs. HA - 0.363	3.268	0.350	3.010	0.279	2.042	1.895
LA - 0.967 vs. HA - 0.484	3.104	0.281	3.258	0.290	1.660	1.763
LA - 0.967 vs. HA - 0.605	3.997	0.427	4.419	0.469	1.777	1.998
LA - 0.967 vs. HA - 0.725	4.676	0.693	5.819	0.860	1.581	1.930
LA - 1.21 vs. HA - 0.121	2.354	0.592	2.328	0.553	1.851	1.844
LA - 1.21 vs. HA - 0.242	2.461	0.237	2.477	0.244	1.802	1.780
LA - 1.21 vs. HA - 0.363	3.144	0.277	2.837	0.216	2.080	1.905
LA - 1.21 vs. HA - 0.484	2.981	0.200	2.971	0.198	1.766	1.794
LA - 1.21 vs. HA - 0.605	3.547	0.249	3.666	0.258	1.880	1.993
LA - 1.21 vs. HA - 0.725	3.768	0.297	4.186	0.332	1.748	1.938
LA - 1.21 vs. HA - 0.967	6.864	0.993	6.608	0.955	1.936	1.863
$\bar{n}_{pre-rejection}$		3.749			1.854	
$S_{pre-rejection}$		1.486			0.161	
$\bar{n}_{post-rejection}$		3.749			1.842	
$S_{post-rejection}$		1.486			0.136	
λ_{95}		0.562			0.036	
$\bar{\epsilon}$		0.800				

Table VI-C. Full data set of $\Delta t = 45s$, LA - HI vs. HA - LI scenario.

$\Delta t = 45s$

HA - HI vs. LA - LI	$n_{0,0,1}$	$\epsilon_{0,0,1}$	$n_{0,0,2}$	$\epsilon_{0,0,2}$	$n_{x,t,1}$	$n_{x,t,2}$
HA - 0.242 vs. LA - 0.121	0.549	0.945	1.724	2.007	2.248	9.373
HA - 0.363 vs. LA - 0.121	0.507	0.580	1.608	1.235	1.017	3.079
HA - 0.363 vs. LA - 0.242	-2.194	0.959	-1.375	0.663	5.861	4.169
HA - 0.484 vs. LA - 0.121	1.162	0.454	1.774	0.978	1.961	2.894
HA - 0.484 vs. LA - 0.242	0.237	0.236	0.196	0.224	1.349	0.954
HA - 0.484 vs. LA - 0.363	-1.698	0.628	-1.074	0.515	1.748	1.147
HA - 0.605 vs. LA - 0.121	1.170	0.389	1.641	0.837	1.777	2.419
HA - 0.605 vs. LA - 0.242	0.477	0.174	0.346	0.164	1.213	0.825
HA - 0.605 vs. LA - 0.363	-0.422	0.201	-0.250	0.215	5.259	4.657
HA - 0.605 vs. LA - 0.484	-3.525	1.070	-3.432	1.053	2.347	2.422
HA - 0.725 vs. LA - 0.121	1.349	0.356	1.699	0.752	1.908	2.408
HA - 0.725 vs. LA - 0.242	0.883	0.154	0.656	0.139	1.712	1.294
HA - 0.725 vs. LA - 0.363	0.459	0.127	0.397	0.143	1.917	1.904
HA - 0.725 vs. LA - 0.484	-0.624	0.167	-0.895	0.207	1.973	2.515
HA - 0.725 vs. LA - 0.605	-3.275	0.973	-3.661	1.092	1.640	1.784
HA - 0.967 vs. LA - 0.121	1.351	0.306	1.783	0.650	1.783	2.353
HA - 0.967 vs. LA - 0.242	0.984	0.124	0.998	0.120	1.555	1.593
HA - 0.967 vs. LA - 0.363	0.725	0.093	0.957	0.112	1.495	2.057
HA - 0.967 vs. LA - 0.484	0.202	0.072	0.434	0.080	0.771	1.793
HA - 0.967 vs. LA - 0.605	-0.433	0.095	-0.008	0.087	3.764	0.061
HA - 0.967 vs. LA - 0.725	-1.805	0.287	-1.333	0.225	2.200	1.544
HA - 1.21 vs. LA - 0.121	1.423	0.279	1.787	0.587	1.812	2.265
HA - 1.21 vs. LA - 0.242	1.137	0.111	1.112	0.107	1.650	1.614
HA - 1.21 vs. LA - 0.363	0.978	0.083	1.117	0.095	1.664	1.930
HA - 1.21 vs. LA - 0.484	0.662	0.062	0.772	0.068	1.466	1.732
HA - 1.21 vs. LA - 0.605	0.379	0.054	0.581	0.065	1.477	2.257
HA - 1.21 vs. LA - 0.725	-0.104	0.054	0.044	0.055	43.045	-2.853
HA - 1.21 vs. LA - 0.967	-2.175	0.328	-2.708	0.400	1.573	1.918
$\bar{n}_{pre-rejection}$		0.058			2.291	
$S_{pre-rejection}$		1.472			2.142	
$\bar{n}_{post-rejection}$		0.058			1.961	
$S_{post-rejection}$		1.472			1.234	
λ_{95}		0.393			0.336	
$\bar{\epsilon}$		0.397				

Table VI-D. Full data set of $\Delta t = 45s$, HA - HI vs. LA - LI scenario.

$\Delta t = 90s$

HA - HI vs. HA - LI	$n_{0,0,1}$	$\epsilon_{0,0,1}$	$n_{0,0,2}$	$\epsilon_{0,0,2}$	$n_{x,t,1}$	$n_{x,t,2}$
HA - 0.242 vs. HA - 0.121	1.967	1.023	1.912	1.039	1.861	1.977
HA - 0.363 vs. HA - 0.121	1.545	0.576	1.822	0.615	1.524	1.786
HA - 0.363 vs. HA - 0.242	0.824	0.520	1.668	0.657	0.876	1.501
HA - 0.484 vs. HA - 0.121	1.849	0.471	1.849	0.483	1.838	1.828
HA - 0.484 vs. HA - 0.242	1.732	0.350	1.785	0.365	1.813	1.691
HA - 0.484 vs. HA - 0.363	3.044	0.954	1.950	0.651	3.085	1.996
HA - 0.605 vs. HA - 0.121	1.777	0.398	1.770	0.408	1.746	1.727
HA - 0.605 vs. HA - 0.242	1.633	0.246	1.663	0.256	1.652	1.556
HA - 0.605 vs. HA - 0.363	2.275	0.403	1.659	0.303	2.216	1.603
HA - 0.605 vs. HA - 0.484	1.326	0.459	1.283	0.455	1.215	1.156
HA - 0.725 vs. HA - 0.121	1.856	0.362	1.783	0.367	1.793	1.748
HA - 0.725 vs. HA - 0.242	1.785	0.212	1.702	0.212	1.749	1.616
HA - 0.725 vs. HA - 0.363	2.348	0.291	1.722	0.218	2.199	1.689
HA - 0.725 vs. HA - 0.484	1.877	0.303	1.561	0.264	1.658	1.486
HA - 0.725 vs. HA - 0.605	2.550	0.760	1.900	0.593	2.158	1.944
HA - 0.967 vs. HA - 0.121	1.851	0.311	1.883	0.320	1.762	1.810
HA - 0.967 vs. HA - 0.242	1.793	0.166	1.869	0.175	1.711	1.734
HA - 0.967 vs. HA - 0.363	2.194	0.188	1.952	0.161	2.009	1.835
HA - 0.967 vs. HA - 0.484	1.855	0.162	1.952	0.170	1.626	1.776
HA - 0.967 vs. HA - 0.605	2.106	0.224	2.270	0.240	1.810	2.074
HA - 0.967 vs. HA - 0.725	1.824	0.278	2.504	0.375	1.583	2.143
HA - 1.21 vs. HA - 0.121	1.845	0.280	1.868	0.288	1.746	1.776
HA - 1.21 vs. HA - 0.242	1.792	0.142	1.849	0.148	1.697	1.700
HA - 1.21 vs. HA - 0.363	2.119	0.147	1.910	0.127	1.934	1.769
HA - 1.21 vs. HA - 0.484	1.838	0.118	1.898	0.121	1.623	1.706
HA - 1.21 vs. HA - 0.605	2.003	0.137	2.096	0.144	1.748	1.882
HA - 1.21 vs. HA - 0.725	1.808	0.144	2.165	0.172	1.596	1.863
HA - 1.21 vs. HA - 0.967	1.786	0.266	1.729	0.258	1.613	1.499
$\bar{n}_{pre-rejection}$		1.878			1.763	
$S_{pre-rejection}$		0.314			0.296	
$\bar{n}_{post-rejection}$		1.876			1.739	
$S_{post-rejection}$		0.238			0.237	
λ_{95}		0.065			0.064	
$\bar{\epsilon}$		0.348				

Table VII-A. Full data set of $\Delta t = 90s$, HA - HI vs. HA - LI scenario.

$\Delta t = 90s$

LA - HI vs. LA - LI	$n_{0,0,1}$	$\epsilon_{0,0,1}$	$n_{0,0,2}$	$\epsilon_{0,0,2}$	$n_{x,t,1}$	$n_{x,t,2}$
LA - 0.242 vs. LA - 0.121	1.924	0.732	2.400	0.899	1.898	2.340
LA - 0.363 vs. LA - 0.121	1.842	0.428	1.960	0.473	1.827	1.912
LA - 0.363 vs. LA - 0.242	1.702	0.537	1.208	0.393	1.702	1.179
LA - 0.484 vs. LA - 0.121	1.888	0.339	1.955	0.369	1.859	1.909
LA - 0.484 vs. LA - 0.242	1.852	0.316	1.509	0.259	1.821	1.477
LA - 0.484 vs. LA - 0.363	2.064	0.612	1.934	0.577	1.980	1.898
LA - 0.605 vs. LA - 0.121	1.848	0.286	1.895	0.309	1.805	1.845
LA - 0.605 vs. LA - 0.242	1.791	0.224	1.513	0.190	1.736	1.471
LA - 0.605 vs. LA - 0.363	1.862	0.292	1.756	0.277	1.762	1.701
LA - 0.605 vs. LA - 0.484	1.601	0.470	1.526	0.451	1.489	1.453
LA - 0.725 vs. LA - 0.121	1.843	0.255	1.901	0.277	1.799	1.846
LA - 0.725 vs. LA - 0.242	1.792	0.183	1.585	0.162	1.738	1.536
LA - 0.725 vs. LA - 0.363	1.845	0.205	1.806	0.201	1.758	1.743
LA - 0.725 vs. LA - 0.484	1.689	0.256	1.716	0.260	1.602	1.636
LA - 0.725 vs. LA - 0.605	1.797	0.521	1.949	0.565	1.747	1.859
LA - 0.967 vs. LA - 0.121	1.742	0.211	1.899	0.238	1.692	1.831
LA - 0.967 vs. LA - 0.242	1.651	0.133	1.648	0.130	1.592	1.580
LA - 0.967 vs. LA - 0.363	1.630	0.124	1.830	0.138	1.548	1.742
LA - 0.967 vs. LA - 0.484	1.450	0.121	1.786	0.147	1.372	1.680
LA - 0.967 vs. LA - 0.605	1.379	0.142	1.910	0.195	1.315	1.785
LA - 0.967 vs. LA - 0.725	1.114	0.167	1.885	0.276	1.049	1.739
LA - 1.21 vs. LA - 0.121	1.778	0.193	1.852	0.211	1.713	1.784
LA - 1.21 vs. LA - 0.242	1.716	0.117	1.615	0.109	1.635	1.548
LA - 1.21 vs. LA - 0.363	1.720	0.104	1.753	0.106	1.614	1.669
LA - 1.21 vs. LA - 0.484	1.612	0.097	1.696	0.102	1.503	1.600
LA - 1.21 vs. LA - 0.605	1.616	0.106	1.750	0.115	1.507	1.647
LA - 1.21 vs. LA - 0.725	1.552	0.120	1.680	0.130	1.426	1.572
LA - 1.21 vs. LA - 0.967	2.117	0.306	1.414	0.207	1.886	1.349
$\bar{n}_{pre-rejection}$		1.745				1.673
$S_{pre-rejection}$		0.211				0.210
$\bar{n}_{post-rejection}$		1.734				1.661
$S_{post-rejection}$		0.194				0.191
λ_{95}		0.052				0.052
$\bar{\epsilon}$		0.274				

Table VII-B. Full data set of $\Delta t = 90s$, LA - HI vs. LA - LI scenario.

$\Delta t = 90s$

LA - HI vs. HA - LI	$n_{0,0,1}$	$\epsilon_{0,0,1}$	$n_{0,0,2}$	$\epsilon_{0,0,2}$	$n_{x,t,1}$	$n_{x,t,2}$
LA - 0.242 vs. HA - 0.121	3.324	1.318	3.597	1.406	1.825	1.992
LA - 0.363 vs. HA - 0.121	2.725	0.711	2.715	0.722	1.795	1.790
LA - 0.363 vs. HA - 0.242	4.022	1.242	4.088	1.267	1.743	1.664
LA - 0.484 vs. HA - 0.121	2.588	0.541	2.553	0.548	1.823	1.806
LA - 0.484 vs. HA - 0.242	3.210	0.554	3.194	0.557	1.801	1.676
LA - 0.484 vs. HA - 0.363	6.572	1.935	5.344	1.572	2.214	1.767
LA - 0.605 vs. HA - 0.121	2.451	0.452	2.411	0.457	1.787	1.768
LA - 0.605 vs. HA - 0.242	2.818	0.363	2.788	0.365	1.750	1.676
LA - 0.605 vs. HA - 0.363	4.400	0.697	3.676	0.579	2.055	1.750
LA - 0.605 vs. HA - 0.484	6.190	1.788	5.901	1.706	1.699	1.663
LA - 0.725 vs. HA - 0.121	2.385	0.399	2.364	0.406	1.784	1.776
LA - 0.725 vs. HA - 0.242	2.648	0.283	2.648	0.287	1.750	1.697
LA - 0.725 vs. HA - 0.363	3.715	0.424	3.222	0.363	2.010	1.767
LA - 0.725 vs. HA - 0.484	4.215	0.634	4.124	0.621	1.708	1.701
LA - 0.725 vs. HA - 0.605	7.750	2.221	7.600	2.180	1.867	1.884
LA - 0.967 vs. HA - 0.121	2.209	0.332	2.297	0.345	1.701	1.771
LA - 0.967 vs. HA - 0.242	2.330	0.199	2.490	0.213	1.641	1.703
LA - 0.967 vs. HA - 0.363	2.952	0.236	2.830	0.219	1.825	1.761
LA - 0.967 vs. HA - 0.484	2.928	0.244	3.195	0.265	1.554	1.710
LA - 0.967 vs. HA - 0.605	3.688	0.376	4.102	0.417	1.632	1.841
LA - 0.967 vs. HA - 0.725	4.409	0.643	5.498	0.800	1.498	1.820
LA - 1.21 vs. HA - 0.121	2.200	0.299	2.212	0.306	1.717	1.738
LA - 1.21 vs. HA - 0.242	2.300	0.168	2.341	0.174	1.669	1.667
LA - 1.21 vs. HA - 0.363	2.797	0.181	2.567	0.161	1.833	1.708
LA - 1.21 vs. HA - 0.484	2.730	0.167	2.761	0.169	1.607	1.655
LA - 1.21 vs. HA - 0.605	3.182	0.210	3.237	0.214	1.680	1.751
LA - 1.21 vs. HA - 0.725	3.408	0.262	3.714	0.286	1.587	1.720
LA - 1.21 vs. HA - 0.967	5.449	0.784	5.275	0.759	1.588	1.535
$\bar{n}_{pre-rejection}$		3.542			1.748	
$S_{pre-rejection}$		1.356			0.123	
$\bar{n}_{post-rejection}$		3.465			1.740	
$S_{post-rejection}$		1.241			0.107	
λ_{95}		0.335			0.029	
$\bar{\epsilon}$		0.625				

Table VII-C. Full data set of $\Delta t = 90s$, LA - HI vs. HA - LI scenario.

$\Delta t = 90s$

HA - HI vs. LA - LI	$n_{0,0,1}$	$\epsilon_{0,0,1}$	$n_{0,0,2}$	$\epsilon_{0,0,2}$	$n_{x,t,1}$	$n_{x,t,2}$
HA - 0.242 vs. LA - 0.121	0.567	0.465	0.716	0.550	2.277	3.816
HA - 0.363 vs. LA - 0.121	0.662	0.285	1.067	0.358	1.312	2.019
HA - 0.363 vs. LA - 0.242	-1.496	0.532	-1.212	0.429	4.083	3.771
HA - 0.484 vs. LA - 0.121	1.149	0.257	1.251	0.295	1.909	2.012
HA - 0.484 vs. LA - 0.242	0.375	0.131	0.101	0.107	1.964	0.463
HA - 0.484 vs. LA - 0.363	-1.496	0.472	-1.460	0.465	1.576	1.588
HA - 0.605 vs. LA - 0.121	1.174	0.222	1.255	0.252	1.752	1.821
HA - 0.605 vs. LA - 0.242	0.606	0.109	0.389	0.087	1.478	0.894
HA - 0.605 vs. LA - 0.363	-0.263	0.099	-0.262	0.103	4.558	7.948
HA - 0.605 vs. LA - 0.484	-3.263	0.950	-3.092	0.903	2.211	2.226
HA - 0.725 vs. LA - 0.121	1.314	0.209	1.321	0.231	1.820	1.838
HA - 0.725 vs. LA - 0.242	0.929	0.111	0.639	0.084	1.726	1.219
HA - 0.725 vs. LA - 0.363	0.477	0.077	0.307	0.070	1.778	1.320
HA - 0.725 vs. LA - 0.484	-0.649	0.118	-0.847	0.147	2.311	2.606
HA - 0.725 vs. LA - 0.605	-3.403	0.980	-3.752	1.082	1.753	1.868
HA - 0.967 vs. LA - 0.121	1.385	0.185	1.484	0.209	1.771	1.901
HA - 0.967 vs. LA - 0.242	1.115	0.097	1.026	0.088	1.675	1.559
HA - 0.967 vs. LA - 0.363	0.872	0.074	0.951	0.079	1.653	1.876
HA - 0.967 vs. LA - 0.484	0.377	0.045	0.544	0.056	1.202	1.844
HA - 0.967 vs. LA - 0.605	-0.203	0.044	0.077	0.041	4.276	-1.211
HA - 0.967 vs. LA - 0.725	-1.471	0.220	-1.109	0.170	2.016	1.443
HA - 1.21 vs. LA - 0.121	1.423	0.169	1.508	0.190	1.750	1.846
HA - 1.21 vs. LA - 0.242	1.208	0.088	1.124	0.080	1.662	1.546
HA - 1.21 vs. LA - 0.363	1.042	0.067	1.096	0.070	1.640	1.747
HA - 1.21 vs. LA - 0.484	0.720	0.048	0.832	0.055	1.420	1.651
HA - 1.21 vs. LA - 0.605	0.437	0.037	0.609	0.047	1.348	1.855
HA - 1.21 vs. LA - 0.725	-0.048	0.026	0.131	0.029	-0.659	1.836
HA - 1.21 vs. LA - 0.967	-1.546	0.228	-2.131	0.309	1.287	1.727
$\bar{n}_{pre-rejection}$		0.081				1.938
$S_{pre-rejection}$		1.340				1.243
$\bar{n}_{post-rejection}$		0.081				1.830
$S_{post-rejection}$		1.340				0.949
λ_{95}		0.358				0.256
$\bar{\epsilon}$		0.231				

Table VII-D. Full data set of $\Delta t = 90s$, HA - HI vs. LA - LI scenario.

$\Delta t = 180s$

HA - HI vs. HA - LI	$n_{0,0,1}$	$\epsilon_{0,0,1}$	$n_{0,0,2}$	$\epsilon_{0,0,2}$	$n_{x,t,1}$	$n_{x,t,2}$
HA - 0.242 vs. HA - 0.121	2.063	0.786	1.937	0.768	1.934	1.987
HA - 0.363 vs. HA - 0.121	1.725	0.419	1.935	0.459	1.681	1.872
HA - 0.363 vs. HA - 0.242	4.448	0.401	1.932	0.614	1.199	1.703
HA - 0.484 vs. HA - 0.121	1.928	0.350	1.963	0.361	1.879	1.902
HA - 0.484 vs. HA - 0.242	1.793	0.307	1.988	0.341	1.819	1.826
HA - 0.484 vs. HA - 0.363	2.702	0.801	2.067	0.618	2.634	2.020
HA - 0.605 vs. HA - 0.121	1.863	0.292	1.895	0.301	1.789	1.806
HA - 0.605 vs. HA - 0.242	1.713	0.215	1.864	0.235	1.674	1.685
HA - 0.605 vs. HA - 0.363	2.161	0.341	1.809	0.286	2.009	1.671
HA - 0.605 vs. HA - 0.484	1.464	0.437	1.477	0.441	1.284	1.274
HA - 0.725 vs. HA - 0.121	1.918	0.267	1.884	0.269	1.801	1.796
HA - 0.725 vs. HA - 0.242	1.826	0.186	1.851	0.191	1.716	1.689
HA - 0.725 vs. HA - 0.363	2.223	0.247	1.803	0.201	1.974	1.680
HA - 0.725 vs. HA - 0.484	1.883	0.285	1.616	0.247	1.572	1.458
HA - 0.725 vs. HA - 0.605	2.396	0.692	1.786	0.522	1.890	1.708
HA - 0.967 vs. HA - 0.121	1.932	0.230	1.968	0.237	1.767	1.816
HA - 0.967 vs. HA - 0.242	1.866	0.147	1.983	0.158	1.687	1.743
HA - 0.967 vs. HA - 0.363	2.163	0.163	2.004	0.150	1.852	1.760
HA - 0.967 vs. HA - 0.484	1.940	0.159	1.978	0.162	1.581	1.667
HA - 0.967 vs. HA - 0.605	2.166	0.220	2.216	0.225	1.708	1.848
HA - 0.967 vs. HA - 0.725	2.021	0.296	2.488	0.363	1.592	1.919
HA - 1.21 vs. HA - 0.121	1.872	0.203	1.897	0.209	1.706	1.737
HA - 1.21 vs. HA - 0.242	1.791	0.121	1.880	0.128	1.611	1.645
HA - 1.21 vs. HA - 0.363	2.007	0.121	1.863	0.112	1.725	1.626
HA - 1.21 vs. HA - 0.484	1.789	0.107	1.799	0.108	1.483	1.519
HA - 1.21 vs. HA - 0.605	1.893	0.124	1.902	0.125	1.542	1.596
HA - 1.21 vs. HA - 0.725	1.714	0.132	1.944	0.150	1.412	1.562
HA - 1.21 vs. HA - 0.967	1.319	0.193	1.242	0.182	1.155	1.055
$\bar{n}_{pre-rejection}$		1.897			1.701	
$S_{pre-rejection}$		0.261			0.244	
$\bar{n}_{post-rejection}$		1.911			1.684	
$S_{post-rejection}$		0.243			0.210	
λ_{95}		0.065			0.057	
$\bar{\epsilon}$		0.293				

Table VIII-A. Full data set of $\Delta t = 180s$, HA - HI vs. HA - LI scenario.

$\Delta t = 180s$

LA - HI vs. LA - LI	$n_{0,0,1}$	$\epsilon_{0,0,1}$	$n_{0,0,2}$	$\epsilon_{0,0,2}$	$n_{x,t,1}$	$n_{x,t,2}$
LA - 0.242 vs. LA - 0.121	1.863	0.625	2.586	0.867	1.821	2.490
LA - 0.363 vs. LA - 0.121	1.739	0.350	2.073	0.425	1.706	1.996
LA - 0.363 vs. LA - 0.242	1.526	0.460	1.196	0.362	1.506	1.152
LA - 0.484 vs. LA - 0.121	1.831	0.285	2.001	0.320	1.777	1.928
LA - 0.484 vs. LA - 0.242	1.800	0.294	1.417	0.232	1.733	1.366
LA - 0.484 vs. LA - 0.363	2.186	0.637	1.729	0.505	2.035	1.666
LA - 0.605 vs. LA - 0.121	1.797	0.239	1.935	0.265	1.729	1.856
LA - 0.605 vs. LA - 0.242	1.748	0.208	1.443	0.172	1.661	1.380
LA - 0.605 vs. LA - 0.363	1.923	0.295	1.639	0.252	1.776	1.558
LA - 0.605 vs. LA - 0.484	1.584	0.457	1.524	0.441	1.448	1.424
LA - 0.725 vs. LA - 0.121	1.771	0.211	1.895	0.233	1.703	1.815
LA - 0.725 vs. LA - 0.242	1.713	0.167	1.459	0.142	1.630	1.393
LA - 0.725 vs. LA - 0.363	1.822	0.198	1.613	0.175	1.698	1.531
LA - 0.725 vs. LA - 0.484	1.564	0.233	1.530	0.229	1.459	1.438
LA - 0.725 vs. LA - 0.605	1.540	0.442	1.538	0.442	1.473	1.455
LA - 0.967 vs. LA - 0.121	1.535	0.159	1.792	0.191	1.481	1.713
LA - 0.967 vs. LA - 0.242	1.371	0.105	1.396	0.106	1.314	1.329
LA - 0.967 vs. LA - 0.363	1.307	0.097	1.479	0.109	1.237	1.400
LA - 0.967 vs. LA - 0.484	0.942	0.078	1.375	0.112	0.898	1.293
LA - 0.967 vs. LA - 0.605	0.638	0.067	1.304	0.132	0.621	1.230
LA - 0.967 vs. LA - 0.725	0.066	0.028	1.156	0.169	0.065	1.088
LA - 1.21 vs. LA - 0.121	1.528	0.143	1.663	0.162	1.466	1.595
LA - 1.21 vs. LA - 0.242	1.384	0.090	1.265	0.082	1.317	1.212
LA - 1.21 vs. LA - 0.363	1.336	0.079	1.289	0.076	1.257	1.232
LA - 1.21 vs. LA - 0.484	1.069	0.064	1.151	0.069	1.009	1.097
LA - 1.21 vs. LA - 0.605	0.904	0.059	1.031	0.068	0.862	0.989
LA - 1.21 vs. LA - 0.725	0.677	0.053	0.850	0.066	0.644	0.819
LA - 1.21 vs. LA - 0.967	1.464	0.212	0.454	0.071	1.338	0.452
$\bar{n}_{pre-rejection}$		1.472				1.403
$S_{pre-rejection}$		0.434				0.415
$\bar{n}_{post-rejection}$		1.497				1.427
$S_{post-rejection}$		0.393				0.376
λ_{95}		0.106				0.101
$\bar{\epsilon}$		0.229				

Table VIII-B. Full data set of $\Delta t = 180s$, LA - HI vs. LA - LI scenario.

$\Delta t = 180s$

LA - HI vs. HA - LI	$n_{0,0,1}$	$\epsilon_{0,0,1}$	$n_{0,0,2}$	$\epsilon_{0,0,2}$	$n_{x,t,1}$	$n_{x,t,2}$
LA - 0.242 vs. HA - 0.121	3.504	1.199	3.818	1.302	1.913	2.100
LA - 0.363 vs. HA - 0.121	2.774	0.589	2.850	0.609	1.813	1.863
LA - 0.363 vs. HA - 0.242	3.990	1.195	4.411	1.322	1.718	1.779
LA - 0.484 vs. HA - 0.121	2.652	0.442	2.617	0.443	1.848	1.833
LA - 0.484 vs. HA - 0.242	3.242	0.532	3.298	0.544	1.796	1.702
LA - 0.484 vs. HA - 0.363	6.192	1.801	5.222	1.519	2.065	1.665
LA - 0.605 vs. HA - 0.121	2.504	0.361	2.466	0.362	1.804	1.789
LA - 0.605 vs. HA - 0.242	2.838	0.342	2.866	0.347	1.739	1.702
LA - 0.605 vs. HA - 0.363	4.179	0.642	3.606	0.554	1.929	1.702
LA - 0.605 vs. HA - 0.484	6.084	1.749	5.592	1.608	1.673	1.583
LA - 0.725 vs. HA - 0.121	2.406	0.313	2.371	0.314	1.778	1.762
LA - 0.725 vs. HA - 0.242	2.623	0.259	2.645	0.263	1.709	1.675
LA - 0.725 vs. HA - 0.363	3.485	0.380	3.062	0.333	1.862	1.665
LA - 0.725 vs. HA - 0.484	4.041	0.601	3.769	0.561	1.635	1.558
LA - 0.725 vs. HA - 0.605	7.195 2.058	2.058	6.573	1.880	1.754	1.660
LA - 0.967 vs. HA - 0.121	2.082	0.242	2.203	0.256	1.594	1.686
LA - 0.967 vs. HA - 0.242	2.092	0.163	2.336	0.182	1.466	1.587
LA - 0.967 vs. HA - 0.363	2.482	0.185	2.503	0.185	1.532	1.553
LA - 0.967 vs. HA - 0.484	2.391	0.195	2.684	0.218	1.280	1.447
LA - 0.967 vs. HA - 0.605	2.831	0.286	3.258	0.328	1.279	1.490
LA - 0.967 vs. HA - 0.725	3.107	0.452	4.190	0.608	1.105	1.440
LA - 1.21 vs. HA - 0.121	2.022	0.214	2.034	0.218	1.573	1.592
LA - 1.21 vs. HA - 0.242	2.005	0.134	2.075	0.140	1.452	1.475
LA - 1.21 vs. HA - 0.363	2.293	0.137	2.123	0.126	1.506	1.417
LA - 1.21 vs. HA - 0.484	2.165	0.129	2.141	0.128	1.289	1.299
LA - 1.21 vs. HA - 0.605	2.391	0.156	2.355	0.153	1.291	1.304
LA - 1.21 vs. HA - 0.725	2.389	0.183	2.558	0.196	1.159	1.232
LA - 1.21 vs. HA - 0.967	2.865	0.412	2.648	0.381	0.929	0.859
$\bar{n}_{pre-rejection}$		3.163			1.588	
$S_{pre-rejection}$		1.229			0.257	
$\bar{n}_{post-rejection}$		3.089			1.588	
$S_{post-rejection}$		1.110			0.257	
λ_{95}		0.299			0.069	
$\bar{\epsilon}$		0.543				

Table VIII-C. Full data set of $\Delta t = 180s$, LA - HI vs. HA - LI scenario.

$\Delta t = 180s$

HA - HI vs. LA - LI	$n_{0,0,1}$	$\epsilon_{0,0,1}$	$n_{0,0,2}$	$\epsilon_{0,0,2}$	$n_{x,t,1}$	$n_{x,t,2}$
HA - 0.242 vs. LA - 0.121	0.421	0.236	0.705	0.346	1.638	3.610
HA - 0.363 vs. LA - 0.121	0.690	0.174	1.158	0.269	1.337	2.136
HA - 0.363 vs. LA - 0.242	-1.316	0.411	-1.283	0.396	3.746	4.182
HA - 0.484 vs. LA - 0.121	1.107	0.185	1.347	0.233	1.782	2.098
HA - 0.484 vs. LA - 0.242	0.351	0.078	0.107	0.052	1.596	0.438
HA - 0.484 vs. LA - 0.363	-1.304	0.389	-1.426	0.423	1.452	1.637
HA - 0.605 vs. LA - 0.121	1.157	0.164	1.365	0.201	1.668	1.912
HA - 0.605 vs. LA - 0.242	0.622	0.083	0.441	0.062	1.401	0.942
HA - 0.605 vs. LA - 0.363	-0.095	0.046	-0.158	0.049	12.132	-9.874
HA - 0.605 vs. LA - 0.484	-3.036	0.874	-2.590	0.747	2.164	1.991
HA - 0.725 vs. LA - 0.121	1.283	0.159	1.408	0.184	1.706	1.883
HA - 0.725 vs. LA - 0.242	0.917	0.093	0.664	0.069	1.578	1.178
HA - 0.725 vs. LA - 0.363	0.560	0.067	0.353	0.047	1.709	1.232
HA - 0.725 vs. LA - 0.484	-0.594	0.094	-0.622	0.099	2.936	2.531
HA - 0.725 vs. LA - 0.605	-3.259	0.933	-3.249	0.930	1.822	1.750
HA - 0.967 vs. LA - 0.121	1.385	0.145	1.557	0.170	1.682	1.891
HA - 0.967 vs. LA - 0.242	1.146	0.088	1.043	0.080	1.583	1.457
HA - 0.967 vs. LA - 0.363	0.988	0.074	0.980	0.073	1.637	1.680
HA - 0.967 vs. LA - 0.484	0.491	0.043	0.669	0.057	1.203	1.696
HA - 0.967 vs. LA - 0.605	-0.027	0.020	0.263	0.034	-0.330	3.578
HA - 0.967 vs. LA - 0.725	-1.021	0.151	-0.546	0.084	1.936	0.993
HA - 1.21 vs. LA - 0.121	1.378	0.131	1.526	0.151	1.614	1.780
HA - 1.21 vs. LA - 0.242	1.170	0.077	1.070	0.070	1.497	1.373
HA - 1.21 vs. LA - 0.363	1.050	0.063	1.028	0.061	1.492	1.484
HA - 1.21 vs. LA - 0.484	0.693	0.042	0.808	0.049	1.180	1.382
HA - 1.21 vs. LA - 0.605	0.406	0.029	0.578	0.040	0.958	1.348
HA - 1.21 vs. LA - 0.725	0.001	0.015	0.235	0.024	0.006	1.150
HA - 1.21 vs. LA - 0.967	-0.082	0.036	-0.952	0.140	0.097	1.056
$\bar{n}_{pre-rejection}$		0.206			1.638	
$S_{pre-rejection}$		1.204			2.250	
$\bar{n}_{post-rejection}$		0.206			1.657	
$S_{post-rejection}$		1.204			0.823	
λ_{95}		0.322			0.224	
$\bar{\epsilon}$		0.179				

Table VIII-D. Full data set of $\Delta t = 180s$, HA - HI vs. LA - LI scenario.

$$I\Delta t = 0.9J$$

HA - HI vs. HA - LI	$n_{0,0,1}$	$\epsilon_{0,0,1}$	$n_{0,0,2}$	$\epsilon_{0,0,2}$	$n_{x,t,1}$	$n_{x,t,2}$
HA - 0.242 vs. HA - 0.121	2.031	0.809	2.007	0.820	1.927	2.081
HA - 0.363 vs. HA - 0.121	1.473	0.427	1.785	0.458	1.462	1.762
HA - 0.363 vs. HA - 0.242	0.520	0.647	1.405	0.680	0.560	1.282
HA - 0.484 vs. HA - 0.121	1.828	0.347	1.893	0.361	1.839	1.892
HA - 0.484 vs. HA - 0.242	1.624	0.367	1.778	0.390	1.739	1.716
HA - 0.484 vs. HA - 0.363	3.484	1.155	2.304	0.883	3.378	2.420
HA - 0.605 vs. HA - 0.121	1.734	0.288	1.706	0.293	1.730	1.690
HA - 0.605 vs. HA - 0.242	1.510	0.261	1.478	0.271	1.568	1.416
HA - 0.605 vs. HA - 0.363	2.295	0.522	1.536	0.414	2.318	1.533
HA - 0.605 vs. HA - 0.484	1.154	0.716	0.546	0.689	1.096	0.512
HA - 0.725 vs. HA - 0.121	1.859	0.265	1.751	0.263	1.837	1.751
HA - 0.725 vs. HA - 0.242	1.751	0.220	1.589	0.222	1.775	1.554
HA - 0.725 vs. HA - 0.363	2.471	0.373	1.696	0.293	2.423	1.732
HA - 0.725 vs. HA - 0.484	1.967	0.411	1.265	0.375	1.830	1.267
HA - 0.725 vs. HA - 0.605	2.962	1.057	2.145	0.971	2.688	2.343
HA - 0.967 vs. HA - 0.121	1.717	0.217	1.823	0.228	1.693	1.815
HA - 0.967 vs. HA - 0.242	1.560	0.163	1.732	0.173	1.568	1.690
HA - 0.967 vs. HA - 0.363	1.990	0.237	1.866	0.198	1.947	1.876
HA - 0.967 vs. HA - 0.484	1.496	0.212	1.685	0.208	1.418	1.664
HA - 0.967 vs. HA - 0.605	1.658	0.303	2.225	0.334	1.570	2.254
HA - 0.967 vs. HA - 0.725	0.832	0.378	2.276	0.486	0.810	2.203
HA - 1.21 vs. HA - 0.121	1.792	0.199	1.821	0.205	1.774	1.813
HA - 1.21 vs. HA - 0.242	1.689	0.141	1.741	0.147	1.705	1.704
HA - 1.21 vs. HA - 0.363	2.083	0.189	1.854	0.156	2.058	1.861
HA - 1.21 vs. HA - 0.484	1.738	0.154	1.713	0.151	1.681	1.696
HA - 1.21 vs. HA - 0.605	1.926	0.194	2.088	0.209	1.874	2.105
HA - 1.21 vs. HA - 0.725	1.557	0.203	2.068	0.246	1.554	2.028
HA - 1.21 vs. HA - 0.967	2.491	0.531	1.799	0.438	2.574	1.796
$\bar{n}_{pre-rejection}$		1.794				1.783
$S_{pre-rejection}$		0.455				0.468
$\bar{n}_{post-rejection}$		1.769				1.754
$S_{post-rejection}$		0.418				0.418
λ_{95}		0.113				0.113
$\bar{\epsilon}$		0.385				

Table IX-A. Full data set of $I\Delta t = 0.9J$, HA - HI vs. HA - LI scenario.

$I\Delta t = 0.9J$

LA - HI vs. LA - LI	$n_{0,0\ 1}$	$\epsilon_{0,0\ 1}$	$n_{0,0\ 2}$	$\epsilon_{0,0\ 2}$	$n_{x,t\ 1}$	$n_{x,t\ 2}$
LA - 0.242 vs. LA - 0.121	1.747	0.593	2.460	0.830	1.731	2.404
LA - 0.363 vs. LA - 0.121	1.702	0.345	1.949	0.405	1.702	1.914
LA - 0.363 vs. LA - 0.242	1.626	0.522	1.076	0.368	1.650	1.066
LA - 0.484 vs. LA - 0.121	1.771	0.277	1.960	0.315	1.766	1.934
LA - 0.484 vs. LA - 0.242	1.795	0.310	1.460	0.255	1.801	1.455
LA - 0.484 vs. LA - 0.363	2.034	0.627	2.000	0.624	2.007	2.013
LA - 0.605 vs. LA - 0.121	1.704	0.228	1.862	0.258	1.691	1.838
LA - 0.605 vs. LA - 0.242	1.671	0.213	1.411	0.181	1.660	1.402
LA - 0.605 vs. LA - 0.363	1.707	0.286	1.676	0.286	1.668	1.671
LA - 0.605 vs. LA - 0.484	1.286	0.431	1.257	0.434	1.240	1.240
LA - 0.725 vs. LA - 0.121	1.693	0.203	1.864	0.230	1.687	1.843
LA - 0.725 vs. LA - 0.242	1.659	0.173	1.488	0.155	1.659	1.483
LA - 0.725 vs. LA - 0.363	1.679	0.200	1.729	0.208	1.664	1.729
LA - 0.725 vs. LA - 0.484	1.427	0.243	1.537	0.261	1.418	1.530
LA - 0.725 vs. LA - 0.605	1.600	0.523	1.880	0.601	1.652	1.893
LA - 0.967 vs. LA - 0.121	1.685	0.173	1.918	0.202	1.673	1.893
LA - 0.967 vs. LA - 0.242	1.654	0.134	1.648	0.131	1.644	1.633
LA - 0.967 vs. LA - 0.363	1.666	0.135	1.884	0.150	1.641	1.868
LA - 0.967 vs. LA - 0.484	1.513	0.139	1.836	0.164	1.490	1.810
LA - 0.967 vs. LA - 0.605	1.621	0.188	2.110	0.233	1.612	2.080
LA - 0.967 vs. LA - 0.725	1.634	0.277	2.256	0.357	1.588	2.195
LA - 1.21 vs. LA - 0.121	1.784	0.164	1.934	0.183	1.761	1.911
LA - 1.21 vs. LA - 0.242	1.799	0.122	1.707	0.115	1.774	1.695
LA - 1.21 vs. LA - 0.363	1.858	0.117	1.920	0.122	1.814	1.908
LA - 1.21 vs. LA - 0.484	1.802	0.116	1.894	0.123	1.754	1.876
LA - 1.21 vs. LA - 0.605	1.969	0.141	2.099	0.150	1.921	2.082
LA - 1.21 vs. LA - 0.725	2.100	0.177	2.178	0.183	2.010	2.149
LA - 1.21 vs. LA - 0.967	2.702	0.418	2.076	0.330	2.536	2.087
$\bar{n}_{pre-rejection}$		1.785			1.765	
$S_{pre-rejection}$		0.278			0.263	
$\bar{n}_{post-rejection}$		1.768			1.765	
$S_{post-rejection}$		0.251			0.263	
λ_{95}		0.068			0.070	
$\bar{\epsilon}$		0.274				

Table IX-B. Full data set of $I\Delta t = 0.9J$, LA - HI vs. LA - LI scenario.

$I\Delta t = 0.9J$

LA - HI vs. HA - LI	$n_{0,0,1}$	$\epsilon_{0,0,1}$	$n_{0,0,2}$	$\epsilon_{0,0,2}$	$n_{x,t,1}$	$n_{x,t,2}$
LA - 0.242 vs. HA - 0.121	3.388	1.168	3.692	1.266	1.863	2.048
LA - 0.363 vs. HA - 0.121	2.738	0.585	2.727	0.590	1.812	1.805
LA - 0.363 vs. HA - 0.242	3.946	1.224	3.956	1.235	1.721	1.620
LA - 0.484 vs. HA - 0.121	2.592	0.435	2.576	0.439	1.841	1.836
LA - 0.484 vs. HA - 0.242	3.153	0.548	3.144	0.553	1.790	1.637
LA - 0.484 vs. HA - 0.363	6.863	2.074	5.595	1.684	2.338	1.802
LA - 0.605 vs. HA - 0.121	2.411	0.352	2.393	0.355	1.777	1.774
LA - 0.605 vs. HA - 0.242	2.698	0.353	2.685	0.356	1.702	1.637
LA - 0.605 vs. HA - 0.363	4.427	0.750	3.700	0.618	2.102	1.786
LA - 0.605 vs. HA - 0.484	6.034	1.784	5.501	1.635	1.673	1.565
LA - 0.725 vs. HA - 0.121	2.328	0.306	2.341	0.312	1.768	1.783
LA - 0.725 vs. HA - 0.242	2.516	0.273	2.551	0.280	1.697	1.665
LA - 0.725 vs. HA - 0.363	3.683	0.464	3.222	0.393	2.038	1.802
LA - 0.725 vs. HA - 0.484	4.040	0.642	3.873	0.618	1.669	1.627
LA - 0.725 vs. HA - 0.605	7.573	2.221	7.944	2.336	1.849	1.991
LA - 0.967 vs. HA - 0.121	2.232	0.254	2.329	0.266	1.748	1.829
LA - 0.967 vs. HA - 0.242	2.333	0.200	2.490	0.214	1.680	1.744
LA - 0.967 vs. HA - 0.363	3.082	0.281	2.938	0.249	1.952	1.878
LA - 0.967 vs. HA - 0.484	3.041	0.279	3.202	0.288	1.650	1.760
LA - 0.967 vs. HA - 0.605	3.938	0.439	4.463	0.493	1.775	2.050
LA - 0.967 vs. HA - 0.725	4.556	0.699	5.931	0.904	1.557	1.993
LA - 1.21 vs. HA - 0.121	2.278	0.233	2.305	0.238	1.813	1.849
LA - 1.21 vs. HA - 0.242	2.384	0.173	2.433	0.179	1.774	1.778
LA - 1.21 vs. HA - 0.363	3.012	0.222	2.779	0.191	2.030	1.904
LA - 1.21 vs. HA - 0.484	2.959	0.200	2.928	0.197	1.789	1.809
LA - 1.21 vs. HA - 0.605	3.540	0.261	3.694	0.276	1.916	2.056
LA - 1.21 vs. HA - 0.725	3.746	0.311	4.247	0.359	1.773	2.012
LA - 1.21 vs. HA - 0.967	7.503	1.118	6.789	1.007	2.136	1.939
$\bar{n}_{pre-rejection}$		3.668				1.825
$S_{pre-rejection}$		1.493				0.155
$\bar{n}_{post-rejection}$		3.668				1.816
$S_{post-rejection}$		1.493				0.140
λ_{95}		0.399				0.038
$\bar{\epsilon}$		0.632				

Table IX-C. Full data set of $I\Delta t = 0.9J$, LA - HI vs. HA - LI scenario.

$\Delta t = 0.9J$

HA - HI vs. LA - LI	$n_{0,0,1}$	$\epsilon_{0,0,1}$	$n_{0,0,2}$	$\epsilon_{0,0,2}$	$n_{x,t,1}$	$n_{x,t,2}$
HA - 0.242 vs. LA - 0.121	0.390	0.287	0.775	0.403	1.593	4.192
HA - 0.363 vs. LA - 0.121	0.438	0.202	1.008	0.269	0.881	1.933
HA - 0.363 vs. LA - 0.242	-1.801	0.691	-1.474	0.552	4.757	4.382
HA - 0.484 vs. LA - 0.121	1.007	0.183	1.277	0.232	1.709	2.091
HA - 0.484 vs. LA - 0.242	0.267	0.167	0.094	0.151	1.575	0.472
HA - 0.484 vs. LA - 0.363	-1.649	0.596	-1.292	0.517	1.682	1.365
HA - 0.605 vs. LA - 0.121	1.027	0.158	1.175	0.190	1.572	1.744
HA - 0.605 vs. LA - 0.242	0.483	0.132	0.204	0.124	1.256	0.498
HA - 0.605 vs. LA - 0.363	-0.425	0.207	-0.489	0.228	4.594	7.292
HA - 0.605 vs. LA - 0.484	-3.594	1.114	-3.697	1.158	2.368	2.577
HA - 0.725 vs. LA - 0.121	1.224	0.157	1.274	0.176	1.751	1.824
HA - 0.725 vs. LA - 0.242	0.894	0.120	0.526	0.102	1.776	1.066
HA - 0.725 vs. LA - 0.363	0.466	0.127	0.204	0.140	2.103	1.067
HA - 0.725 vs. LA - 0.484	-0.646	0.202	-1.070	0.269	1.900	2.832
HA - 0.725 vs. LA - 0.605	-3.011	0.943	-3.919	1.216	1.487	1.883
HA - 0.967 vs. LA - 0.121	1.170	0.130	1.413	0.160	1.571	1.897
HA - 0.967 vs. LA - 0.242	0.881	0.095	0.889	0.088	1.439	1.469
HA - 0.967 vs. LA - 0.363	0.573	0.095	0.812	0.099	1.252	1.853
HA - 0.967 vs. LA - 0.484	-0.033	0.109	0.319	0.102	-0.144	1.535
HA - 0.967 vs. LA - 0.605	-0.659	0.172	-0.127	0.143	4.208	0.725
HA - 0.967 vs. LA - 0.725	-2.091	0.394	-1.399	0.300	2.403	1.528
HA - 1.21 vs. LA - 0.121	1.298	0.126	1.450	0.147	1.694	1.884
HA - 1.21 vs. LA - 0.242	1.105	0.087	1.015	0.079	1.670	1.537
HA - 1.21 vs. LA - 0.363	0.929	0.080	0.995	0.084	1.681	1.833
HA - 1.21 vs. LA - 0.484	0.582	0.075	0.679	0.079	1.427	1.693
HA - 1.21 vs. LA - 0.605	0.355	0.089	0.493	0.094	1.730	2.420
HA - 1.21 vs. LA - 0.725	-0.089	0.112	-0.002	0.113	1.326	0.025
HA - 1.21 vs. LA - 0.967	-2.310	0.412	-2.913	0.479	1.561	1.937
$\bar{n}_{pre-rejection}$		-0.089				1.935
$S_{pre-rejection}$		1.414				1.224
$\bar{n}_{post-rejection}$		-0.089				1.838
$S_{post-rejection}$		1.414				0.992
λ_{95}		0.378				0.268
$\bar{\epsilon}$		0.267				

Table IX-D. Full data set of $\Delta t = 0.9J$, HA - HI vs. LA - LI scenario.

$I\Delta t = 1.8J$

HA - HI vs. HA - LI	$n_{0,0,1}$	$\epsilon_{0,0,1}$	$n_{0,0,2}$	$\epsilon_{0,0,2}$	$n_{x,t,1}$	$n_{x,t,2}$
HA - 0.242 vs. HA - 0.121	2.216	0.759	1.938	0.675	2.088	1.999
HA - 0.363 vs. HA - 0.121	1.744	0.372	1.899	0.394	1.720	1.862
HA - 0.363 vs. HA - 0.242	0.936	0.391	1.833	0.602	1.005	1.656
HA - 0.484 vs. HA - 0.121	1.958	0.314	1.896	0.304	1.954	1.883
HA - 0.484 vs. HA - 0.242	1.700	0.301	1.855	0.329	1.803	1.775
HA - 0.484 vs. HA - 0.363	2.777	0.860	1.886	0.610	2.896	1.969
HA - 0.605 vs. HA - 0.121	1.852	0.256	1.791	0.247	1.834	1.761
HA - 0.605 vs. HA - 0.242	1.576	0.207	1.680	0.222	1.624	1.595
HA - 0.605 vs. HA - 0.363	2.084	0.359	1.559	0.280	2.082	1.542
HA - 0.605 vs. HA - 0.484	1.191	0.451	1.136	0.444	1.128	1.053
HA - 0.725 vs. HA - 0.121	1.927	0.236	1.789	0.220	1.888	1.777
HA - 0.725 vs. HA - 0.242	1.745	0.182	1.696	0.182	1.753	1.645
HA - 0.725 vs. HA - 0.363	2.218	0.264	1.616	0.202	2.148	1.638
HA - 0.725 vs. HA - 0.484	1.822	0.304	1.423	0.262	1.679	1.414
HA - 0.725 vs. HA - 0.605	2.594	0.801	1.775	0.609	2.314	1.933
HA - 0.967 vs. HA - 0.121	1.847	0.195	1.862	0.194	1.803	1.836
HA - 0.967 vs. HA - 0.242	1.662	0.135	1.824	0.148	1.652	1.760
HA - 0.967 vs. HA - 0.363	1.962	0.162	1.821	0.147	1.893	1.807
HA - 0.967 vs. HA - 0.484	1.623	0.152	1.793	0.164	1.519	1.745
HA - 0.967 vs. HA - 0.605	1.828	0.215	2.105	0.238	1.701	2.097
HA - 0.967 vs. HA - 0.725	1.343	0.252	2.314	0.375	1.285	2.188
HA - 1.21 vs. HA - 0.121	1.863	0.176	1.846	0.174	1.826	1.820
HA - 1.21 vs. HA - 0.242	1.711	0.117	1.807	0.125	1.707	1.748
HA - 1.21 vs. HA - 0.363	1.972	0.129	1.798	0.116	1.922	1.782
HA - 1.21 vs. HA - 0.484	1.719	0.115	1.771	0.118	1.642	1.727
HA - 1.21 vs. HA - 0.605	1.889	0.141	1.975	0.146	1.809	1.960
HA - 1.21 vs. HA - 0.725	1.637	0.148	2.047	0.179	1.610	1.968
HA - 1.21 vs. HA - 0.967	2.017	0.338	1.701	0.296	2.057	1.673
$\bar{n}_{pre-rejection}$		1.819				1.785
$S_{pre-rejection}$		0.297				0.294
$\bar{n}_{post-rejection}$		1.801				1.765
$S_{post-rejection}$		0.270				0.254
λ_{95}		0.073				0.069
$\bar{\epsilon}$		0.292				

Table X-A. Full data set of $I\Delta t = 1.8J$, HA - HI vs. HA - LI scenario.

$$|\Delta t| = 1.8J$$

LA - HI vs. LA - LI	$n_{0,0,1}$	$\epsilon_{0,0,1}$	$n_{0,0,2}$	$\epsilon_{0,0,2}$	$n_{x,t,1}$	$n_{x,t,2}$
LA - 0.242 vs. LA - 0.121	1.791	0.584	2.427	0.790	1.765	2.352
LA - 0.363 vs. LA - 0.121	1.715	0.333	1.941	0.379	1.705	1.895
LA - 0.363 vs. LA - 0.242	1.585	0.479	1.110	0.339	1.599	1.098
LA - 0.484 vs. LA - 0.121	1.764	0.266	1.905	0.288	1.748	1.870
LA - 0.484 vs. LA - 0.242	1.737	0.285	1.383	0.228	1.730	1.374
LA - 0.484 vs. LA - 0.363	1.950	0.574	1.769	0.523	1.908	1.769
LA - 0.605 vs. LA - 0.121	1.733	0.222	1.840	0.238	1.709	1.805
LA - 0.605 vs. LA - 0.242	1.689	0.202	1.395	0.167	1.666	1.382
LA - 0.605 vs. LA - 0.363	1.771	0.275	1.621	0.254	1.716	1.608
LA - 0.605 vs. LA - 0.484	1.540	0.455	1.432	0.427	1.475	1.404
LA - 0.725 vs. LA - 0.121	1.733	0.199	1.846	0.213	1.714	1.814
LA - 0.725 vs. LA - 0.242	1.697	0.166	1.479	0.145	1.682	1.466
LA - 0.725 vs. LA - 0.363	1.762	0.194	1.696	0.187	1.729	1.682
LA - 0.725 vs. LA - 0.484	1.629	0.248	1.644	0.251	1.601	1.622
LA - 0.725 vs. LA - 0.605	1.737	0.510	1.904	0.558	1.765	1.892
LA - 0.967 vs. LA - 0.121	1.682	0.165	1.884	0.186	1.660	1.846
LA - 0.967 vs. LA - 0.242	1.628	0.123	1.613	0.122	1.607	1.588
LA - 0.967 vs. LA - 0.363	1.645	0.123	1.821	0.135	1.610	1.790
LA - 0.967 vs. LA - 0.484	1.519	0.127	1.843	0.152	1.486	1.798
LA - 0.967 vs. LA - 0.605	1.508	0.158	2.038	0.210	1.492	1.984
LA - 0.967 vs. LA - 0.725	1.363	0.208	2.122	0.315	1.326	2.040
LA - 1.21 vs. LA - 0.121	1.772	0.157	1.907	0.169	1.737	1.869
LA - 1.21 vs. LA - 0.242	1.764	0.114	1.683	0.108	1.725	1.657
LA - 1.21 vs. LA - 0.363	1.824	0.108	1.876	0.111	1.766	1.844
LA - 1.21 vs. LA - 0.484	1.785	0.108	1.909	0.115	1.722	1.868
LA - 1.21 vs. LA - 0.605	1.864	0.124	2.063	0.137	1.803	2.016
LA - 1.21 vs. LA - 0.725	1.909	0.149	2.120	0.166	1.815	2.060
LA - 1.21 vs. LA - 0.967	2.642	0.383	2.117	0.312	2.414	2.086
$\bar{n}_{pre-rejection}$		1.770				1.735
$S_{pre-rejection}$		0.247				0.227
$\bar{n}_{post-rejection}$		1.754				1.735
$S_{post-rejection}$		0.220				0.227
λ_{95}		0.059				0.061
$\bar{\epsilon}$		0.255				

Table X-B. Full data set of $|\Delta t| = 1.8J$, LA - HI vs. LA - LI scenario.

$I\Delta t = 1.8J$

LA - HI vs. HA - LI	$n_{0,0,1}$	$\epsilon_{0,0,1}$	$n_{0,0,2}$	$\epsilon_{0,0,2}$	$n_{x,t,1}$	$n_{x,t,2}$
LA - 0.242 vs. HA - 0.121	3.658	1.201	3.818	1.250	2.002	2.107
LA - 0.363 vs. HA - 0.121	2.893	0.573	2.819	0.558	1.905	1.858
LA - 0.363 vs. HA - 0.242	4.049	1.214	4.325	1.298	1.761	1.763
LA - 0.484 vs. HA - 0.121	2.697	0.417	2.601	0.401	1.905	1.845
LA - 0.484 vs. HA - 0.242	3.178	0.522	3.264	0.539	1.796	1.710
LA - 0.484 vs. HA - 0.363	6.337	1.853	5.280	1.544	2.148	1.757
LA - 0.605 vs. HA - 0.121	2.537	0.336	2.439	0.323	1.860	1.799
LA - 0.605 vs. HA - 0.242	2.779	0.335	2.818	0.342	1.745	1.710
LA - 0.605 vs. HA - 0.363	4.242	0.660	3.599	0.560	2.003	1.733
LA - 0.605 vs. HA - 0.484	6.130	1.771	5.807	1.680	1.697	1.650
LA - 0.725 vs. HA - 0.121	2.455	0.291	2.384	0.282	1.852	1.806
LA - 0.725 vs. HA - 0.242	2.606	0.258	2.666	0.266	1.747	1.730
LA - 0.725 vs. HA - 0.363	3.583	0.398	3.153	0.349	1.969	1.757
LA - 0.725 vs. HA - 0.484	4.155	0.625	4.052	0.611	1.709	1.696
LA - 0.725 vs. HA - 0.605	7.783	2.236	7.621	2.190	1.892	1.909
LA - 0.967 vs. HA - 0.121	2.304	0.235	2.348	0.238	1.794	1.833
LA - 0.967 vs. HA - 0.242	2.348	0.181	2.553	0.198	1.683	1.776
LA - 0.967 vs. HA - 0.363	2.932	0.224	2.851	0.215	1.847	1.811
LA - 0.967 vs. HA - 0.484	2.996	0.250	3.251	0.270	1.621	1.777
LA - 0.967 vs. HA - 0.605	3.853	0.397	4.255	0.436	1.732	1.947
LA - 0.967 vs. HA - 0.725	4.651	0.683	5.827	0.854	1.591	1.950
LA - 1.21 vs. HA - 0.121	2.334	0.214	2.326	0.213	1.846	1.852
LA - 1.21 vs. HA - 0.242	2.385	0.157	2.493	0.165	1.764	1.808
LA - 1.21 vs. HA - 0.363	2.873	0.176	2.715	0.164	1.923	1.847
LA - 1.21 vs. HA - 0.484	2.903	0.177	2.975	0.181	1.747	1.824
LA - 1.21 vs. HA - 0.605	3.454	0.230	3.567	0.238	1.860	1.972
LA - 1.21 vs. HA - 0.725	3.760	0.293	4.206	0.328	1.774	1.978
LA - 1.21 vs. HA - 0.967	6.878	0.995	6.645	0.961	1.962	1.896
$\bar{n}_{pre-rejection}$		3.668			1.826	
$S_{pre-rejection}$		1.421			0.113	
$\bar{n}_{post-rejection}$		3.668			1.826	
$S_{post-rejection}$		1.421			0.113	
λ_{95}		0.380			0.030	
$\bar{\epsilon}$		0.599				

Table X-C. Full data set of $I\Delta t = 1.8J$, LA - HI vs. HA - LI scenario.

$\Delta t = 1.8J$

HA - HI vs. LA - LI	$n_{0,0,1}$	$\epsilon_{0,0,1}$	$n_{0,0,2}$	$\epsilon_{0,0,2}$	$n_{x,t,1}$	$n_{x,t,2}$
HA - 0.242 vs. LA - 0.121	0.350	0.168	0.547	0.233	1.405	2.899
HA - 0.363 vs. LA - 0.121	0.566	0.135	1.021	0.213	1.130	1.936
HA - 0.363 vs. LA - 0.242	-1.528	0.489	-1.382	0.436	4.052	4.130
HA - 0.484 vs. LA - 0.121	1.025	0.160	1.201	0.189	1.720	1.947
HA - 0.484 vs. LA - 0.242	0.259	0.086	-0.025	0.073	1.460	-0.125
HA - 0.484 vs. LA - 0.363	-1.610	0.495	-1.625	0.502	1.660	1.732
HA - 0.605 vs. LA - 0.121	1.048	0.139	1.192	0.160	1.589	1.751
HA - 0.605 vs. LA - 0.242	0.486	0.080	0.258	0.061	1.242	0.620
HA - 0.605 vs. LA - 0.363	-0.386	0.109	-0.419	0.113	4.552	7.349
HA - 0.605 vs. LA - 0.484	-3.399	0.995	-3.239	0.951	2.248	2.281
HA - 0.725 vs. LA - 0.121	1.205	0.141	1.251	0.149	1.706	1.775
HA - 0.725 vs. LA - 0.242	0.836	0.089	0.509	0.064	1.631	1.021
HA - 0.725 vs. LA - 0.363	0.398	0.071	0.158	0.066	1.711	0.793
HA - 0.725 vs. LA - 0.484	-0.704	0.136	-0.984	0.178	2.147	2.672
HA - 0.725 vs. LA - 0.605	-3.451	1.003	-3.942	1.147	1.719	1.906
HA - 0.967 vs. LA - 0.121	1.224	0.122	1.398	0.141	1.625	1.855
HA - 0.967 vs. LA - 0.242	0.941	0.076	0.884	0.071	1.511	1.438
HA - 0.967 vs. LA - 0.363	0.675	0.062	0.791	0.068	1.434	1.752
HA - 0.967 vs. LA - 0.484	0.145	0.049	0.385	0.056	0.601	1.722
HA - 0.967 vs. LA - 0.605	-0.517	0.086	-0.112	0.068	3.710	0.726
HA - 0.967 vs. LA - 0.725	-1.946	0.302	-1.390	0.227	2.285	1.561
HA - 1.21 vs. LA - 0.121	1.301	0.116	1.428	0.129	1.678	1.832
HA - 1.21 vs. LA - 0.242	1.090	0.073	0.997	0.067	1.621	1.487
HA - 1.21 vs. LA - 0.363	0.923	0.060	0.959	0.062	1.634	1.726
HA - 1.21 vs. LA - 0.484	0.601	0.048	0.705	0.053	1.425	1.693
HA - 1.21 vs. LA - 0.605	0.299	0.045	0.471	0.052	1.350	2.121
HA - 1.21 vs. LA - 0.725	-0.215	0.055	-0.040	0.054	4.192	0.693
HA - 1.21 vs. LA - 0.967	-2.249	0.343	-2.827	0.421	1.559	1.920
$\bar{n}_{pre-rejection}$		-0.080				1.925
$S_{pre-rejection}$		1.389				1.150
$\bar{n}_{post-rejection}$		-0.080				1.827
$S_{post-rejection}$		1.389				0.893
λ_{95}		0.371				0.241
$\bar{\epsilon}$		0.210				

Table X-D. Full data set of $\Delta t = 1.8J$, HA - HI vs. LA - LI scenario.

$I\Delta t = 3.6J$

HA - HI vs. HA - LI	$n_{0,0,1}$	$\epsilon_{0,0,1}$	$n_{0,0,2}$	$\epsilon_{0,0,2}$	$n_{x,t,1}$	$n_{x,t,2}$
HA - 0.242 vs. HA - 0.121	2.138	0.700	1.779	0.584	1.990	1.819
HA - 0.363 vs. HA - 0.121	1.790	0.351	1.789	0.349	1.747	1.736
HA - 0.363 vs. HA - 0.242	1.196	0.376	1.807	0.549	1.272	1.612
HA - 0.484 vs. HA - 0.121	1.941	0.294	1.820	0.275	1.908	1.783
HA - 0.484 vs. HA - 0.242	1.743	0.287	1.861	0.307	1.815	1.750
HA - 0.484 vs. HA - 0.363	2.545	0.741	1.938	0.575	2.544	1.972
HA - 0.605 vs. HA - 0.121	1.854	0.240	1.743	0.225	1.810	1.693
HA - 0.605 vs. HA - 0.242	1.639	0.198	1.715	0.207	1.662	1.605
HA - 0.605 vs. HA - 0.363	1.990	0.312	1.643	0.259	1.946	1.599
HA - 0.605 vs. HA - 0.484	1.315	0.401	1.263	0.388	1.232	1.164
HA - 0.725 vs. HA - 0.121	1.900	0.219	1.736	0.200	1.832	1.701
HA - 0.725 vs. HA - 0.242	1.750	0.171	1.709	0.168	1.727	1.631
HA - 0.725 vs. HA - 0.363	2.075	0.229	1.652	0.184	1.964	1.644
HA - 0.725 vs. HA - 0.484	1.763	0.270	1.449	0.226	1.595	1.419
HA - 0.725 vs. HA - 0.605	2.311	0.676	1.676	0.503	2.008	1.779
HA - 0.967 vs. HA - 0.121	1.881	0.186	1.820	0.179	1.802	1.762
HA - 0.967 vs. HA - 0.242	1.753	0.133	1.840	0.140	1.704	1.737
HA - 0.967 vs. HA - 0.363	1.983	0.148	1.854	0.138	1.861	1.792
HA - 0.967 vs. HA - 0.484	1.763	0.147	1.819	0.151	1.606	1.723
HA - 0.967 vs. HA - 0.605	1.975	0.205	2.084	0.215	1.776	1.999
HA - 0.967 vs. HA - 0.725	1.763	0.266	2.342	0.348	1.620	2.118
HA - 1.21 vs. HA - 0.121	1.858	0.165	1.799	0.159	1.788	1.743
HA - 1.21 vs. HA - 0.242	1.738	0.112	1.808	0.117	1.697	1.713
HA - 1.21 vs. HA - 0.363	1.920	0.114	1.808	0.107	1.825	1.750
HA - 1.21 vs. HA - 0.484	1.734	0.105	1.767	0.107	1.617	1.685
HA - 1.21 vs. HA - 0.605	1.869	0.125	1.929	0.129	1.740	1.860
HA - 1.21 vs. HA - 0.725	1.711	0.136	2.020	0.159	1.635	1.885
HA - 1.21 vs. HA - 0.967	1.644	0.249	1.604	0.244	1.656	1.562
$\bar{n}_{pre-rejection}$		1.814			1.743	
$S_{pre-rejection}$		0.225			0.208	
$\bar{n}_{post-rejection}$		1.801			1.729	
$S_{post-rejection}$		0.206			0.179	
λ_{95}		0.056			0.048	
$\bar{\epsilon}$		0.263				

Table XI-A. Full data set of $I\Delta t = 3.6J$, HA - HI vs. HA - LI scenario.

$$I\Delta t = 3.6J$$

LA - HI vs. LA - LI	$n_{0,0,1}$	$\epsilon_{0,0,1}$	$n_{0,0,2}$	$\epsilon_{0,0,2}$	$n_{x,t,1}$	$n_{x,t,2}$
LA - 0.242 vs. LA - 0.121	1.838	0.594	2.205	0.713	1.795	2.116
LA - 0.363 vs. LA - 0.121	1.660	0.320	1.830	0.352	1.639	1.774
LA - 0.363 vs. LA - 0.242	1.356	0.404	1.190	0.355	1.365	1.174
LA - 0.484 vs. LA - 0.121	1.769	0.264	1.787	0.267	1.736	1.741
LA - 0.484 vs. LA - 0.242	1.701	0.275	1.369	0.222	1.677	1.354
LA - 0.484 vs. LA - 0.363	2.187	0.636	1.622	0.473	2.095	1.610
LA - 0.605 vs. LA - 0.121	1.746	0.222	1.746	0.222	1.706	1.701
LA - 0.605 vs. LA - 0.242	1.677	0.198	1.400	0.165	1.639	1.379
LA - 0.605 vs. LA - 0.363	1.932	0.295	1.566	0.240	1.845	1.541
LA - 0.605 vs. LA - 0.484	1.604	0.463	1.495	0.433	1.526	1.454
LA - 0.725 vs. LA - 0.121	1.730	0.196	1.746	0.198	1.695	1.703
LA - 0.725 vs. LA - 0.242	1.661	0.160	1.457	0.140	1.631	1.435
LA - 0.725 vs. LA - 0.363	1.840	0.199	1.613	0.175	1.781	1.588
LA - 0.725 vs. LA - 0.484	1.593	0.238	1.607	0.240	1.554	1.573
LA - 0.725 vs. LA - 0.605	1.580	0.455	1.744	0.502	1.590	1.719
LA - 0.967 vs. LA - 0.121	1.642	0.160	1.776	0.173	1.609	1.726
LA - 0.967 vs. LA - 0.242	1.544	0.115	1.561	0.117	1.516	1.528
LA - 0.967 vs. LA - 0.363	1.621	0.119	1.714	0.125	1.576	1.672
LA - 0.967 vs. LA - 0.484	1.387	0.113	1.753	0.142	1.356	1.698
LA - 0.967 vs. LA - 0.605	1.283	0.131	1.875	0.190	1.272	1.812
LA - 0.967 vs. LA - 0.725	1.096	0.163	1.958	0.286	1.076	1.869
LA - 1.21 vs. LA - 0.121	1.722	0.151	1.784	0.156	1.677	1.736
LA - 1.21 vs. LA - 0.242	1.672	0.106	1.603	0.102	1.626	1.569
LA - 1.21 vs. LA - 0.363	1.779	0.104	1.741	0.101	1.710	1.701
LA - 1.21 vs. LA - 0.484	1.651	0.098	1.779	0.105	1.589	1.728
LA - 1.21 vs. LA - 0.605	1.666	0.108	1.871	0.122	1.609	1.817
LA - 1.21 vs. LA - 0.725	1.696	0.130	1.916	0.147	1.616	1.851
LA - 1.21 vs. LA - 0.967	2.474	0.357	1.861	0.270	2.266	1.826
$\bar{n}_{pre-rejection}$		1.691				1.646
$S_{pre-rejection}$		0.230				0.206
$\bar{n}_{post-rejection}$		1.676				1.635
$S_{post-rejection}$		0.206				0.190
λ_{95}		0.055				0.051
$\bar{\epsilon}$		0.241				

Table XI-B. Full data set of $I\Delta t = 3.6J$, LA - HI vs. LA - LI scenario.

$I\Delta t = 3.6J$

LA - HI vs. HA - LI	$n_{0,0,1}$	$\epsilon_{0,0,1}$	$n_{0,0,2}$	$\epsilon_{0,0,2}$	$n_{x,t,1}$	$n_{x,t,2}$
LA - 0.242 vs. HA - 0.121	3.629	1.175	3.580	1.158	1.973	1.964
LA - 0.363 vs. HA - 0.121	2.790	0.540	2.698	0.521	1.827	1.770
LA - 0.363 vs. HA - 0.242	3.905	1.161	4.270	1.270	1.697	1.737
LA - 0.484 vs. HA - 0.121	2.665	0.400	2.475	0.371	1.868	1.747
LA - 0.484 vs. HA - 0.242	3.192	0.517	3.171	0.514	1.794	1.670
LA - 0.484 vs. HA - 0.363	6.005	1.744	5.093	1.479	2.028	1.699
LA - 0.605 vs. HA - 0.121	2.518	0.322	2.339	0.299	1.832	1.716
LA - 0.605 vs. HA - 0.242	2.805	0.332	2.762	0.327	1.751	1.670
LA - 0.605 vs. HA - 0.363	4.083	0.625	3.521	0.539	1.919	1.695
LA - 0.605 vs. HA - 0.484	6.104	1.755	5.562	1.600	1.698	1.594
LA - 0.725 vs. HA - 0.121	2.422	0.277	2.278	0.260	1.813	1.716
LA - 0.725 vs. HA - 0.242	2.602	0.252	2.593	0.251	1.734	1.675
LA - 0.725 vs. HA - 0.363	3.424	0.371	3.054	0.331	1.872	1.699
LA - 0.725 vs. HA - 0.484	4.070	0.606	3.845	0.573	1.678	1.618
LA - 0.725 vs. HA - 0.605	7.442	2.129	7.006	2.005	1.821	1.771
LA - 0.967 vs. HA - 0.121	2.239	0.220	2.234	0.218	1.733	1.733
LA - 0.967 vs. HA - 0.242	2.289	0.172	2.462	0.185	1.634	1.705
LA - 0.967 vs. HA - 0.363	2.741	0.201	2.732	0.200	1.723	1.732
LA - 0.967 vs. HA - 0.484	2.835	0.231	3.062	0.249	1.540	1.678
LA - 0.967 vs. HA - 0.605	3.557	0.359	3.916	0.395	1.611	1.800
LA - 0.967 vs. HA - 0.725	4.347	0.632	5.336	0.775	1.510	1.804
LA - 1.21 vs. HA - 0.121	2.261	0.200	2.198	0.194	1.777	1.741
LA - 1.21 vs. HA - 0.242	2.315	0.148	2.378	0.152	1.705	1.717
LA - 1.21 vs. HA - 0.363	2.691	0.158	2.571	0.150	1.796	1.744
LA - 1.21 vs. HA - 0.484	2.747	0.163	2.770	0.164	1.656	1.701
LA - 1.21 vs. HA - 0.605	3.208	0.209	3.255	0.212	1.735	1.804
LA - 1.21 vs. HA - 0.725	3.528	0.270	3.818	0.292	1.682	1.808
LA - 1.21 vs. HA - 0.967	5.803	0.835	5.721	0.823	1.707	1.679
$\bar{n}_{pre-rejection}$		3.481			1.741	
$S_{pre-rejection}$		1.286			0.097	
$\bar{n}_{post-rejection}$		3.481			1.741	
$S_{post-rejection}$		1.286			0.097	
λ_{95}		0.344			0.026	
$\bar{\epsilon}$		0.563				

Table XI-C. Full data set of $I\Delta t = 3.6J$, LA - HI vs. HA - LI scenario.

$I\Delta t = 3.6J$

HA - HI vs. LA - LI	$n_{0,0\ 1}$	$\epsilon_{0,0\ 1}$	$n_{0,0\ 2}$	$\epsilon_{0,0\ 2}$	$n_{x,t\ 1}$	$n_{x,t\ 2}$
HA - 0.242 vs. LA - 0.121	0.347	0.127	0.403	0.146	1.337	2.042
HA - 0.363 vs. LA - 0.121	0.660	0.132	0.921	0.180	1.293	1.711
HA - 0.363 vs. LA - 0.242	-1.353	0.409	-1.273	0.384	3.686	3.942
HA - 0.484 vs. LA - 0.121	1.045	0.157	1.132	0.170	1.714	1.796
HA - 0.484 vs. LA - 0.242	0.252	0.054	0.060	0.036	1.289	0.273
HA - 0.484 vs. LA - 0.363	-1.303	0.386	-1.533	0.451	1.404	1.700
HA - 0.605 vs. LA - 0.121	1.082	0.139	1.150	0.147	1.608	1.659
HA - 0.605 vs. LA - 0.242	0.511	0.065	0.353	0.048	1.253	0.821
HA - 0.605 vs. LA - 0.363	-0.160	0.050	-0.312	0.065	2.817	9.142
HA - 0.605 vs. LA - 0.484	-3.186	0.918	-2.805	0.810	2.158	2.038
HA - 0.725 vs. LA - 0.121	1.207	0.138	1.204	0.138	1.673	1.675
HA - 0.725 vs. LA - 0.242	0.810	0.080	0.572	0.058	1.524	1.112
HA - 0.725 vs. LA - 0.363	0.490	0.060	0.211	0.037	1.879	0.948
HA - 0.725 vs. LA - 0.484	-0.714	0.114	-0.790	0.127	2.422	2.366
HA - 0.725 vs. LA - 0.605	-3.551	1.018	-3.586	1.029	1.828	1.793
HA - 0.967 vs. LA - 0.121	1.284	0.125	1.361	0.133	1.663	1.763
HA - 0.967 vs. LA - 0.242	1.007	0.076	0.940	0.071	1.558	1.474
HA - 0.967 vs. LA - 0.363	0.863	0.065	0.836	0.063	1.715	1.736
HA - 0.967 vs. LA - 0.484	0.314	0.034	0.510	0.047	1.125	1.934
HA - 0.967 vs. LA - 0.605	-0.298	0.043	0.042	0.032	3.410	-0.427
HA - 0.967 vs. LA - 0.725	-1.489	0.221	-1.036	0.158	1.927	1.287
HA - 1.21 vs. LA - 0.121	1.319	0.116	1.385	0.122	1.662	1.738
HA - 1.21 vs. LA - 0.242	1.096	0.070	1.032	0.066	1.577	1.492
HA - 1.21 vs. LA - 0.363	1.008	0.060	0.978	0.058	1.697	1.679
HA - 1.21 vs. LA - 0.484	0.638	0.041	0.776	0.048	1.409	1.727
HA - 1.21 vs. LA - 0.605	0.327	0.029	0.545	0.041	1.256	2.070
HA - 1.21 vs. LA - 0.725	-0.120	0.027	0.117	0.028	79.09	-25.4
HA - 1.21 vs. LA - 0.967	-1.688	0.249	-2.256	0.329	1.282	1.657
$\bar{n}_{pre-rejection}$		0.024			2.732	
$S_{pre-rejection}$		1.287			11.074	
$\bar{n}_{post-rejection}$		0.024			1.343	
$S_{post-rejection}$		1.287			3.871	
λ_{95}		0.344			1.044	
$\bar{\epsilon}$		0.179				

Table XI-D. Full data set of $I\Delta t = 3.6J$, HA - HI vs. LA - LI scenario.

$\Delta A / \bar{A} = 5\%$

HA - HI vs. HA - LI	$n_{0,0,1}$	$\epsilon_{0,0,1}$	$n_{0,0,2}$	$\epsilon_{0,0,2}$	$n_{x,t,1}$	$n_{x,t,2}$
HA - 0.242 vs. HA - 0.121	2.120	0.717	1.964	0.676	2.025	2.050
HA - 0.363 vs. HA - 0.121	1.645	0.346	1.846	0.383	1.638	1.831
HA - 0.363 vs. HA - 0.242	0.831	0.457	1.645	0.632	0.893	1.504
HA - 0.484 vs. HA - 0.121	1.854	0.299	1.886	0.303	1.880	1.899
HA - 0.484 vs. HA - 0.242	1.588	0.345	1.809	0.372	1.716	1.758
HA - 0.484 vs. HA - 0.363	2.655	0.958	2.041	0.806	2.890	2.174
HA - 0.605 vs. HA - 0.121	1.754	0.245	1.693	0.236	1.763	1.685
HA - 0.605 vs. HA - 0.242	1.476	0.250	1.488	0.247	1.545	1.431
HA - 0.605 vs. HA - 0.363	1.988	0.448	1.364	0.371	2.039	1.368
HA - 0.605 vs. HA - 0.484	1.129	0.833	0.491	0.710	1.077	0.458
HA - 0.725 vs. HA - 0.121	1.895	0.225	1.726	0.217	1.882	1.738
HA - 0.725 vs. HA - 0.242	1.753	0.201	1.577	0.218	1.785	1.553
HA - 0.725 vs. HA - 0.363	2.293	0.305	1.537	0.295	2.264	1.585
HA - 0.725 vs. HA - 0.484	2.035	0.436	1.179	0.449	1.887	1.189
HA - 0.725 vs. HA - 0.605	3.145	1.151	2.021	1.086	2.817	2.264
HA - 0.967 vs. HA - 0.121	1.748	0.179	1.803	0.186	1.731	1.806
HA - 0.967 vs. HA - 0.242	1.562	0.146	1.722	0.161	1.575	1.691
HA - 0.967 vs. HA - 0.363	1.864	0.188	1.754	0.185	1.833	1.777
HA - 0.967 vs. HA - 0.484	1.536	0.226	1.636	0.229	1.452	1.623
HA - 0.967 vs. HA - 0.605	1.729	0.335	2.179	0.352	1.628	2.231
HA - 0.967 vs. HA - 0.725	0.832	0.378	2.279	0.583	0.810	2.212
HA - 1.21 vs. HA - 0.121	1.804	0.169	1.778	0.172	1.803	1.788
HA - 1.21 vs. HA - 0.242	1.668	0.138	1.698	0.152	1.700	1.681
HA - 1.21 vs. HA - 0.363	1.950	0.167	1.715	0.173	1.954	1.747
HA - 1.21 vs. HA - 0.484	1.728	0.193	1.613	0.208	1.690	1.621
HA - 1.21 vs. HA - 0.605	1.921	0.254	1.974	0.275	1.893	2.035
HA - 1.21 vs. HA - 0.725	1.485	0.272	1.958	0.375	1.517	1.961
HA - 1.21 vs. HA - 0.967	2.326	0.665	1.544	0.734	2.542	1.613
$\bar{n}_{pre-rejection}$		1.754			1.759	
$S_{pre-rejection}$		0.409			0.415	
$\bar{n}_{post-rejection}$		1.752			1.783	
$S_{post-rejection}$		0.328			0.379	
λ_{95}		0.089			0.102	
$\bar{\epsilon}$		0.381				

Table XII-A. Full data set of $\Delta A / \bar{A} = 5\%$, HA - HI vs. HA - LI scenario.

$$\Delta A / \bar{A} = 5\%$$

LA - HI vs. LA - LI	$n_{0,0,1}$	$\epsilon_{0,0,1}$	$n_{0,0,2}$	$\epsilon_{0,0,2}$	$n_{x,t,1}$	$n_{x,t,2}$
LA - 0.242 vs. LA - 0.121	1.777	0.616	2.216	0.751	1.771	2.186
LA - 0.363 vs. LA - 0.121	1.788	0.368	1.829	0.379	1.797	1.806
LA - 0.363 vs. LA - 0.242	1.805	0.669	1.166	0.519	1.841	1.154
LA - 0.484 vs. LA - 0.121	1.557	0.262	1.838	0.294	1.565	1.825
LA - 0.484 vs. LA - 0.242	1.337	0.341	1.459	0.320	1.355	1.459
LA - 0.484 vs. LA - 0.363	0.677	0.624	1.871	0.737	0.680	1.901
LA - 0.605 vs. LA - 0.121	1.605	0.222	1.712	0.241	1.602	1.701
LA - 0.605 vs. LA - 0.242	1.474	0.244	1.330	0.241	1.473	1.329
LA - 0.605 vs. LA - 0.363	1.211	0.335	1.461	0.387	1.192	1.471
LA - 0.605 vs. LA - 0.484	1.900	0.977	0.931	0.729	1.822	0.927
LA - 0.725 vs. LA - 0.121	1.558	0.200	1.714	0.213	1.564	1.707
LA - 0.725 vs. LA - 0.242	1.420	0.215	1.397	0.198	1.432	1.400
LA - 0.725 vs. LA - 0.363	1.195	0.277	1.533	0.276	1.197	1.547
LA - 0.725 vs. LA - 0.484	1.562	0.552	1.292	0.399	1.562	1.299
LA - 0.725 vs. LA - 0.605	1.148	0.950	1.734	1.066	1.212	1.764
LA - 0.967 vs. LA - 0.121	1.624	0.176	1.750	0.189	1.624	1.743
LA - 0.967 vs. LA - 0.242	1.547	0.171	1.517	0.167	1.551	1.519
LA - 0.967 vs. LA - 0.363	1.440	0.196	1.663	0.207	1.434	1.672
LA - 0.967 vs. LA - 0.484	1.757	0.318	1.576	0.257	1.742	1.578
LA - 0.967 vs. LA - 0.605	1.689	0.370	1.882	0.433	1.702	1.890
LA - 0.967 vs. LA - 0.725	2.033	0.742	1.976	0.655	1.991	1.968
LA - 1.21 vs. LA - 0.121	1.742	0.165	1.676	0.169	1.735	1.676
LA - 1.21 vs. LA - 0.242	1.726	0.148	1.443	0.152	1.720	1.452
LA - 1.21 vs. LA - 0.363	1.700	0.156	1.536	0.181	1.680	1.554
LA - 1.21 vs. LA - 0.484	2.021	0.233	1.431	0.215	1.988	1.446
LA - 1.21 vs. LA - 0.605	2.060	0.238	1.592	0.314	2.043	1.616
LA - 1.21 vs. LA - 0.725	2.385	0.400	1.541	0.397	2.316	1.563
LA - 1.21 vs. LA - 0.967	2.840	0.856	0.980	0.943	2.728	1.019
$\bar{n}_{pre-rejection}$		1.618				1.616
$S_{pre-rejection}$		0.349				0.333
$\bar{n}_{post-rejection}$		1.596				1.596
$S_{post-rejection}$		0.310				0.299
λ_{95}		0.084				0.081
$\bar{\epsilon}$		0.394				

Table XII-B. Full data set of $\Delta A / \bar{A} = 5\%$, LA - HI vs. LA - LI scenario.

$$\Delta A / \bar{A} = 5\%$$

LA - HI vs. HA - LI	$n_{0,0,1}$	$\epsilon_{0,0,1}$	$n_{0,0,2}$	$\epsilon_{0,0,2}$	$n_{x,t,1}$	$n_{x,t,2}$
LA - 0.242 vs. HA - 0.121	3.512	1.157	3.559	1.170	1.951	1.996
LA - 0.363 vs. HA - 0.121	2.882	0.569	2.676	0.532	1.925	1.786
LA - 0.363 vs. HA - 0.242	4.184	1.294	3.893	1.218	1.845	1.608
LA - 0.484 vs. HA - 0.121	2.425	0.385	2.509	0.387	1.740	1.803
LA - 0.484 vs. HA - 0.242	2.729	0.515	3.054	0.536	1.569	1.561
LA - 0.484 vs. HA - 0.363	5.403	1.698	5.039	1.543	1.876	1.611
LA - 0.605 vs. HA - 0.121	2.352	0.310	2.290	0.309	1.749	1.712
LA - 0.605 vs. HA - 0.242	2.527	0.334	2.537	0.354	1.610	1.561
LA - 0.605 vs. HA - 0.363	3.873	0.653	3.245	0.599	1.864	1.585
LA - 0.605 vs. HA - 0.484	5.443	1.694	4.797	1.577	1.524	1.380
LA - 0.725 vs. HA - 0.121	2.229	0.272	2.233	0.268	1.709	1.716
LA - 0.725 vs. HA - 0.242	2.298	0.277	2.404	0.273	1.567	1.583
LA - 0.725 vs. HA - 0.363	3.156	0.434	2.847	0.382	1.773	1.611
LA - 0.725 vs. HA - 0.484	3.512	0.700	3.420	0.638	1.468	1.452
LA - 0.725 vs. HA - 0.605	6.427	2.117	7.004	2.177	1.593	1.785
LA - 0.967 vs. HA - 0.121	2.202	0.228	2.198	0.229	1.741	1.744
LA - 0.967 vs. HA - 0.242	2.243	0.207	2.315	0.215	1.632	1.640
LA - 0.967 vs. HA - 0.363	2.826	0.271	2.592	0.260	1.815	1.679
LA - 0.967 vs. HA - 0.484	2.898	0.345	2.820	0.339	1.590	1.572
LA - 0.967 vs. HA - 0.605	3.737	0.534	3.926	0.540	1.706	1.837
LA - 0.967 vs. HA - 0.725	4.113	0.805	5.134	0.973	1.433	1.755
LA - 1.21 vs. HA - 0.121	2.264	0.206	2.080	0.203	1.821	1.689
LA - 1.21 vs. HA - 0.242	2.326	0.171	2.130	0.189	1.751	1.578
LA - 1.21 vs. HA - 0.363	2.829	0.202	2.293	0.220	1.935	1.597
LA - 1.21 vs. HA - 0.484	2.884	0.232	2.372	0.268	1.767	1.491
LA - 1.21 vs. HA - 0.605	3.448	0.309	2.978	0.358	1.895	1.693
LA - 1.21 vs. HA - 0.725	3.557	0.360	3.319	0.491	1.717	1.605
LA - 1.21 vs. HA - 0.967	7.070	1.155	4.660	1.115	2.069	1.369
$\bar{n}_{pre-rejection}$		3.316				1.690
$S_{pre-rejection}$		1.227				0.153
$\bar{n}_{post-rejection}$		3.178				1.690
$S_{post-rejection}$		1.010				0.153
λ_{95}		0.275				0.041
$\bar{\epsilon}$		0.621				

Table XII-C. Full data set of $\Delta A / \bar{A} = 5\%$, LA - HI vs. HA - LI scenario.

$$\Delta A / \bar{A} = 5\%$$

HA - HI vs. LA - LI	$n_{0,0,1}$	$\epsilon_{0,0,1}$	$n_{0,0,2}$	$\epsilon_{0,0,2}$	$n_{x,t,1}$	$n_{x,t,2}$
HA - 0.242 vs. LA - 0.121	0.386	0.247	0.621	0.309	1.539	3.300
HA - 0.363 vs. LA - 0.121	0.550	0.174	0.999	0.241	1.097	1.912
HA - 0.363 vs. LA - 0.242	-1.548	0.616	-1.082	0.509	4.345	3.409
HA - 0.484 vs. LA - 0.121	0.987	0.184	1.215	0.214	1.678	1.996
HA - 0.484 vs. LA - 0.242	0.196	0.246	0.214	0.232	1.136	1.051
HA - 0.484 vs. LA - 0.363	-2.071	0.806	-1.127	0.622	2.145	1.208
HA - 0.605 vs. LA - 0.121	1.007	0.161	1.115	0.172	1.544	1.656
HA - 0.605 vs. LA - 0.242	0.424	0.194	0.282	0.176	1.097	0.678
HA - 0.605 vs. LA - 0.363	-0.673	0.326	-0.420	0.304	7.844	7.382
HA - 0.605 vs. LA - 0.484	-2.414	1.108	-3.375	1.155	1.631	2.411
HA - 0.725 vs. LA - 0.121	1.224	0.157	1.207	0.165	1.751	1.736
HA - 0.725 vs. LA - 0.242	0.875	0.159	0.570	0.161	1.725	1.153
HA - 0.725 vs. LA - 0.363	0.331	0.194	0.222	0.231	1.438	1.151
HA - 0.725 vs. LA - 0.484	0.086	0.426	-0.948	0.393	-0.274	2.571
HA - 0.725 vs. LA - 0.605	-2.135	0.904	-3.249	1.346	1.083	1.585
HA - 0.967 vs. LA - 0.121	1.170	0.130	1.355	0.149	1.571	1.827
HA - 0.967 vs. LA - 0.242	0.866	0.126	0.925	0.125	1.408	1.527
HA - 0.967 vs. LA - 0.363	0.478	0.141	0.825	0.152	1.030	1.882
HA - 0.967 vs. LA - 0.484	0.395	0.253	0.391	0.183	1.622	1.846
HA - 0.967 vs. LA - 0.605	-0.319	0.265	0.135	0.337	2.349	-0.820
HA - 0.967 vs. LA - 0.725	-1.248	0.628	-0.879	0.511	1.519	0.986
HA - 1.21 vs. LA - 0.121	1.282	0.128	1.374	0.140	1.684	1.801
HA - 1.21 vs. LA - 0.242	1.069	0.121	1.011	0.122	1.627	1.544
HA - 1.21 vs. LA - 0.363	0.821	0.130	0.958	0.145	1.498	1.793
HA - 1.21 vs. LA - 0.484	0.866	0.206	0.672	0.169	2.126	1.708
HA - 1.21 vs. LA - 0.605	0.533	0.200	0.588	0.261	2.630	2.992
HA - 1.21 vs. LA - 0.725	0.313	0.357	0.179	0.324	4.950	-2.130
HA - 1.21 vs. LA - 0.967	-1.904	0.799	-2.137	0.871	1.303	1.437
$\bar{n}_{pre-rejection}$		0.057				1.693
$S_{pre-rejection}$		1.205				1.715
$\bar{n}_{post-rejection}$		0.057				1.595
$S_{post-rejection}$		1.205				0.950
λ_{95}		0.322				0.261
$\bar{\epsilon}$		0.341				

Table XII-D. Full data set of $\Delta A / \bar{A} = 5\%$, HA - HI vs. LA - LI scenario.

$\Delta A / \bar{A} = 10\%$

HA - HI vs. HA - LI	$n_{0,0,1}$	$\epsilon_{0,0,1}$	$n_{0,0,2}$	$\epsilon_{0,0,2}$	$n_{x,t,1}$	$n_{x,t,2}$
HA - 0.242 vs. HA - 0.121	2.008	0.658	1.679	0.554	1.917	1.749
HA - 0.363 vs. HA - 0.121	1.660	0.326	1.734	0.341	1.646	1.719
HA - 0.363 vs. HA - 0.242	1.066	0.364	1.828	0.577	1.132	1.672
HA - 0.484 vs. HA - 0.121	1.820	0.277	1.729	0.264	1.844	1.741
HA - 0.484 vs. HA - 0.242	1.632	0.288	1.779	0.311	1.761	1.732
HA - 0.484 vs. HA - 0.363	2.431	0.754	1.709	0.574	2.682	1.831
HA - 0.605 vs. HA - 0.121	1.699	0.224	1.655	0.215	1.713	1.642
HA - 0.605 vs. HA - 0.242	1.466	0.204	1.637	0.208	1.542	1.568
HA - 0.605 vs. HA - 0.363	1.784	0.332	1.486	0.266	1.863	1.477
HA - 0.605 vs. HA - 0.484	0.950	0.527	1.198	0.476	0.928	1.090
HA - 0.725 vs. HA - 0.121	1.819	0.212	1.669	0.194	1.817	1.678
HA - 0.725 vs. HA - 0.242	1.700	0.183	1.662	0.175	1.749	1.635
HA - 0.725 vs. HA - 0.363	2.072	0.257	1.565	0.203	2.092	1.611
HA - 0.725 vs. HA - 0.484	1.816	0.353	1.463	0.295	1.730	1.464
HA - 0.725 vs. HA - 0.605	2.877	0.997	1.787	0.653	2.660	2.039
HA - 0.967 vs. HA - 0.121	1.722	0.171	1.719	0.172	1.707	1.726
HA - 0.967 vs. HA - 0.242	1.580	0.129	1.738	0.143	1.596	1.715
HA - 0.967 vs. HA - 0.363	1.792	0.149	1.701	0.150	1.775	1.735
HA - 0.967 vs. HA - 0.484	1.527	0.164	1.698	0.185	1.451	1.698
HA - 0.967 vs. HA - 0.605	1.801	0.260	1.935	0.258	1.689	2.030
HA - 0.967 vs. HA - 0.725	1.119	0.330	2.029	0.413	1.060	2.025
HA - 1.21 vs. HA - 0.121	1.761	0.157	1.724	0.155	1.759	1.734
HA - 1.21 vs. HA - 0.242	1.655	0.115	1.744	0.123	1.686	1.728
HA - 1.21 vs. HA - 0.363	1.853	0.123	1.715	0.122	1.862	1.749
HA - 1.21 vs. HA - 0.484	1.672	0.130	1.717	0.139	1.634	1.725
HA - 1.21 vs. HA - 0.605	1.904	0.178	1.884	0.169	1.862	1.958
HA - 1.21 vs. HA - 0.725	1.557	0.203	1.919	0.223	1.554	1.933
HA - 1.21 vs. HA - 0.967	2.121	0.450	1.777	0.472	2.279	1.810
$\bar{n}_{pre-rejection}$		1.728				1.736
$S_{pre-rejection}$		0.287				0.300
$\bar{n}_{post-rejection}$		1.707				1.701
$S_{post-rejection}$		0.243				0.243
λ_{95}		0.065				0.066
$\bar{\epsilon}$		0.295				

Table XIII-A. Full data set of $\Delta A / \bar{A} = 10\%$, HA - HI vs. HA - LI scenario.

$$\Delta A / \bar{A} = 10\%$$

LA - HI vs. LA - LI	$n_{0,0,1}$	$\epsilon_{0,0,1}$	$n_{0,0,2}$	$\epsilon_{0,0,2}$	$n_{x,t,1}$	$n_{x,t,2}$
LA - 0.242 vs. LA - 0.121	1.676	0.552	2.170	0.709	1.674	2.140
LA - 0.363 vs. LA - 0.121	1.670	0.328	1.767	0.346	1.682	1.745
LA - 0.363 vs. LA - 0.242	1.661	0.538	1.076	0.368	1.697	1.066
LA - 0.484 vs. LA - 0.121	1.715	0.260	1.771	0.269	1.721	1.761
LA - 0.484 vs. LA - 0.242	1.755	0.306	1.371	0.248	1.768	1.375
LA - 0.484 vs. LA - 0.363	1.888	0.615	1.785	0.581	1.866	1.824
LA - 0.605 vs. LA - 0.121	1.606	0.208	1.697	0.221	1.605	1.686
LA - 0.605 vs. LA - 0.242	1.553	0.204	1.338	0.179	1.553	1.338
LA - 0.605 vs. LA - 0.363	1.468	0.278	1.546	0.279	1.443	1.557
LA - 0.605 vs. LA - 0.484	0.927	0.408	1.237	0.512	0.905	1.224
LA - 0.725 vs. LA - 0.121	1.643	0.190	1.716	0.199	1.647	1.710
LA - 0.725 vs. LA - 0.242	1.622	0.172	1.430	0.154	1.630	1.433
LA - 0.725 vs. LA - 0.363	1.599	0.209	1.636	0.207	1.593	1.653
LA - 0.725 vs. LA - 0.484	1.395	0.263	1.530	0.302	1.397	1.533
LA - 0.725 vs. LA - 0.605	1.967	0.691	1.890	0.701	2.035	1.922
LA - 0.967 vs. LA - 0.121	1.626	0.162	1.757	0.174	1.627	1.749
LA - 0.967 vs. LA - 0.242	1.601	0.135	1.550	0.128	1.604	1.550
LA - 0.967 vs. LA - 0.363	1.576	0.146	1.746	0.148	1.566	1.754
LA - 0.967 vs. LA - 0.484	1.446	0.159	1.729	0.181	1.441	1.725
LA - 0.967 vs. LA - 0.605	1.693	0.243	1.963	0.261	1.704	1.965
LA - 0.967 vs. LA - 0.725	1.519	0.346	2.010	0.398	1.504	1.992
LA - 1.21 vs. LA - 0.121	1.720	0.157	1.754	0.157	1.718	1.753
LA - 1.21 vs. LA - 0.242	1.739	0.130	1.575	0.112	1.737	1.583
LA - 1.21 vs. LA - 0.363	1.766	0.138	1.743	0.120	1.751	1.761
LA - 1.21 vs. LA - 0.484	1.727	0.149	1.730	0.137	1.714	1.742
LA - 1.21 vs. LA - 0.605	1.985	0.199	1.889	0.173	1.981	1.913
LA - 1.21 vs. LA - 0.725	1.991	0.250	1.889	0.216	1.963	1.909
LA - 1.21 vs. LA - 0.967	2.604	0.623	1.733		2.548	1.797
$\bar{n}_{pre-rejection}$		1.681				1.683
$S_{pre-rejection}$		0.253				0.254
$\bar{n}_{post-rejection}$		1.665				1.681
$S_{post-rejection}$		0.222				0.203
λ_{95}		0.060				0.055
$\bar{\epsilon}$		0.282				

Table XIII-B. Full data set of $\Delta A / \bar{A} = 10\%$, LA - HI vs. LA - LI scenario.

$$\Delta A / \bar{A} = 10\%$$

LA - HI vs. HA - LI	$n_{0,0,1}$	$\epsilon_{0,0,1}$	$n_{0,0,2}$	$\epsilon_{0,0,2}$	$n_{x,t,1}$	$n_{x,t,2}$
LA - 0.242 vs. HA - 0.121	3.285	1.067	3.377	1.095	1.835	1.902
LA - 0.363 vs. HA - 0.121	2.686	0.522	2.528	0.490	1.801	1.693
LA - 0.363 vs. HA - 0.242	3.845	1.160	3.979	1.195	1.709	1.655
LA - 0.484 vs. HA - 0.121	2.520	0.378	2.374	0.358	1.811	1.712
LA - 0.484 vs. HA - 0.242	3.033	0.500	3.069	0.509	1.747	1.621
LA - 0.484 vs. HA - 0.363	5.805	1.698	4.818	1.425	2.033	1.647
LA - 0.605 vs. HA - 0.121	2.299	0.296	2.216	0.286	1.715	1.661
LA - 0.605 vs. HA - 0.242	2.520	0.308	2.623	0.321	1.613	1.621
LA - 0.605 vs. HA - 0.363	3.674	0.578	3.253	0.521	1.788	1.600
LA - 0.605 vs. HA - 0.484	5.277	1.555	5.244	1.551	1.492	1.519
LA - 0.725 vs. HA - 0.121	2.265	0.260	2.183	0.251	1.739	1.681
LA - 0.725 vs. HA - 0.242	2.428	0.242	2.501	0.251	1.659	1.654
LA - 0.725 vs. HA - 0.363	3.225	0.361	2.895	0.332	1.823	1.647
LA - 0.725 vs. HA - 0.484	3.788	0.590	3.736	0.589	1.591	1.595
LA - 0.725 vs. HA - 0.605	7.263	2.128	6.842	1.997	1.797	1.771
LA - 0.967 vs. HA - 0.121	2.162	0.213	2.159	0.213	1.713	1.716
LA - 0.967 vs. HA - 0.242	2.239	0.177	2.399	0.187	1.635	1.704
LA - 0.967 vs. HA - 0.363	2.725	0.215	2.635	0.207	1.762	1.714
LA - 0.967 vs. HA - 0.484	2.846	0.261	3.019	0.269	1.571	1.688
LA - 0.967 vs. HA - 0.605	3.747	0.429	3.884	0.418	1.714	1.836
LA - 0.967 vs. HA - 0.725	4.298	0.700	5.213	0.800	1.489	1.797
LA - 1.21 vs. HA - 0.121	2.205	0.199	2.118	0.188	1.780	1.722
LA - 1.21 vs. HA - 0.242	2.289	0.162	2.307	0.155	1.733	1.713
LA - 1.21 vs. HA - 0.363	2.702	0.182	2.468	0.158	1.865	1.724
LA - 1.21 vs. HA - 0.484	2.787	0.207	2.706	0.183	1.721	1.704
LA - 1.21 vs. HA - 0.605	3.378	0.283	3.191	0.234	1.865	1.829
LA - 1.21 vs. HA - 0.725	3.557	0.360	3.693	0.323	1.717	1.797
LA - 1.21 vs. HA - 0.967	6.699	1.088	5.838	0.919	1.982	1.710
$\bar{n}_{pre-rejection}$		3.372			1.720	
$S_{pre-rejection}$		1.283			0.106	
$\bar{n}_{post-rejection}$		3.301			1.720	
$S_{post-rejection}$		1.179			0.106	
λ_{95}		0.318			0.028	
$\bar{\epsilon}$		0.563				

Table XIII-C. Full data set of $\Delta A / \bar{A} = 10\%$, LA - HI vs. HA - LI scenario.

$\Delta A / \bar{A} = 10\%$

HA - HI vs. LA - LI	$n_{0,0,1}$	$\epsilon_{0,0,1}$	$n_{0,0,2}$	$\epsilon_{0,0,2}$	$n_{x,t,1}$	$n_{x,t,2}$
HA - 0.242 vs. LA - 0.121	0.398	0.167	0.473	0.190	1.542	2.383
HA - 0.363 vs. LA - 0.121	0.644	0.139	0.973	0.200	1.262	1.841
HA - 0.363 vs. LA - 0.242	-1.118	0.387	-1.075	0.371	3.405	3.562
HA - 0.484 vs. LA - 0.121	1.015	0.160	1.126	0.177	1.713	1.838
HA - 0.484 vs. LA - 0.242	0.355	0.136	0.081	0.114	1.928	0.382
HA - 0.484 vs. LA - 0.363	-1.486	0.524	-1.323	0.468	1.587	1.445
HA - 0.605 vs. LA - 0.121	1.006	0.138	1.136	0.151	1.542	1.670
HA - 0.605 vs. LA - 0.242	0.500	0.121	0.353	0.089	1.286	0.826
HA - 0.605 vs. LA - 0.363	-0.422	0.201	-0.222	0.142	5.259	6.259
HA - 0.605 vs. LA - 0.484	-3.400	1.046	-2.809	0.875	2.284	2.092
HA - 0.725 vs. LA - 0.121	1.197	0.143	1.202	0.143	1.719	1.717
HA - 0.725 vs. LA - 0.242	0.894	0.120	0.591	0.090	1.776	1.177
HA - 0.725 vs. LA - 0.363	0.446	0.142	0.307	0.113	1.978	1.501
HA - 0.725 vs. LA - 0.484	-0.577	0.212	-0.742	0.227	1.736	2.152
HA - 0.725 vs. LA - 0.605	-2.419	0.834	-3.165	1.007	1.213	1.579
HA - 0.967 vs. LA - 0.121	1.186	0.120	1.316	0.133	1.590	1.775
HA - 0.967 vs. LA - 0.242	0.941	0.092	0.889	0.088	1.522	1.469
HA - 0.967 vs. LA - 0.363	0.643	0.097	0.812	0.099	1.371	1.853
HA - 0.967 vs. LA - 0.484	0.127	0.098	0.408	0.125	0.520	1.906
HA - 0.967 vs. LA - 0.605	-0.253	0.161	0.014	0.179	1.993	-0.086
HA - 0.967 vs. LA - 0.725	-1.660	0.340	-1.175	0.331	2.025	1.318
HA - 1.21 vs. LA - 0.121	1.276	0.116	1.361	0.124	1.671	1.779
HA - 1.21 vs. LA - 0.242	1.105	0.087	1.012	0.082	1.670	1.539
HA - 1.21 vs. LA - 0.363	0.917	0.088	0.991	0.088	1.653	1.838
HA - 1.21 vs. LA - 0.484	0.612	0.083	0.741	0.103	1.490	1.849
HA - 1.21 vs. LA - 0.605	0.511	0.115	0.582	0.129	2.394	2.841
HA - 1.21 vs. LA - 0.725	-0.008	0.138	0.115	0.163	0.153	-1.574
HA - 1.21 vs. LA - 0.967	-1.978	0.471	-2.328	0.493	1.384	1.586
$\bar{n}_{pre-rejection}$		0.037				1.753
$S_{pre-rejection}$		1.225				1.086
$\bar{n}_{post-rejection}$		0.037				1.665
$S_{post-rejection}$		1.225				0.633
λ_{95}		0.327				0.174
$\bar{\epsilon}$		0.232				

Table XIII-D. Full data set of $\Delta A / \bar{A} = 10\%$, HA - HI vs. LA - LI scenario.

$$\Delta A / \bar{A} = 20\%$$

HA - HI vs. HA - LI	$n_{0,0,1}$	$\epsilon_{0,0,1}$	$n_{0,0,2}$	$\epsilon_{0,0,2}$	$n_{x,t,1}$	$n_{x,t,2}$
HA - 0.242 vs. HA - 0.121	1.839	0.596	1.552	0.504	1.750	1.624
HA - 0.363 vs. HA - 0.121	1.631	0.315	1.609	0.311	1.612	1.600
HA - 0.363 vs. HA - 0.242	1.276	0.390	1.706	0.516	1.349	1.563
HA - 0.484 vs. HA - 0.121	1.769	0.265	1.619	0.243	1.783	1.632
HA - 0.484 vs. HA - 0.242	1.699	0.280	1.685	0.279	1.821	1.639
HA - 0.484 vs. HA - 0.363	2.297	0.679	1.656	0.501	2.506	1.763
HA - 0.605 vs. HA - 0.121	1.698	0.217	1.602	0.204	1.699	1.593
HA - 0.605 vs. HA - 0.242	1.591	0.192	1.640	0.198	1.657	1.571
HA - 0.605 vs. HA - 0.363	1.841	0.291	1.588	0.254	1.894	1.578
HA - 0.605 vs. HA - 0.484	1.253	0.401	1.499	0.464	1.201	1.372
HA - 0.725 vs. HA - 0.121	1.763	0.201	1.586	0.181	1.750	1.599
HA - 0.725 vs. HA - 0.242	1.715	0.169	1.607	0.159	1.750	1.584
HA - 0.725 vs. HA - 0.363	1.972	0.219	1.549	0.178	1.971	1.597
HA - 0.725 vs. HA - 0.484	1.742	0.275	1.473	0.242	1.643	1.486
HA - 0.725 vs. HA - 0.605	2.340	0.702	1.441	0.469	2.167	1.661
HA - 0.967 vs. HA - 0.121	1.699	0.166	1.671	0.163	1.685	1.679
HA - 0.967 vs. HA - 0.242	1.629	0.125	1.731	0.132	1.651	1.705
HA - 0.967 vs. HA - 0.363	1.774	0.136	1.742	0.133	1.768	1.770
HA - 0.967 vs. HA - 0.484	1.558	0.140	1.777	0.155	1.498	1.773
HA - 0.967 vs. HA - 0.605	1.702	0.194	1.910	0.209	1.640	1.990
HA - 0.967 vs. HA - 0.725	1.298	0.239	2.206	0.351	1.283	2.167
HA - 1.21 vs. HA - 0.121	1.723	0.152	1.667	0.147	1.721	1.678
HA - 1.21 vs. HA - 0.242	1.673	0.109	1.717	0.112	1.707	1.700
HA - 1.21 vs. HA - 0.363	1.807	0.110	1.721	0.106	1.822	1.752
HA - 1.21 vs. HA - 0.484	1.653	0.107	1.741	0.112	1.628	1.748
HA - 1.21 vs. HA - 0.605	1.782	0.130	1.819	0.132	1.771	1.886
HA - 1.21 vs. HA - 0.725	1.583	0.146	1.954	0.171	1.615	1.955
HA - 1.21 vs. HA - 0.967	1.951	0.342	1.629	0.301	2.075	1.670
$\bar{n}_{pre-rejection}$		1.703				1.710
$S_{pre-rejection}$		0.202				0.213
$\bar{n}_{post-rejection}$		1.691				1.695
$S_{post-rejection}$		0.184				0.185
λ_{95}		0.050				0.050
$\bar{\epsilon}$		0.254				

Table XIV-A. Full data set of $\Delta A / \bar{A} = 20\%$, HA - HI vs. HA - LI scenario.

$$\Delta A / \bar{A} = 20\%$$

LA - HI vs. LA - LI	$n_{0,0,1}$	$\epsilon_{0,0,1}$	$n_{0,0,2}$	$\epsilon_{0,0,2}$	$n_{x,t,1}$	$n_{x,t,2}$
LA - 0.242 vs. LA - 0.121	1.711	0.555	2.157	0.698	1.705	2.124
LA - 0.363 vs. LA - 0.121	1.635	0.316	1.727	0.333	1.645	1.712
LA - 0.363 vs. LA - 0.242	1.504	0.457	0.992	0.309	1.540	0.995
LA - 0.484 vs. LA - 0.121	1.718	0.257	1.748	0.261	1.724	1.740
LA - 0.484 vs. LA - 0.242	1.724	0.284	1.340	0.223	1.744	1.348
LA - 0.484 vs. LA - 0.363	2.035	0.608	1.829	0.551	2.023	1.849
LA - 0.605 vs. LA - 0.121	1.639	0.209	1.693	0.216	1.639	1.683
LA - 0.605 vs. LA - 0.242	1.584	0.192	1.342	0.163	1.589	1.344
LA - 0.605 vs. LA - 0.363	1.647	0.266	1.619	0.261	1.627	1.621
LA - 0.605 vs. LA - 0.484	1.147	0.382	1.348	0.428	1.124	1.332
LA - 0.725 vs. LA - 0.121	1.635	0.186	1.698	0.193	1.641	1.694
LA - 0.725 vs. LA - 0.242	1.587	0.157	1.409	0.140	1.599	1.417
LA - 0.725 vs. LA - 0.363	1.635	0.187	1.653	0.189	1.633	1.666
LA - 0.725 vs. LA - 0.484	1.351	0.225	1.528	0.250	1.355	1.537
LA - 0.725 vs. LA - 0.605	1.600	0.523	1.748	0.550	1.652	1.797
LA - 0.967 vs. LA - 0.121	1.635	0.160	1.762	0.172	1.633	1.755
LA - 0.967 vs. LA - 0.242	1.596	0.122	1.565	0.119	1.597	1.567
LA - 0.967 vs. LA - 0.363	1.635	0.126	1.802	0.138	1.620	1.804
LA - 0.967 vs. LA - 0.484	1.468	0.131	1.790	0.156	1.453	1.785
LA - 0.967 vs. LA - 0.605	1.621	0.188	2.000	0.219	1.612	2.003
LA - 0.967 vs. LA - 0.725	1.634	0.277	2.160	0.347	1.588	2.128
LA - 1.21 vs. LA - 0.121	1.718	0.151	1.780	0.156	1.712	1.778
LA - 1.21 vs. LA - 0.242	1.721	0.112	1.618	0.105	1.716	1.626
LA - 1.21 vs. LA - 0.363	1.794	0.110	1.829	0.112	1.773	1.840
LA - 1.21 vs. LA - 0.484	1.718	0.111	1.829	0.117	1.695	1.837
LA - 1.21 vs. LA - 0.605	1.902	0.140	1.983	0.141	1.880	2.002
LA - 1.21 vs. LA - 0.725	2.010	0.176	2.067	0.180	1.957	2.074
LA - 1.21 vs. LA - 0.967	2.495	0.402	1.948	0.334	2.435	2.002
$\bar{n}_{pre-rejection}$		1.698			1.696	
$S_{pre-rejection}$		0.249			0.244	
$\bar{n}_{post-rejection}$		1.683			1.682	
$S_{post-rejection}$		0.226			0.224	
λ_{95}		0.061			0.060	
$\bar{\epsilon}$		0.251				

Table XIV-B. Full data set of $\Delta A / \bar{A} = 20\%$, LA - HI vs. LA - LI scenario.

$$\Delta A / \bar{A} = 20\%$$

LA - HI vs. HA - LI	$n_{0,0\ 1}$	$\epsilon_{0,0\ 1}$	$n_{0,0\ 2}$	$\epsilon_{0,0\ 2}$	$n_{x,t\ 1}$	$n_{x,t\ 2}$
LA - 0.242 vs. HA - 0.121	3.214	1.038	3.247	1.048	1.807	1.848
LA - 0.363 vs. HA - 0.121	2.583	0.498	2.415	0.465	1.742	1.636
LA - 0.363 vs. HA - 0.242	3.855	1.148	3.890	1.159	1.736	1.644
LA - 0.484 vs. HA - 0.121	2.469	0.369	2.293	0.342	1.785	1.667
LA - 0.484 vs. HA - 0.242	3.099	0.504	3.034	0.493	1.806	1.636
LA - 0.484 vs. HA - 0.363	5.670	1.649	4.907	1.429	2.023	1.686
LA - 0.605 vs. HA - 0.121	2.286	0.291	2.162	0.275	1.714	1.632
LA - 0.605 vs. HA - 0.242	2.624	0.313	2.624	0.312	1.696	1.636
LA - 0.605 vs. HA - 0.363	3.694	0.569	3.352	0.517	1.825	1.667
LA - 0.605 vs. HA - 0.484	5.496	1.591	5.538	1.601	1.592	1.632
LA - 0.725 vs. HA - 0.121	2.216	0.252	2.120	0.241	1.710	1.645
LA - 0.725 vs. HA - 0.242	2.454	0.239	2.478	0.241	1.691	1.653
LA - 0.725 vs. HA - 0.363	3.144	0.343	2.930	0.321	1.800	1.686
LA - 0.725 vs. HA - 0.484	3.744	0.565	3.834	0.579	1.603	1.663
LA - 0.725 vs. HA - 0.605	6.793	1.955	6.691	1.926	1.734	1.766
LA - 0.967 vs. HA - 0.121	2.136	0.208	2.125	0.207	1.696	1.699
LA - 0.967 vs. HA - 0.242	2.284	0.172	2.412	0.182	1.675	1.724
LA - 0.967 vs. HA - 0.363	2.701	0.200	2.704	0.201	1.758	1.772
LA - 0.967 vs. HA - 0.484	2.868	0.238	3.139	0.260	1.599	1.774
LA - 0.967 vs. HA - 0.605	3.635	0.374	3.918	0.402	1.691	1.874
LA - 0.967 vs. HA - 0.725	4.456	0.658	5.488	0.807	1.576	1.915
LA - 1.21 vs. HA - 0.121	2.170	0.190	2.108	0.185	1.755	1.722
LA - 1.21 vs. HA - 0.242	2.313	0.149	2.348	0.151	1.757	1.752
LA - 1.21 vs. HA - 0.363	2.663	0.158	2.564	0.152	1.847	1.801
LA - 1.21 vs. HA - 0.484	2.777	0.169	2.849	0.173	1.729	1.808
LA - 1.21 vs. HA - 0.605	3.268	0.219	3.284	0.219	1.829	1.897
LA - 1.21 vs. HA - 0.725	3.599	0.286	3.941	0.311	1.765	1.933
LA - 1.21 vs. HA - 0.967	6.566	0.962	6.178	0.904	1.951	1.841
$\bar{n}_{pre-rejection}$		3.381			1.741	
$S_{pre-rejection}$		1.284			0.097	
$\bar{n}_{post-rejection}$		3.381			1.741	
$S_{post-rejection}$		1.284			0.097	
λ_{95}		0.343			0.026	
$\bar{\epsilon}$		0.543				

Table XIV-C. Full data set of $\Delta A / \bar{A} = 20\%$, LA - HI vs. HA - LI scenario.

$$\Delta A / \bar{A} = 20\%$$

HA - HI vs. LA - LI	$n_{0,0,1}$	$\epsilon_{0,0,1}$	$n_{0,0,2}$	$\epsilon_{0,0,2}$	$n_{x,t,1}$	$n_{x,t,2}$
HA - 0.242 vs. LA - 0.121	0.336	0.123	0.462	0.160	1.218	2.151
HA - 0.363 vs. LA - 0.121	0.683	0.136	0.921	0.180	1.305	1.711
HA - 0.363 vs. LA - 0.242	-1.075	0.333	-1.191	0.365	3.606	4.286
HA - 0.484 vs. LA - 0.121	1.018	0.154	1.074	0.162	1.683	1.728
HA - 0.484 vs. LA - 0.242	0.324	0.078	-0.010	0.054	1.575	-0.042
HA - 0.484 vs. LA - 0.363	-1.338	0.414	-1.422	0.439	1.520	1.656
HA - 0.605 vs. LA - 0.121	1.051	0.135	1.133	0.145	1.578	1.649
HA - 0.605 vs. LA - 0.242	0.551	0.078	0.358	0.057	1.343	0.817
HA - 0.605 vs. LA - 0.363	-0.206	0.089	-0.146	0.087	5.166	23.94
HA - 0.605 vs. LA - 0.484	-3.096	0.906	-2.691	0.792	2.230	2.088
HA - 0.725 vs. LA - 0.121	1.182	0.135	1.164	0.134	1.670	1.651
HA - 0.725 vs. LA - 0.242	0.848	0.089	0.538	0.062	1.626	1.056
HA - 0.725 vs. LA - 0.363	0.464	0.079	0.272	0.071	1.820	1.214
HA - 0.725 vs. LA - 0.484	-0.651	0.137	-0.833	0.161	2.340	2.610
HA - 0.725 vs. LA - 0.605	-2.852	0.850	-3.502	1.025	1.527	1.798
HA - 0.967 vs. LA - 0.121	1.198	0.118	1.308	0.128	1.597	1.748
HA - 0.967 vs. LA - 0.242	0.941	0.076	0.884	0.071	1.511	1.438
HA - 0.967 vs. LA - 0.363	0.708	0.068	0.839	0.076	1.486	1.837
HA - 0.967 vs. LA - 0.484	0.158	0.062	0.428	0.068	0.613	1.816
HA - 0.967 vs. LA - 0.605	-0.312	0.104	-0.008	0.087	2.958	0.061
HA - 0.967 vs. LA - 0.725	-1.524	0.268	-1.121	0.221	1.938	1.346
HA - 1.21 vs. LA - 0.121	1.271	0.112	1.339	0.118	1.654	1.738
HA - 1.21 vs. LA - 0.242	1.081	0.073	0.987	0.067	1.621	1.485
HA - 1.21 vs. LA - 0.363	0.939	0.065	0.985	0.068	1.669	1.783
HA - 1.21 vs. LA - 0.484	0.594	0.057	0.721	0.062	1.404	1.733
HA - 1.21 vs. LA - 0.605	0.416	0.072	0.519	0.069	1.802	2.314
HA - 1.21 vs. LA - 0.725	-0.006	0.085	0.080	0.087	0.189	-1.868
HA - 1.21 vs. LA - 0.967	-2.120	0.353	-2.601	0.416	1.514	1.848
$\bar{n}_{pre-rejection}$		0.019				2.067
$S_{pre-rejection}$		1.247				3.127
$\bar{n}_{post-rejection}$		0.019				1.669
$S_{post-rejection}$		1.247				0.969
λ_{95}		0.333				0.261
$\bar{\epsilon}$		0.191				

Table XIV-D. Full data set of $\Delta A / \bar{A} = 20\%$, HA - HI vs. LA - LI scenario.

$$\Delta A / \bar{A} = 50\%$$

HA - HI vs. HA - LI	$n_{0,0,1}$	$\epsilon_{0,0,1}$	$n_{0,0,2}$	$\epsilon_{0,0,2}$	$n_{x,t,1}$	$n_{x,t,2}$
HA - 0.242 vs. HA - 0.121	1.583	0.511	1.517	0.490	1.536	1.588
HA - 0.363 vs. HA - 0.121	1.547	0.297	1.552	0.298	1.527	1.554
HA - 0.363 vs. HA - 0.242	1.485	0.442	1.611	0.479	1.510	1.503
HA - 0.484 vs. HA - 0.121	1.656	0.247	1.514	0.226	1.687	1.545
HA - 0.484 vs. HA - 0.242	1.730	0.280	1.510	0.245	1.854	1.503
HA - 0.484 vs. HA - 0.363	2.074	0.604	1.368	0.401	2.408	1.505
HA - 0.605 vs. HA - 0.121	1.618	0.205	1.539	0.195	1.634	1.546
HA - 0.605 vs. HA - 0.242	1.645	0.194	1.556	0.184	1.713	1.516
HA - 0.605 vs. HA - 0.363	1.771	0.271	1.512	0.233	1.882	1.528
HA - 0.605 vs. HA - 0.484	1.381	0.403	1.697	0.493	1.322	1.554
HA - 0.725 vs. HA - 0.121	1.667	0.189	1.532	0.174	1.662	1.555
HA - 0.725 vs. HA - 0.242	1.721	0.166	1.542	0.149	1.745	1.535
HA - 0.725 vs. HA - 0.363	1.859	0.201	1.502	0.163	1.882	1.557
HA - 0.725 vs. HA - 0.484	1.705	0.256	1.597	0.241	1.584	1.590
HA - 0.725 vs. HA - 0.605	2.103	0.607	1.473	0.431	1.883	1.645
HA - 0.967 vs. HA - 0.121	1.666	0.162	1.620	0.157	1.662	1.636
HA - 0.967 vs. HA - 0.242	1.707	0.128	1.671	0.125	1.728	1.659
HA - 0.967 vs. HA - 0.363	1.799	0.132	1.696	0.124	1.818	1.729
HA - 0.967 vs. HA - 0.484	1.684	0.138	1.832	0.150	1.615	1.813
HA - 0.967 vs. HA - 0.605	1.828	0.187	1.896	0.194	1.755	1.952
HA - 0.967 vs. HA - 0.725	1.654	0.246	2.463	0.319	1.664	2.123
HA - 1.21 vs. HA - 0.121	1.656	0.145	1.611	0.141	1.662	1.629
HA - 1.21 vs. HA - 0.242	1.687	0.107	1.651	0.105	1.719	1.646
HA - 1.21 vs. HA - 0.363	1.755	0.102	1.665	0.097	1.789	1.698
HA - 1.21 vs. HA - 0.484	1.655	0.099	1.758	0.105	1.625	1.754
HA - 1.21 vs. HA - 0.605	1.744	0.115	1.778	0.117	1.725	1.826
HA - 1.21 vs. HA - 0.725	1.615	0.127	1.887	0.147	1.661	1.884
HA - 1.21 vs. HA - 0.967	1.565	0.237	1.530	0.232	1.656	1.563
$\bar{n}_{pre-rejection}$		1.667				1.679
$S_{pre-rejection}$		0.158				0.171
$\bar{n}_{post-rejection}$		1.658				1.666
$S_{post-rejection}$		0.144				0.141
λ_{95}		0.039				0.038
$\bar{\epsilon}$		0.236				

Table XV-A. Full data set of $\Delta A / \bar{A} = 50\%$, HA - HI vs. HA - LI scenario.

$\Delta A / \bar{A} = 50\%$

LA - HI vs. LA - LI	$n_{0,0,1}$	$\epsilon_{0,0,1}$	$n_{0,0,2}$	$\epsilon_{0,0,2}$	$n_{x,t,1}$	$n_{x,t,2}$
LA - 0.242 vs. LA - 0.121	1.749	0.565	2.038	0.658	1.744	2.015
LA - 0.363 vs. LA - 0.121	1.590	0.305	1.725	0.331	1.599	1.704
LA - 0.363 vs. LA - 0.242	1.319	0.393	1.190	0.355	1.345	1.174
LA - 0.484 vs. LA - 0.121	1.700	0.253	1.626	0.242	1.701	1.620
LA - 0.484 vs. LA - 0.242	1.650	0.267	1.215	0.197	1.657	1.219
LA - 0.484 vs. LA - 0.363	2.117	0.616	1.249	0.366	2.082	1.285
LA - 0.605 vs. LA - 0.121	1.671	0.212	1.674	0.212	1.672	1.663
LA - 0.605 vs. LA - 0.242	1.612	0.190	1.399	0.165	1.617	1.395
LA - 0.605 vs. LA - 0.363	1.845	0.283	1.564	0.240	1.826	1.574
LA - 0.605 vs. LA - 0.484	1.493	0.434	1.970	0.570	1.491	1.929
LA - 0.725 vs. LA - 0.121	1.676	0.190	1.688	0.191	1.681	1.683
LA - 0.725 vs. LA - 0.242	1.631	0.157	1.468	0.142	1.641	1.470
LA - 0.725 vs. LA - 0.363	1.813	0.196	1.630	0.177	1.811	1.649
LA - 0.725 vs. LA - 0.484	1.597	0.240	1.900	0.285	1.614	1.900
LA - 0.725 vs. LA - 0.605	1.724	0.501	1.815	0.526	1.768	1.862
LA - 0.967 vs. LA - 0.121	1.628	0.158	1.739	0.169	1.630	1.729
LA - 0.967 vs. LA - 0.242	1.567	0.117	1.589	0.119	1.572	1.585
LA - 0.967 vs. LA - 0.363	1.670	0.122	1.754	0.128	1.664	1.758
LA - 0.967 vs. LA - 0.484	1.484	0.122	1.963	0.160	1.487	1.948
LA - 0.967 vs. LA - 0.605	1.480	0.153	1.960	0.200	1.485	1.957
LA - 0.967 vs. LA - 0.725	1.325	0.201	2.053	0.303	1.312	2.014
LA - 1.21 vs. LA - 0.121	1.711	0.149	1.767	0.154	1.709	1.766
LA - 1.21 vs. LA - 0.242	1.694	0.108	1.650	0.105	1.693	1.657
LA - 1.21 vs. LA - 0.363	1.821	0.106	1.805	0.105	1.808	1.823
LA - 1.21 vs. LA - 0.484	1.727	0.103	1.980	0.118	1.720	1.988
LA - 1.21 vs. LA - 0.605	1.803	0.120	1.983	0.131	1.794	2.008
LA - 1.21 vs. LA - 0.725	1.831	0.144	2.043	0.160	1.803	2.060
LA - 1.21 vs. LA - 0.967	2.483	0.367	2.032	0.302	2.428	2.122
$\bar{n}_{pre-rejection}$		1.712				1.713
$S_{pre-rejection}$		0.239				0.234
$\bar{n}_{post-rejection}$		1.698				1.700
$S_{post-rejection}$		0.217				0.215
λ_{95}		0.058				0.058
$\bar{\epsilon}$		0.243				

Table XV-B. Full data set of $\Delta A / \bar{A} = 50\%$, LA - HI vs. LA - LI scenario.

$$\Delta A / \bar{A} = 50\%$$

LA - HI vs. HA - LI	$n_{0,0,1}$	$\epsilon_{0,0,1}$	$n_{0,0,2}$	$\epsilon_{0,0,2}$	$n_{x,t,1}$	$n_{x,t,2}$
LA - 0.242 vs. HA - 0.121	2.978	0.961	2.956	0.954	1.747	1.760
LA - 0.363 vs. HA - 0.121	2.366	0.454	2.304	0.443	1.646	1.607
LA - 0.363 vs. HA - 0.242	3.704	1.099	3.650	1.083	1.737	1.620
LA - 0.484 vs. HA - 0.121	2.314	0.344	2.085	0.311	1.714	1.558
LA - 0.484 vs. HA - 0.242	3.045	0.492	2.654	0.429	1.770	1.604
LA - 0.484 vs. HA - 0.363	5.245	1.521	4.123	1.197	1.859	1.681
LA - 0.605 vs. HA - 0.121	2.200	0.279	2.069	0.263	1.690	1.599
LA - 0.605 vs. HA - 0.242	2.667	0.314	2.487	0.293	1.770	1.604
LA - 0.605 vs. HA - 0.363	3.606	0.550	3.183	0.486	1.876	1.648
LA - 0.605 vs. HA - 0.484	5.581	1.604	5.522	1.587	1.696	1.700
LA - 0.725 vs. HA - 0.121	2.152	0.244	2.044	0.232	1.696	1.619
LA - 0.725 vs. HA - 0.242	2.511	0.242	2.376	0.229	1.770	1.632
LA - 0.725 vs. HA - 0.363	3.111	0.335	2.823	0.305	1.859	1.681
LA - 0.725 vs. HA - 0.484	3.846	0.572	3.855	0.573	1.710	1.732
LA - 0.725 vs. HA - 0.605	6.864	1.964	6.496	1.858	1.843	1.798
LA - 0.967 vs. HA - 0.121	2.037	0.198	2.045	0.198	1.653	1.665
LA - 0.967 vs. HA - 0.242	2.265	0.169	2.309	0.172	1.698	1.692
LA - 0.967 vs. HA - 0.363	2.587	0.189	2.597	0.189	1.750	1.748
LA - 0.967 vs. HA - 0.484	2.800	0.227	3.107	0.252	1.614	1.801
LA - 0.967 vs. HA - 0.605	3.474	0.351	3.776	0.380	1.684	1.865
LA - 0.967 vs. HA - 0.725	4.342	0.632	5.236	0.760	1.631	1.910
LA - 1.21 vs. HA - 0.121	2.081	0.182	2.044	0.178	1.716	1.700
LA - 1.21 vs. HA - 0.242	2.295	0.146	2.270	0.144	1.778	1.735
LA - 1.21 vs. HA - 0.363	2.568	0.149	2.492	0.145	1.842	1.796
LA - 1.21 vs. HA - 0.484	2.723	0.161	2.845	0.168	1.744	1.850
LA - 1.21 vs. HA - 0.605	3.155	0.205	3.215	0.209	1.826	1.912
LA - 1.21 vs. HA - 0.725	3.530	0.271	3.836	0.294	1.814	1.955
LA - 1.21 vs. HA - 0.967	5.949	0.858	5.992	0.863	1.874	1.886
$\bar{n}_{pre-rejection}$		3.257				1.739
$S_{pre-rejection}$		1.243				0.095
$\bar{n}_{post-rejection}$		3.257				1.739
$S_{post-rejection}$		1.243				0.095
λ_{95}		0.332				0.025
$\bar{\epsilon}$		0.516				

Table XV-C. Full data set of $\Delta A / \bar{A} = 50\%$, LA - HI vs. HA - LI scenario.

$$\Delta A / \bar{A} = 50\%$$

HA - HI vs. LA - LI	$n_{0,0,1}$	$\epsilon_{0,0,1}$	$n_{0,0,2}$	$\epsilon_{0,0,2}$	$n_{x,t,1}$	$n_{x,t,2}$
HA - 0.242 vs. LA - 0.121	0.354	0.117	0.599	0.194	1.076	2.089
HA - 0.363 vs. LA - 0.121	0.771	0.149	0.972	0.187	1.352	1.687
HA - 0.363 vs. LA - 0.242	-0.900	0.270	-0.849	0.255	5.326	5.102
HA - 0.484 vs. LA - 0.121	1.042	0.155	1.054	0.157	1.652	1.633
HA - 0.484 vs. LA - 0.242	0.334	0.059	0.071	0.028	1.293	0.255
HA - 0.484 vs. LA - 0.363	-1.053	0.310	-1.506	0.440	1.388	1.995
HA - 0.605 vs. LA - 0.121	1.089	0.138	1.144	0.145	1.582	1.616
HA - 0.605 vs. LA - 0.242	0.589	0.072	0.467	0.058	1.309	0.978
HA - 0.605 vs. LA - 0.363	0.010	0.033	-0.107	0.036	0.350	-2.037
HA - 0.605 vs. LA - 0.484	-2.707	0.780	-1.854	0.538	2.174	1.636
HA - 0.725 vs. LA - 0.121	1.192	0.135	1.177	0.133	1.629	1.620
HA - 0.725 vs. LA - 0.242	0.840	0.082	0.634	0.063	1.499	1.159
HA - 0.725 vs. LA - 0.363	0.561	0.065	0.309	0.041	1.779	1.127
HA - 0.725 vs. LA - 0.484	-0.544	0.089	-0.358	0.068	2.972	1.618
HA - 0.725 vs. LA - 0.605	-3.038	0.872	-3.207	0.920	1.860	1.841
HA - 0.967 vs. LA - 0.121	1.256	0.122	1.314	0.128	1.635	1.712
HA - 0.967 vs. LA - 0.242	1.009	0.076	0.952	0.072	1.551	1.475
HA - 0.967 vs. LA - 0.363	0.881	0.066	0.853	0.064	1.714	1.731
HA - 0.967 vs. LA - 0.484	0.368	0.037	0.688	0.061	1.205	2.345
HA - 0.967 vs. LA - 0.605	-0.166	0.041	0.080	0.036	6.614	-1.542
HA - 0.967 vs. LA - 0.725	-1.364	0.206	-1.020	0.159	2.069	1.451
HA - 1.21 vs. LA - 0.121	1.286	0.112	1.335	0.117	1.638	1.694
HA - 1.21 vs. LA - 0.242	1.086	0.070	1.032	0.066	1.571	1.492
HA - 1.21 vs. LA - 0.363	1.008	0.060	0.978	0.058	1.697	1.679
HA - 1.21 vs. LA - 0.484	0.660	0.042	0.893	0.056	1.430	1.940
HA - 1.21 vs. LA - 0.605	0.391	0.036	0.547	0.043	1.362	1.954
HA - 1.21 vs. LA - 0.725	-0.084	0.034	0.094	0.035	-2.019	2.957
HA - 1.21 vs. LA - 0.967	-1.901	0.284	-2.431	0.357	1.576	1.959
$\bar{n}_{pre-rejection}$		0.122				1.651
$S_{pre-rejection}$		1.173				1.336
$\bar{n}_{post-rejection}$		0.122				1.561
$S_{post-rejection}$		1.173				1.164
λ_{95}		0.313				0.314
$\bar{\epsilon}$		0.161				

Table XV-D. Full data set of $\Delta A / \bar{A} = 50\%$, HA - HI vs. LA - LI scenario.

R002594125